AN EXPERIMENTAL STUDY OF THE

HYDRODYNAMIC SUSPENSION OF CYLINDERS

IN A VERTICAL PIPELINE

AN EXPERIMENTAL STUDY OF THE
HYDRODYNAMIC SUSPENSION OF CYLINDERS
IN A VERTICAL PIPELINE

By

S.W. Lee, B. Eng. (McMaster)

A Thesis

Submitted to the Faculty of Graduate Studies

In Partial Fulfilment of the Requirements

for the Degree

Master of Engineering

McMaster University

December, 1974

TITLE : An Experimental Study of the Hydrodynamic Suspension
of Cylinders in a Vertical Pipeline.

AUTHOR : Stephen W. Lee . B. Eng. (McMaster University)

SUPERVOSOR : Dr. B. Latto

NUMBER OF PAGES : 179.

SCOPE AND CONTENTS :

This thesis describes an experimental study of hydro-
dynamically suspended cylinders and cylinders modified by end
cap(s) in a vertical pipeline, using water and polymer solution
as the fluid medium.

The experiments involved hydrodynamically suspending
steel and aluminium cylinders in a pipeline for the sphere to
pipe diameter ratios of 0.434 to 0.864. Drag coefficients were
found from a force balance which involved measuring the average
velocity of flow near the cylinders as well as the pressure
drops across the cylinders. The experiments on cylinders were
done in both water and dilute aqueous polymer solutions, while
the tests on cylinders modified by end caps were done in water
only. The length to diameter ratios of cylinders used in this
study ranged from three to fourteen.

Comparison of results from this study to those
obtained by other authors especially Hoerner[13], McNown &
Newlin[18] and Aly[30] were made.

ACKNOWLEDGEMENTS

TABLE OF CONTENTS

NOMENCLATURE

A Area

A_s Area of body facing the flow.

c Concentration of polymer solution

C_d Drag coefficient based on local velocity U_l .

C_d^* Drag coefficient based on free stream velocity U_o .

d diameter of cylindrical bodies

D Diameter of test section of pipeline

f Skin Friction factor (Darcy's). $= 4 C_f$ (local),

K Constants.

L Length of cylindrical bodies

L_T Length of test section of pipeline.

ΔP_o Total pressure drop across test section with no cylindrical bodies in it but having the same fluid flow rate as the case of flow with cylindrical bodies hydrodynamically suspended in the pipeline.

ΔP_m Total pressure drop across test section with cylindrical bodies hydrodynamically suspended in test section of pipeline.

q Dynamic pressure head $\rho U_o^2 / 2 g_c$.

T_o Skin friction on pipe wall.

U_o Average velocity of fluid in pipeline away from the cylindrical bodies.

U_1 Average velocity of fluid in the annulus adjacent to the cylindrical bodies.

V Volume of bodies.

Greek Symbols

σ Specific weight of the bodies.

ρ Specific weight of the fluids.

σ_m Specific weight of mercury in the manometers.

θ Angle of inclination of pipeline to the horizontal ($= 90^o$ in these experiments.)

Subscripts

o   Without bodies in the test section.

1   Local, i.e. adjacent to the bodies.

m   With bodies in the test section.

p   Polymer.

I INTRODUCTION

In recent years, expecially with an increasing world-wide demand for energy and the need for more efficient, convenient, and non-polluting methods of transportation of raw materials, there is an increasing interest in pipeline transportation. This is of particular importance in North America where vast distances and sometimes difficult terrains as well as adverse climatic zones separate the source of energy and minerals from the processors and consumers. It is not surprising then to find an increase in interest in slurry and/or capsule pipelines that sometimes cover distances of several hundred miles. [37]

The problem of transporting fluids and raw materials as well as finished products is complex for many reasons, most of which are non-scientific. However, it is found that transportation through pipelines can be economically competitive with rail and road transportation particularly in regions where sufficient transportation systems do not exist and in localities where construction and maintence of new transportation facilities is difficult and expensive. Furthermore, pipelining can considerably shorten the distance between the origin and destination by avoiding existing indirect routes. Pipelines can also operate continuously under automatic control systems and can be monitored by computer systems. The economics of pipelining becomes even more attractive if a fluid need to be transported in the same direction (to the consumers) as the

solid materials,in which case both solid and liquid are carried in the pipeline and no problem with disposal of the carrier fluid has to be considered. In the instances of the solids transported being chemically reactive to the carrier fluid or if the final separation process is not desirable, the solids can be compacted and placed in capsules.

The use of pipelining[33] extends to areas such as mining, dredging and filling, sewage treatment and disposal or chemical processes in general, so that it is not an understatement to say that long distance pipelines have demonstrated the technical and economic feasibility of this mode of transportation and that it deserves further investigation of the fluid dynamic, engineering and energy problems which are generally encountered.

In the current research, the hydrodynamics of cylindrical shaped bodies of different densities and diameter ratios are investigated to supplement existing knowledge of capsule transportation. The underlying principles and existing knowledge and difficulties of pipelining will also be discussed.

The results presented in this thesis stems from an investigation of hydrodynamically suspended metal cylinders (aluminium, S.G.=2.7 and steel, S.G.=7.8) of diameter ratios 0.43 to 0.86 in a 2" diameter vertical pipeline having a plexiglass test section of 10' in length.

The present research also involved the investigation of the effects of modifying the cylindrical shapes in an attempt to "streamline" them by attaching to them semi-hemispherical caps of the same material either as fore or afterbodies. The hydraulic pumping power requirements for these blunt cylinders and modified bodies were also compared as well as for blunt cylinders with and without the use of the polymer additive.

The experiment was directed towards investigating the effects of diameter, length and specific gravity of the blunt cylinder and modified cylinders as well as the effects of viscous shear friction along the cylinder, the skin friction of the inner pipe wall and the inertial mass effects of the cylindrical bodies. It is intended that the results obtained from the present experiments will help in the design of future pipeline transportation systems.

II   LITERATURE SURVEY

Since 1851 when Stokes[1] derived the mathematical relation for the flow of a sphere in a fluid medium, the majority of the more important researches related to the flow of fluids past bodies have been done by aerodynamicists and naval architects on the research of both aerial and undersea weapons.

In general, the results of these researches since the 1920's involve the flow of air or water past blunt cylindrical bodies[13],[32] without the restrictions of a boundary medium. In particular, experiments done on torpedos[13] have found to be most useful to the current work even though the flow regimes in these experiments are usually hyper or supersonic flows. However, dimensional similarities have rendered them useful comparisions to the present research.

It was not until 1951 that another useful set of results was published by McNown and Newlin[18] who studied the effects of a change of diameter on rigidly mounted spheres in air flowing inside a tube. However, these experiments were done in the flow of air at very low Reynolds number and are not generally of value to pipeline transportation problems. The experiments did produced an important prediction for the form drag coefficients as a function of the diameter ratio d/D in the form,

$$C_d^* = (d/D / (1 - (d/D)^2))^2 \qquad (2.1)$$

This relationship was shown to hold for diameter ratios up to about 0.8, but unfortunately, attempts to apply this relationship to a viscous fluid medium has been unsuccessful.[29]

Yet, the outcome of McNown and Newlin's work has proved useful and led to an increased activity on the research of flow of bodies in a bounded medium, in particular, pipeline transportation research. The work of the Alberta Research Council[3-12] and many other independent researchers in the past twenty years sufficiently indicate current interest shown in single and multi-phase flows as well as capsule transportation problems.

The results from these researches are in their own rights important but they do not necessarily apply to the current research; yet they do establish a few parameters that are useful in the description of similar flows, such as,

(1) Flow Reynolds number[6-9]

It defines the relative importance of dynamic instability resulting from the rotation component of the velocity vector and also the significance of the inertial force term.

(2) Pressure drop with bodies in the pipeline[3],[5],[11]

It defines the form drag and is useful in determining the required hydraulic pumping power for a pipeline.

(3) Body diameter to pipe diameter ratio[4],[6-8]

It defines the mass throughput for the pipe with respect to different shapes and sizes of the body. It is also related to the viscous shear losses along the sides of the bodies. Increasing diameter ratios usually results in greater pressure drops.

(4) Length to diameter ratio[4],[6-9]

For capsules of the same diameter under low velocity flow, longer capsules generally move slower than short ones.

(5) Surface roughness of bodies and pipe wall[2],[4],[6],[8]

Effects of surface roughness is noticeable at low flow velocities but decreases uniformly with an increase of flow velocity.

(6) Density of body and carrier fluid[4],[6],[8]

A body with low body to fluid density ratio is very sensitive to the velocity of the fluid but the effect decreases with an increase of density ratio.

(7) Presence of fore or afterbodies[2],[4],[6-8]

Fore and afterbodies of either ellipsoidal or conical shapes are sometimes added to the cylindrical capsules at the leading or both ends of the capsules. In a horizontal pipe, this generates little effects, particularly for capsules of large diameter ratios. They do however provide an increase of the flow velocity and a change of the flow pattern.

(8) Viscosity of carrier fluid[4],[6-8]

The results on water and industrial oils of different viscosities show an obvious increase of pressure drop associated with bodies particularly those of low density as the viscosity of the fluid is increased. This is of great significance for the consideration of polymer solutions which will be discussed later.

The above parameters are found useful also for the description of flows in an inclined pipeline. Round and Kruyer experimented with the flow of water[10] and air[12] past single spheres and sphere trains, and found that at a "bounce point", the spheres become stationary and there are no inertial effects except for gravity. Also, the Reynolds number for the spheres become irrevelent and the independent variables are the fluid velocity and the pressure drop across the spheres. They also found that at a pipe inclination of between 20° and 65°, the square of the sustaining velocity varies linearly with the sine of the angle of inclination, while at inclination close to 90°, the velocity becomes unpredictable.

On the other hand, the drag coefficient was found to be dependent on the diameter ratio only while the lift coefficient was found to be about one half of the value of the drag coefficient of the spheres or sphere trains.

The flow pattern of similar bodies in a fluid changes with the addition of certain polymeric (natural or synthetic) and non-polymeric solutions to the flow. Experi-

ments have shown that this drag reducing effect or ' Tom's phenomenon' is exhibited by guar gum, polyethylene oxides, polyacryamides and certain myceller solutions as well as certain fine fibre suspensions such as asbestos.

The actual phenomenon of drag reduction is not totally understood and certainly many contradictory theories have been suggested throughout the years as Hoyt[17] and Gadd[15] have indicated in their recent survey on the subject.

In pipe flow for instance, the drag reducing mechism is believed to be related to the inner wall region of the boundary layer. It is thought that the small chain-like struture of the additives actually dampens the circulation of high frequency small scale eddies that causes active turbulent mixing and also reduces the heat and mass transfer rates in the buffer or inner wall region just outside the viscous sublayer. Outside of this region, the turbulence eddies are usually large perturbations so that little, if any, damping action may exist. The net result is a steeper velocity profile near the wall with a more typical turbulent flow velocity profile towards the edge of the boundary layer and a thickening of the buffer zone.

Another hypothesis suggests that an anisotropic layer exists near the wall so that shear in the normal direction to the flow is dampened and that the flow in the axial direction is enhanced with the benefit of less energy loss. This hypothesis, however, has not been found useful to explain the paradox and uncertainties in polymer solution flows.

The characteristics of a drag reducing solution are many fold. Indeed, there is usually an optimum drag reducing effect associated with a certain polymer concentration that changes with different flow systems. On the basis of work done on a simple capillary tube gravity flow rheometer, Latto[*] has shown that such an optimum concentration to be between 10 to 1000 wppm depending on the nature of the additive as shown in the enclosed figure 2.1.

Polymer solutions also appear to show a delay of transition from the laminar to the turbulent flow regime, and this is believed to be associated with a higher shear stress necessary to affect the expanded buffer zone.

Another characteristic is the necessity for polymer solutions to be "aged" so that the molecules can relax to an entangled mass of interlocking chains. However, researchers such as White[20] have reported damage to the drag reducing property if this process is prolonged. Indeed it has been found that room temperature oxidation, exposure to sunlight, biological attack[22] and most often, mechanical shear [21] can degrade the polymer solutions by breaking up the molecular chains. However, the rate of degradation appears to be dependent on the type of polymer used.

Whereas polymer solutions can reduce drag, there is usually a maximum drag reduction capability for a given Reynolds number. These maximum drag asymptotes have been empirically

[*] Private communciation
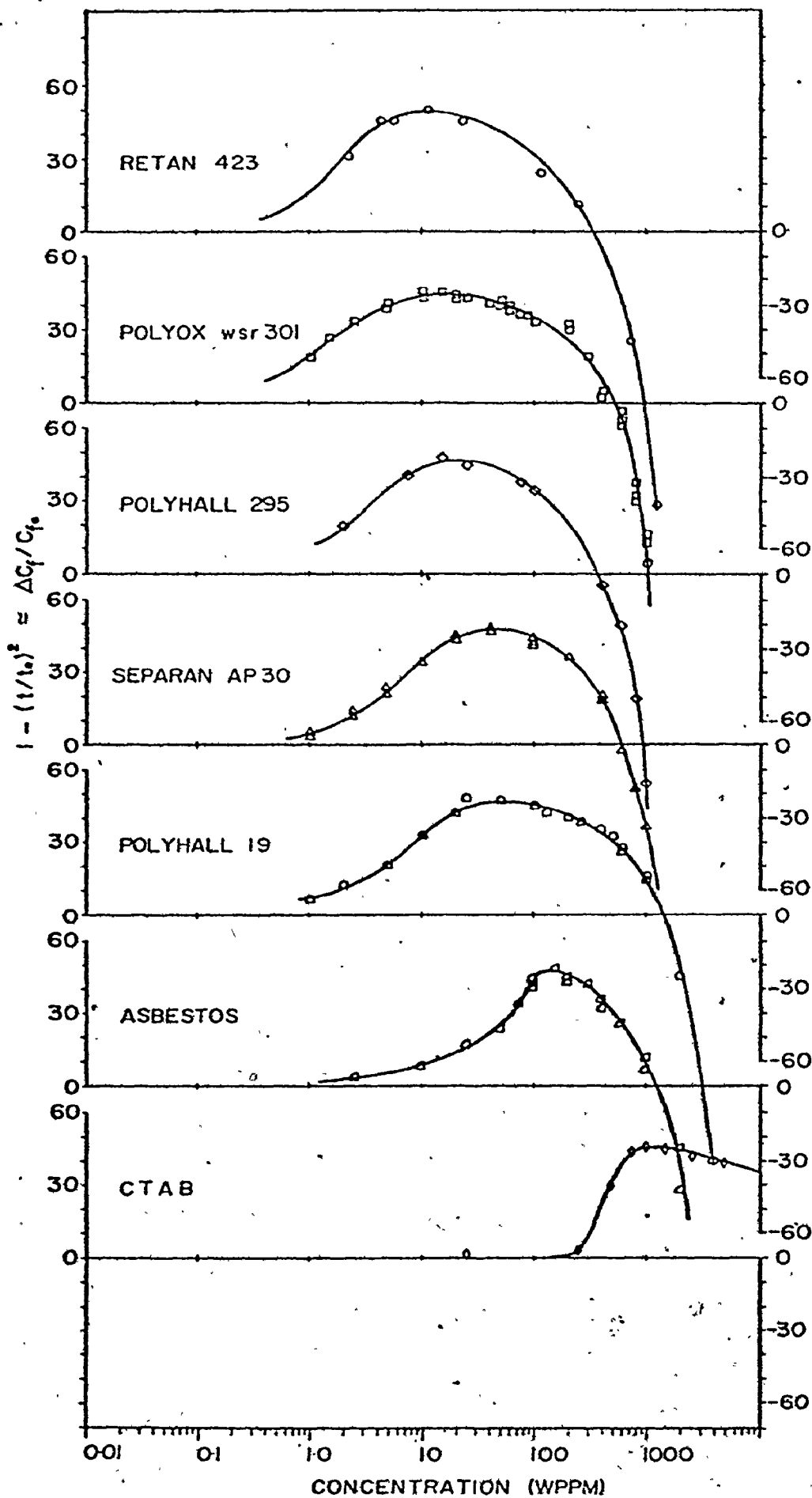
obtained. Indeed, the relationship for drag of such a solution
is similar to that of a Newtonian turbulent friction equation
for a smooth pipe.

$$f^{-0.5} = 19 \log (\text{Re} \times f^{0.5}) - 32.4 \quad (\text{Virk}[23]) \quad (2.2)$$

$$f^{-0.5} = 4.0 \log (\text{Re} \times f^{0.5}) - 0.4 \quad (\text{water}) \quad (2.3)$$

The form of the two equations suggest simpler relationships such
as :

$$f = 1.4 \text{ Re}^{-0.667} \qquad (\text{Castro et al}) \qquad (2.4a)$$

$$f = 0.42 \text{ Re}^{-0.55} \qquad (\text{Virk et al}) \qquad (2.4b)$$

$$f = 0.25 \text{ Re}^{-0.5} \qquad (\text{Giles et al}) \qquad (2.4c)$$

These relationships will be discussed later in this thesis.
Meanwhile it must be said that although these equations expresses
friction loss as solely dependent on Reynolds number, the pipe
size effect is implicitly related.

In spite of the confusion caused by so many contrad-
ictory hypotheses regarding the drag reducing mechanism, many
experiments were done to relate the flow of polymer solutions
for particular situations.[24],[25] In fact, White[26] experimented
on the Stokean flow of spheres in a polymer solution and found
that within the laminar regime, there is possibly a delay of
the separation point to a location further downstream if the
Reynolds number is increased, and he attributed this to a
visco-elastic effect.

The effects of the walls on a polymer (pipe) flow was investigated in the work of Stow and Ellict[27] who experimented with single spheres of a fixed diameter ratio (0.39) tethered in a cylindrical boundary using four different types of polymer solutions that had previously been found to show drag reduction capabilities. The amazing result that no drag reduction was observed led them to conclude that the flow of the polymer solutions were effectively the same as in Stoke's experiment where water was used as the fluid medium. Moreover, the Reynold number was fairly high (up to 80,000) so that the only affecting factor seems to be that of the wall.

Recently, an investigation was made by Iatto, Round and Anzenavs[28] using single spheres and sphere trains hydrodynamically suspended in a 2" diameter vertical glass tube. Diameter ratios ranging from 0.2 to 0.97 were used and measurements were made using polymer solutions of different concentrations and results were compared to that obtained using water. It was found that the drag coefficient was not affected for diameter ratios greater than 0.7 but there was an obvious increase for diameter ratios less than this value. These data also correlated well with theoretical force and momentum equations indicating that the results are valid. It was believed that this increase of drag coefficient at low diameter ratios (by as much as 30%) was accompanied by a decrease in skin friction losses along the inside wall of the pipe as well as reduced shear losses at the sphere surface.

The results using sphere trains indicate a size, density and length effects on the drag coefficient. Moreover, the type of connection between the spheres was also significant. Flexible connections were found to result in higher drag coefficients than for rigidly attached spheres. Furthermore, at high aspect ratios, the drag coefficient asympototically approached a constant value.

However, such an investigation was not capable of ascertaining the wall effects and correction factors for the wall such as suggested by McNown and Lee[34] fail to include the inertial terms and for spheres in free fall as in Stoke's experiment, they gave a factor K such that

$$K = 1 + \frac{9}{4} \left(\frac{d}{D} \right) + \left(\frac{9}{4} \frac{d}{D} \right)^2 \qquad (2.5)$$

This compared well with Ladenburg's correction factor

$$K = 1 + 2.4 \left(\frac{d}{D} \right) \qquad (2.6)$$

or Faxen's correction factor,

$$K = 1 + 2.1 \left(\frac{d}{D} \right) \qquad (2.7)$$

Unfortunately these corrections are valid only for small diameter ratios of up to 0.4. For large diameter ratios close to 1.0, McNown and Lee suggested a correction of the form

$$K = 1.67 \left(1 - \frac{d}{D} \right)^{-2.5} \qquad (2.8)$$

Indeed, this constant was related to the annuluar spacing rather than to the sphere sizes as previous equations show and suggest the similarity to a flow pattern between two parallel plates.

The other parameter affecting wall effects was found to be the Reynolds number such that

$$C_d = f \left(Re, \frac{d}{D} \right) \tag{2.9}$$

McNown and Newlin[18] actually investigated the Reynolds number effect on the drag coefficient for different diameter ratics and found that there was an increase of drag coefficient with increase of diameter ratio. They also observed that at Reynolds number close to 50,000, the drag coefficient tend towards a constant value.

Unfortunately, they excluded the inertial term effects but managed to estimate the contribution of the viscous shear effects by separating the total drag coefficient into two parts, as follows :

$$(C_d)_{total} = (C_d)_{\substack{pressure \\ drag}} + (C_d)_{\substack{shear \\ losses}} \tag{2.10}$$

and they estimated the magnitude of each term by using the following equation,

$$(C_d)_{\substack{shear \\ losses}} = \frac{2.5}{Re^{0.5}} \left(\frac{U_{max}}{U_o} \right)^{1.5} \tag{2.11}$$

U_{max} being the centerline velocity of the sphere and U_o the velocity of the free stream. They obatined the drag coeffic- ient associated with pressure drag from a measured pressure distribution and found that the pressure drag was 93% of the total drag.

Another related work was that of Aly[30] who showed that for nylon spheres and cylinders, the drag coefficient tend towards a constant value at large aspect ratios. He also observed that on a per sphere basis, the drag coefficient for a cylinder train is less than that for a sphere train. This has far reaching effects when the economics of capsule transportation is considered, as Kruyer and Ellis indicate in their recent publication[31] based on measurements of an actual pipeline.

However, not much research has been done with streamlined capsules in a viscous flow in a bounded medium, except for the investigation on horizontal pipelines[2],[4],[6-8] which indicate minimal effects; however, it is believed that perhaps more careful measurements might reveal better results.

In the absence of publications on viscous incomp- ressible fluid flows past streamlined bodies, the publication by Hoener[13] and Chang[32] on aerodynamic drag will have to be referred to on discussions in this area.

In conclusion, it appears that there is a necessity for more research that may prove useful in providing inform- ation for the design of slurry and capsule pipelines in the future.

III THEORY

In an attempt to model the pipeline system used in the current research to obtain a relationship between the flow and physical parameters for hydrodynamic suspension of cylinders in pipelines, the following approach was adopted.

If the control volume depicted in Fig. 3.1 is considered, a force balance between the gravity, buoyancy and frictional forces as well as the applied pressure force exists. These forces may be classified as the inertial force, the shear or viscous drag force on the side of the body, the skin friction drag associated with the wall of the pipe and the pressure drag force experienced by the body. These forces are defined in the following discussion.

The inertial forces are those body forces that effectively change the momentum of the body and for a body hydrodynamically suspended in a fluid where there is no momentum change, the only body force is the gravitational force.

Shear or viscous drag is related to the frictional losses on the surface of the body. Since it is a surface force, it acts tangentially to the surface and in the present case, is along the axis of the cylinder and pipe.

Pressure drag force acts normally to the body and is the pressure drop between the front and back end of the
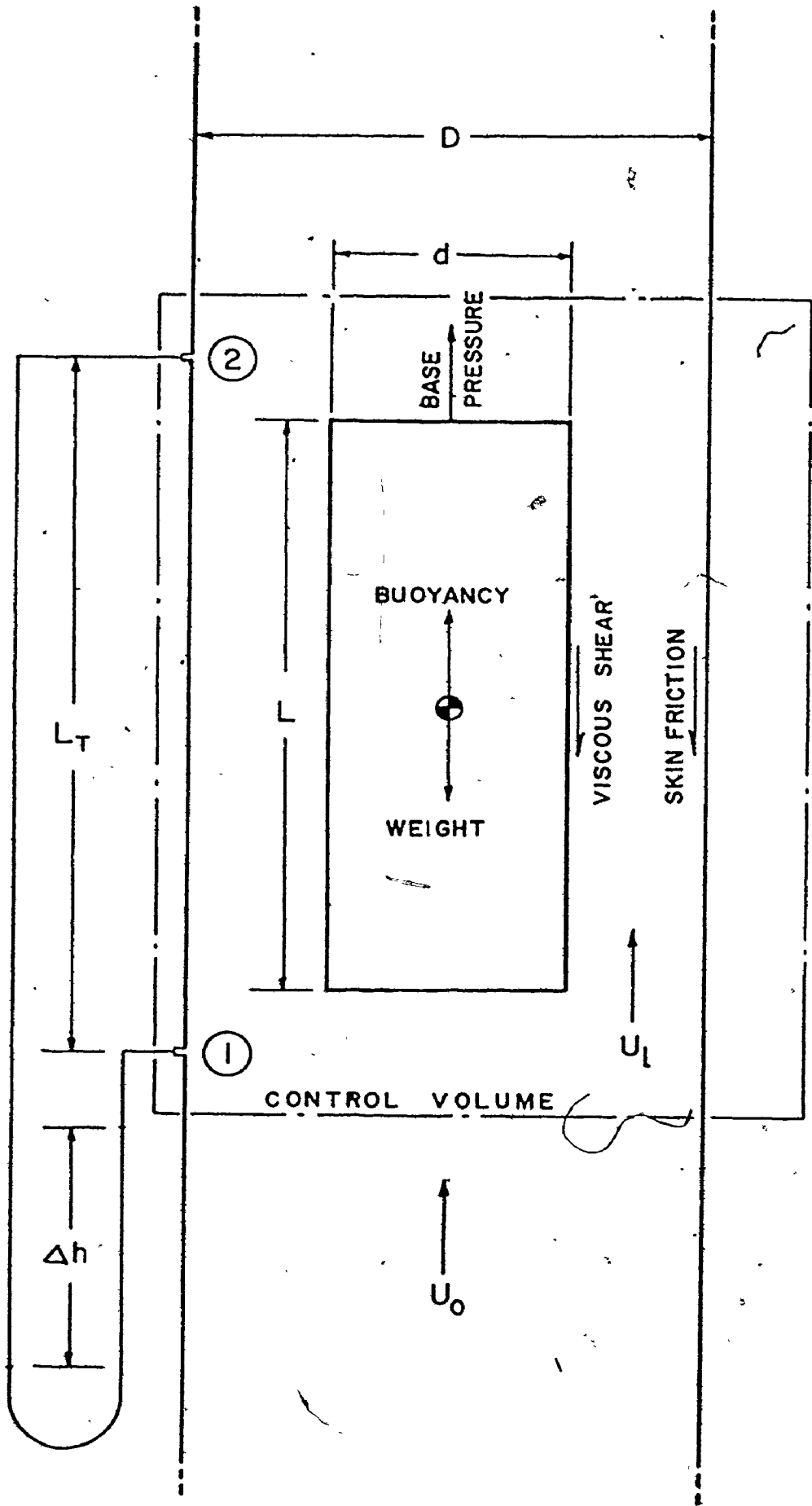
FIG.3·1: SCHEMATIC OF CONTROL VOLUME IN TEST SECTION

cylinder giving rise to a net pressure force at the end surfaces. This force may be separated into two forces, the base drag and the fore or afterbody drag.

Base drag is solely a pressure loss term resulting from the change of geometry at the back end of the cylinder which either changes the streamline direction of a potential flow or causes vortices and a wake depending on the nature of the flow.

The fore or afterbody drag is in itself a combination of pressure and viscous shear forces. This may be explained if a blunt cylinder and a cylinder modified by the addition of end cap(s) are compared. It may be envisaged that the modified cylinder will have a different pressure drag because the pressure variation over this modified body is different from the blunt cylinder due to a less abrupt change of geometry at the end(s) of the cylindrical body. However, since a modified cylinder has more surface area, the viscous shear force it experiences is different from that of the blunt cylinder.

There is also skin friction associated with the friction loss along the inner wall of the pipe. This loss is exhibited as a pressure head loss and is essentially a viscous shear force term that accompanies the pipe flow with or without the cylinder in it.

The sum of these forces may be expressed as follows :

$$\Delta P_m = \Delta P_B + \Delta P_A + \Delta P_V + \Delta P_F \qquad (3.1)$$

where ΔP_m is the total pressure loss with cylinder.

ΔP_B is the base pressure loss.

ΔP_A is the pressure drop associated with the addition of the fore(after)body.

ΔP_V is the pressure drop associated with shear or viscous drag loss.

ΔP_F is the pressure drag associated with the skin friction loss along the pipe wall.

Note that the pressure drag term is actually defined as $(\Delta P_B + \Delta P_A)$. Furthermore, we may write an expression for the case of no cylinders in the pipe as, (for the description of notations, see NOMENCLATURE)

$$\Delta P_o (\tfrac{\pi}{4} D^2) - \Delta P_F (\pi D I_T') = \frac{\rho U_o^2}{2 g_c} \; \frac{\pi}{4} D^2$$

i.e.

$$\Delta P_F = \frac{D}{4 I_T} (\Delta P_o - \frac{\rho U_o^2}{2 g_c})$$

$$= K_1 (\Delta P_o - K_2 U_o^2)$$

$$\Delta P_F = f_1 (\Delta P_o , U_o) \qquad (3.2)$$

Since K_1 and K_2 are constants, ΔP_F varies with the flow rate (hence the mean velocity term) and the pressure term ΔP_o so that for a flow rate of the same magnitude as that of the case with a cylinder suspended in the pipe, the value of ΔP_F is the same with or without the cylinders, that is,

$$P_F = f_2(\Delta P_O) \qquad (3.3)$$

Rewriting eqn. 3.1, we get,

$$\Delta P_m - \Delta P_O = \Delta P_B + \Delta P_A + \Delta P_V \qquad (3.4)$$

If the right hand side terms are grouped according to whether they are associated with pressure loss or viscous or shear drag in origin, we obtain,

$$\Delta P_m - \Delta P_O = (\Delta P_B + (\Delta P_A)_P) + (\Delta P_V + (\Delta P_A)_V) \qquad (3.5)$$

Here, the subscripts p and v stand for pressure and viscous nature of the forces. Furthermore, this conforms to the manner the fore(after)body pressure drop is separated in Chapter II. If no end cap(s) are used, eqn. 3.5 reduces to the form for a blunt cylinder, that is,

$$\Delta P_m - \Delta P_O = \Delta P_B + \Delta P_V \qquad (3.6)$$

A comparision of eqn. 3.4 with eqn. 3.6 establishes the effectiveness of the addition of end cap(s).

It is possible to investigate each term presented in eqn. 3.5 using a "theoretical" approach. If F_A is the drag force associated with the presence of the end cap(s), then, we may write, using cylindrical coordinate notations,

$$F_A = \int_0^{\frac{1}{2}\pi} (\Delta P_A)_P \cos \emptyset (r \, d\emptyset \, (2\pi r \sin\emptyset)) +$$
$$\int_0^{\frac{1}{2}\pi} (\Delta P_A)_V \sin \emptyset (r \, d\emptyset \, (2\pi r \sin\emptyset)) \qquad (3.7)$$

Now, if the drag coefficient is defined as, for any i,

$$(\text{Drag})_i = (C_d)_i \frac{\rho U_0^2}{2 g_c} A$$

$$(C_A)_P = \int_0^{\frac{1}{2}\pi} \frac{(\triangle P_A)_P}{q} (2 \sin 2\phi \, d\phi)$$

$$(C_A)_V = \int_0^{\frac{1}{2}\pi} \frac{(\triangle P_A)_V}{q} (2 \sin^2\phi \, d\phi) \qquad (3.8)$$

Note that eqn. 3.8 is based on the existence of only one end cap so that if there are two end caps, the effect would have to be a summation of a' $(C_A)_P$ and a $(C_A)_V$ term from each cap. However, this more complex form is not presented here.

The actual values of $(C_A)_P$ and $(C_A)_V$ may be obtained if the variation of $(\triangle P_A)_P$ and $(\triangle P_A)_V$ with the angle ϕ is available from pressure measurements or from a vigorous mathematical derivation of simple geometrical shapes such as a sphere or a cylinder or a cylinder normal to the flow. Unfortunately, the mathematics for the present flow system is very complex so that a theretical derivation of the pressure variation with the angle ϕ is not available.

A similar set of relationship may be obtained for the viscous shear drag term $\triangle P_V$ for a blunt cylinder and indeed, if x is the direction along the axis of the cylinder and dx is an elemental length on it, then,

$$\int_0^L (\pi d \, dx) \triangle P_V = C_V (q) (\frac{\pi}{4} d^2)$$

i.e.
$$C_V = \int_0^L \frac{\Delta P_V}{q} \frac{4}{\pi} \, dx \qquad (3.9)$$

This equation gives the relationship for the drag coefficient associated with the viscous shear loss on a blunt cylinder. However, as before, the relationship between the pressure drop ΔP_V and x is not available so that the integration may not be completed.

The evaluation of the base pressure term may not be as simple. However, Chapman[35] managed to set up an empirical relationship of the form,

$$P_B = f_3 \left(\Delta P_B^* , \text{ Re } , \text{ L/d } , q_1/q_0 , \Delta P_0^* \right) \qquad (3.10)$$

where the subscript 1 and 0 stand for positions at the end tip of the cylinder and at the free stream respectively. Each of the above terms may be defined as follows :

(1) ΔP_B^* is the ratio of the static pressure and the dynamic pressure at the particular flow situation when separation is observed to occur with the stream flow detaching from the trailing end of the cylinder. If the subscript b is used to represent a position in space just behind the back end of the cylinder surface, then,

$$\Delta P_B^* \text{ (separation) } = \left(P_b - P_1 \right) / \tfrac{1}{2} \rho_1 \left(U_1 \right)_{local}^2$$

(2)   The ratio of the dynamic pressures, using the same subscripts, is,

$$\frac{q_1}{q_0} = \frac{\frac{1}{2}\rho_1 (U_1)^2_{local}}{\frac{1}{2}\rho_0 U_0^2}$$

(3) $\Delta P_0^{'}$ is the pressure coefficient at free stream, i.e.

$$\Delta P_0^{'} = (P_1 - P_0)/ \frac{1}{2}\rho_0 U_0^2$$

(4)   Reynolds number, which exists as a power law term Re^{-n} depends on the nature of the flow and relates to the boundary layer.

Now, we may expand eqn. 3.10 in the form,

$$\Delta P_B = \Delta\overline{P}_B^{*} (1 - K Re^n (L/d)) (q_1/q_0) + \Delta P_0^{'} \qquad (3.11)$$

It is obvious from such an expression that allowance has been made for the variation of the dynamic pressure and viscosity with the change of flow velocity so that the flows are very intimately related. Indeed, back pressures are closely associated with the existence of vortices and wakes, and are affected by the existence of separated flows as well as back flows.

To conclude this portion of the analysis, one may consider again eqn. 3.4 and eqn. 3.6 and write the corresponding relationships for drag coefficients as :

$$C_{blunt \atop cylinder} = C_B + C_V$$

$$C_{modified \atop cylindrical \atop body} = C_B + C_V + C_A$$

so that combining the two equations gives,

$$C_{\substack{\text{modified} \\ \text{body}}} = C_{\substack{\text{blunt} \\ \text{body}}} + C_{\substack{\text{after or} \\ \text{forebody}}} \qquad (3.12)$$

In fact, the drag coefficient associated with the fore or afterbody must be negative in order that the drag for a blunt cydrical body is greater than that for a cylindrical body modified by end cap(s). This feature will be discussed later in Chapter VI.

To fully understand the present system, the useful flow parameters must first be identified. A dimensional analysis is useful in this regards.

The variables considered to be involved here are related by :

$$P = f_4 (d , D, L , \sigma , \rho , U_o , \mu , g_c , g) \qquad (3.13)$$

If the fundamental dimensions are F,M,L and t, then the nine independent variables shown above may be related by (9-4) or 6 dimensionless groups. If we choose U_o, ρ, D and g_c as the repeating quantities, then,

$$\Pi_1 = (U_o^a \, D^b \, \rho^c \, g_c^e) \; P$$

$$\Pi_2 = (\qquad " \qquad) \; d$$

$$\Pi_3 = (\qquad " \qquad) \; \mu$$

$$\Pi_4 = (\qquad " \qquad) \; L$$

$$\Pi_5 = (\qquad " \qquad) \; \sigma$$

$$\Pi_6 = (\qquad " \qquad) \; g$$

For dimensional homogenity, the solutions are :

$$\Pi_1 = \Delta P\, g_c\, /\, U_o^2\, \rho$$

or $\quad \Pi_1 = \Delta P\, /\, (L/d)\, \dfrac{\rho\, U_o^2}{2 g_c} = C_f = $ skin friction factor

$$\Pi_2 = d/D$$

$$\Pi_3 = \mu/\, U_o\, D\, g$$

$$\Pi_4 = L/d$$

$\Pi_5 = \sigma/\rho \quad$ which can be written as $\quad \dfrac{\sigma - \rho}{\rho}$

$$\Pi_6 = g\, D\, /\, U_o^2 = (\dfrac{\sigma - \rho}{\rho})\, 2\, g\, D\, /\, U_o^2$$

$$= \text{drag coefficient}$$

The final solution becomes,

$$f_5 = (\, C_f\, ,\, \frac{d}{D}\, ,\, Re\, ,\, \frac{L}{d}\, ,\, \frac{\sigma - \rho}{\rho}\, ,\, C_d\,) = 0 \quad (3.14)$$

However, this equation does not include all the parameters relating to the flow system. Indeed, dimensional analysis only relates dimensionless groups so that parameters such as the rotational component of the velocity are not included in eqn. 3.14. Of course, important parameters that are in themselves dimensionless may not have been included because of the way we set the original equations for Π. Falling into this category of important parameters are for instance the surface roughness of both the cylindrical bodies and the inner pipe wall or the eccentricity of the cylinder's position from the central axis of the pipeline.

It must be said that the exclusion of these other parameters in eqn. 3.14 does not make the relationship unrealistic. For instance, the rotation and eccentricity contribution may be ignored if experimental results are collected for minimal rotational velocity and that the cylindrical bodies are suspended centrally in the pipe. The surface roughness effects are ignored because it is hoped that they stay the same throughout the experiment and that this parameter is characteristic of the pipeline system. However, in the case of a flow with aqueous solutions of polymer added to the flow, the concentration of the polymer solution should be included and since this is already a dimensionless group, we write,

$$f_5 = (\ C_f \ , \ \frac{d}{D} \ , \ Re \ , \ \frac{L}{d} \ , \ \frac{\sigma - \rho}{\rho} \ , \ C_d \ , \ c \ ) = 0 \qquad (3.15)$$

To further the analysis of the flow system, a force and momentum balance using all the above mentioned dimensionless groups should be made as follows :

(A) Force balance

A force balance on the free body of the cylinder gives,

$$weight = buoyancy + total \ drag.$$

i.e. $$V \sigma = V \rho + C_d^* \frac{\rho \ U_o^2}{2 \ g} \ A_s \qquad (3.16)$$

or

$$c_d^* = (\frac{\sigma - \rho}{\rho}) 2 g L / U_o^2$$ (3.17)

which may be rewritten as,

$$\frac{c_d^*}{(L/d)} = (\frac{\sigma - \rho}{\rho}) 2 g d / U_o^2$$ (3.18)

Note that for cylinders of the same material,

$$\frac{c_d^*}{(L/d)} = K d / U_o^2$$ (3.19)

If the average local velocity in the annular spacing between the cylinders is used instead, we write,

$$D^2 U_o = (D^2 - d^2) U_1$$ (3.20)

and eqn. 3.16 becomes,

$$V (\sigma - \rho) = C_d \frac{\rho U_1^2}{2 g} A_s$$ (3.21)

or combining eqn. 3.20 and eqn. 3.21 to get,

$$\frac{U_o^2}{(\frac{L}{d}) D g (\frac{\sigma - \rho}{\rho}) \sin \theta} = \frac{2}{C_d} (\frac{d}{D}) (1 - (\frac{d}{D})^2)^2$$

$$= \text{velocity function}$$ (3.22)

(B) Momentum balance

A momentum balance may also be made of a control volume as shown in Fig. 3.1 and one gets,

$$P_1 A_1 + (\rho U A)_1 U_1 = P_2 A_2 + (\rho U A)_2 U_2 + T_o \pi D L_T +$$

$$\rho (\frac{\pi}{4} D^2 L_T - \frac{\pi}{4} d^2 L) + \frac{\pi}{4} d^2 L \sigma$$

For steady-state steady flow,

$$U_1 = U_2 \quad ; \quad A_1 = A_2 \quad ; \quad (\rho U A)_1 = (\rho U A)_2$$

the last relationship exists for no momentum generation within the control volume, so we may write,

$$(P_1 - P_2)_m \frac{\pi}{4} D^2 = T_0 \pi D L_T - \frac{1}{4} \pi D^2 L_T \rho +$$

$$\frac{1}{4} \pi d^2 L (\sigma - \rho) \qquad (3.23)$$

If no cylinders were present in the pipe, the same analysis gives, assuming that T_0 is independent of velocity and pressure,

$$(P_1 - P_2)_o \frac{\pi}{4} D^2 = T_0 \pi D L_T + \frac{\pi}{4} D^2 L_T \rho \qquad (3.24)$$

then, eqn. 3.23 and eqn. 3.24 gives,

$$\Delta P_m - \Delta P_o = (\frac{d}{D})^2 L (\sigma - \rho) \qquad (3.25)$$

alternatively, one gets,

$$\frac{\Delta P_m - \Delta P_o}{(\frac{L}{d}) D (\sigma - \rho) \sin \theta} = (\frac{d}{D})^3 \qquad (3.26)$$

Or allowing for discrepancies arising from the assumption of the shear T_0 being independent of the velocity and pressure,

$$\frac{\Delta P_m - \Delta P_o}{(\frac{L}{d}) D (\sigma - \rho)} = c' (\frac{d}{D})^n \qquad (3.27)$$

$$= \text{Pressure function}$$

where c' and n are constants.

The pressure and velocity developed in this section of the chapter will be repeatedly referred to in Chapter VI because they are dimensionless groups and are useful in comparing the effects of different physical and flow changes of the system such as the density, the use of polymer additives and modification of the bodies using end caps.

IV EXPERIMENTAL APPARATUS

The apparatus used for the main experiment will be discussed as separate sub-systems :

(a) The water flow system

This system consists of a 2" I.D. steel pipe of about 80 ft in length and assembled as shown schematically in Fig. 4.1 while a photograph of the main components is shown in Plate I.

Hydraulic power to the flow system is supplied through the water mains' line pressure and augumented by an auxillary single stage centrifugal pump which is a Worthington Model 2CN-32 type powered by a 3 hp, 3600 rpm General Electric induction motor.

The whole pipeline system is built to operate either as a closed system with the fluid re-circulated via a 300 litre capacity aluminium reservoir or alternatively, as is done in the present research, the water flows down a tail pipe to a lower floor and is discharged to the sewers. The normal line pressure from the mains is about 30 to 50 psi but is increased to about 80 psi with the use of the pump. Small variation in the line pressure is damped out using a 15 litre variable volume surge chamber which uses compressed air from the air mains line to minimize flow fluctuations.

The flow rate through the system is measured using two Brooks rotameters installed in a parallel circuit
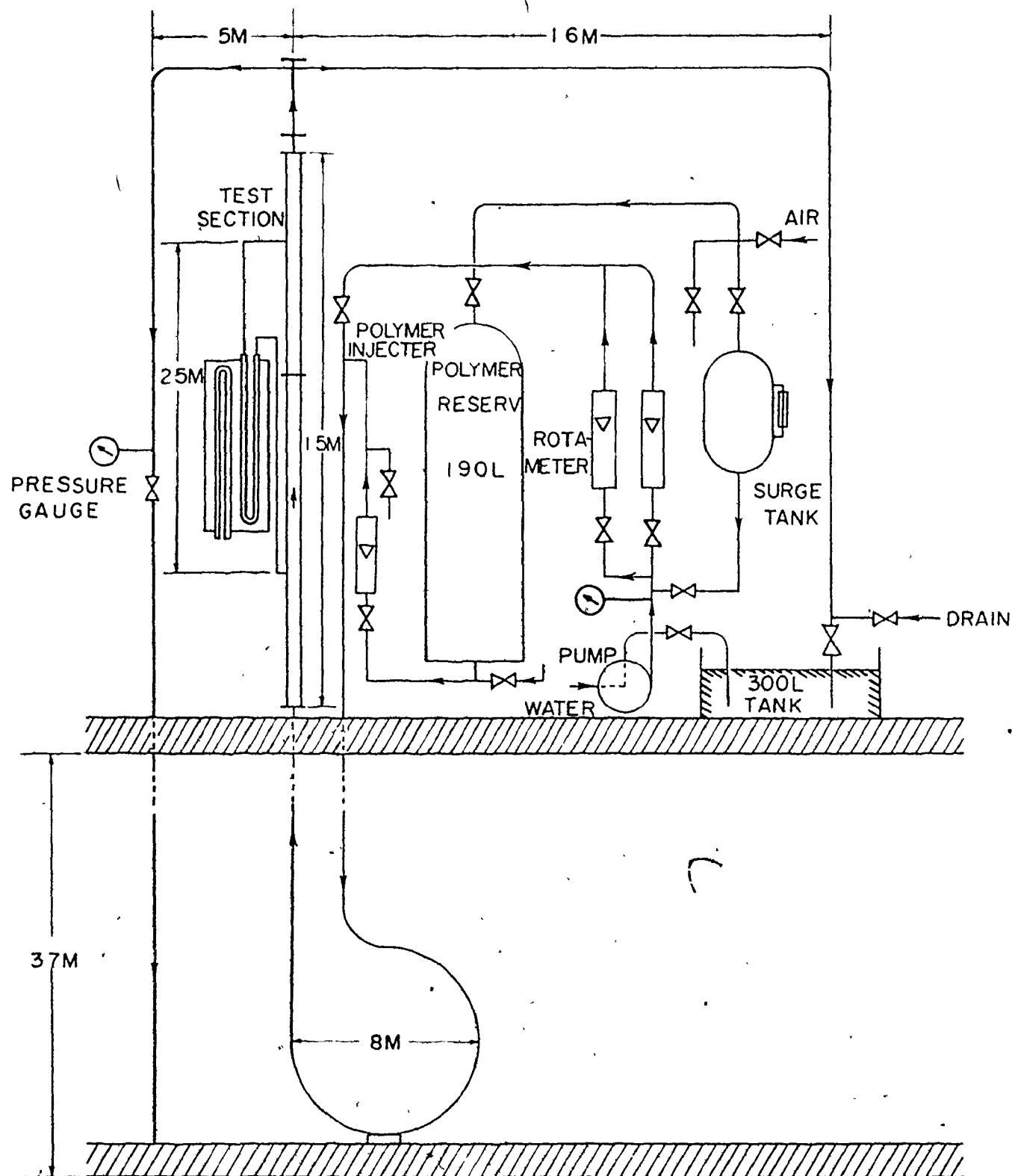
FIG. 4·1: SCHEMATIC OF PIPE FLOW SYSTEM
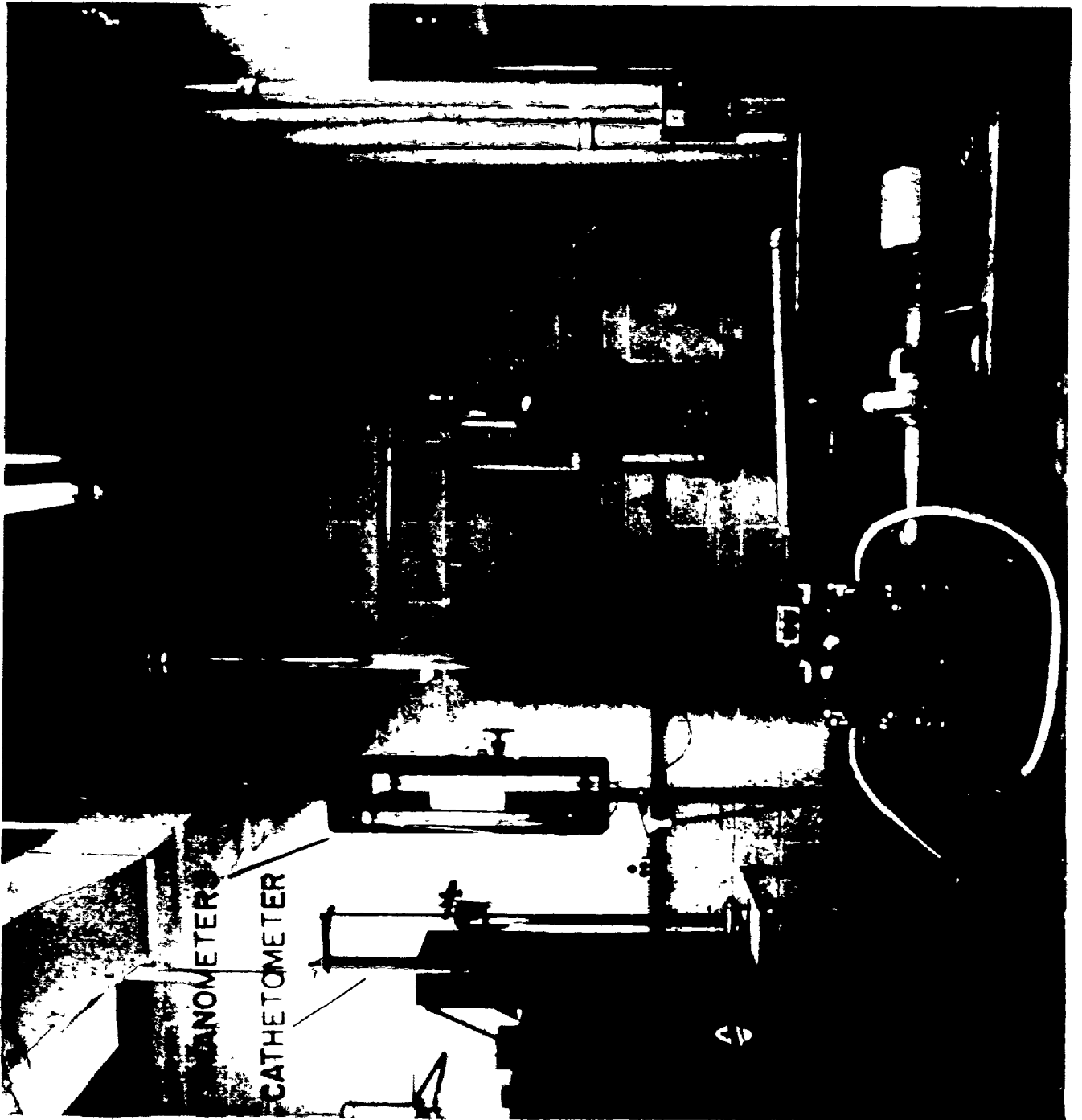
PLATE I. MAIN APPARATUS.

so that either one. or both may be used at any time. At the beginning of the experiment, one large (capacity of about 5000 c.c./sec) and a small (capacity of about 1000 c.c./sec) flow meter were used. But this arrangement was later changed to accomodate two flow meters of the large type because of capacity requirements.

After leaving the flow meters, the fluid passes through a 60 ft long loop down and back up to the level of the main apparatus through a vertical section that joins with a 10 ft long plexiglass test section, after which it either goes to the reservoir or flows down to the lower floor drains.

Two gate valves at appropriate locations control the open or closed circuit flow while a third valve on the drain section of the pipeline regulates the suction (back) pressure, which exists since the long drain pipe gives a suction head of about 30 ft.

A honeycomb filter placed at the entrance to the plexiglass test section produces homogeneous turbulence for the flow while the long length of the pipeline loop is sufficient to provide a developed turbulent flow.

The test section is accurately set vertical to avoid attenuation of any flow irregularity such as a swirling flow. The lower portion of the test section is connected to the metal pipe through flanges to ensure proper alignment, while the top portion of the test section is joined

to a flexible tygon bellows piece to prevent breakage of the tube and allow for expansion and contraction in the support. The test section consists of two equal 5 ft lengths joined together by flanges and sealed by a rubber O-ring. This sectioning of the pipe was necessary since precision I.D. pipe of long lengths is not available. Above the tygon bellows is a metal screw cap which permits insertion and easy retrieval of the cylindrical sections.

(b) The polymer injection system

The polymer injection system is connected to the main flow system at about 40 ft from the test section and always operates with an open circuit system since the recirculation system will csuse mechanical degradation of the aqueous solution.

The injection apparatus consists of a 190 litre capacity pressure vessel which holds a polymer solution, usually having a concentration of 2000 wppm but sometimes 500 wppm solutions were used if low concentration at the test section is desired. After filling the polymer vessel with the pump, the pressure vessel is charged with air from the air mains line and is regulated to a pressure of about 70 psi. The polymer solution is then discharged from the bottom of the vessel via a Brooks rotameter which then measures the flow rate of the fluid that passes into the main water system through a $\frac{1}{2}$" tubing as shown in Plate II.

BACK PRESSURE
REGULATION
VALVE

POLYMER
INJECTION
POINT
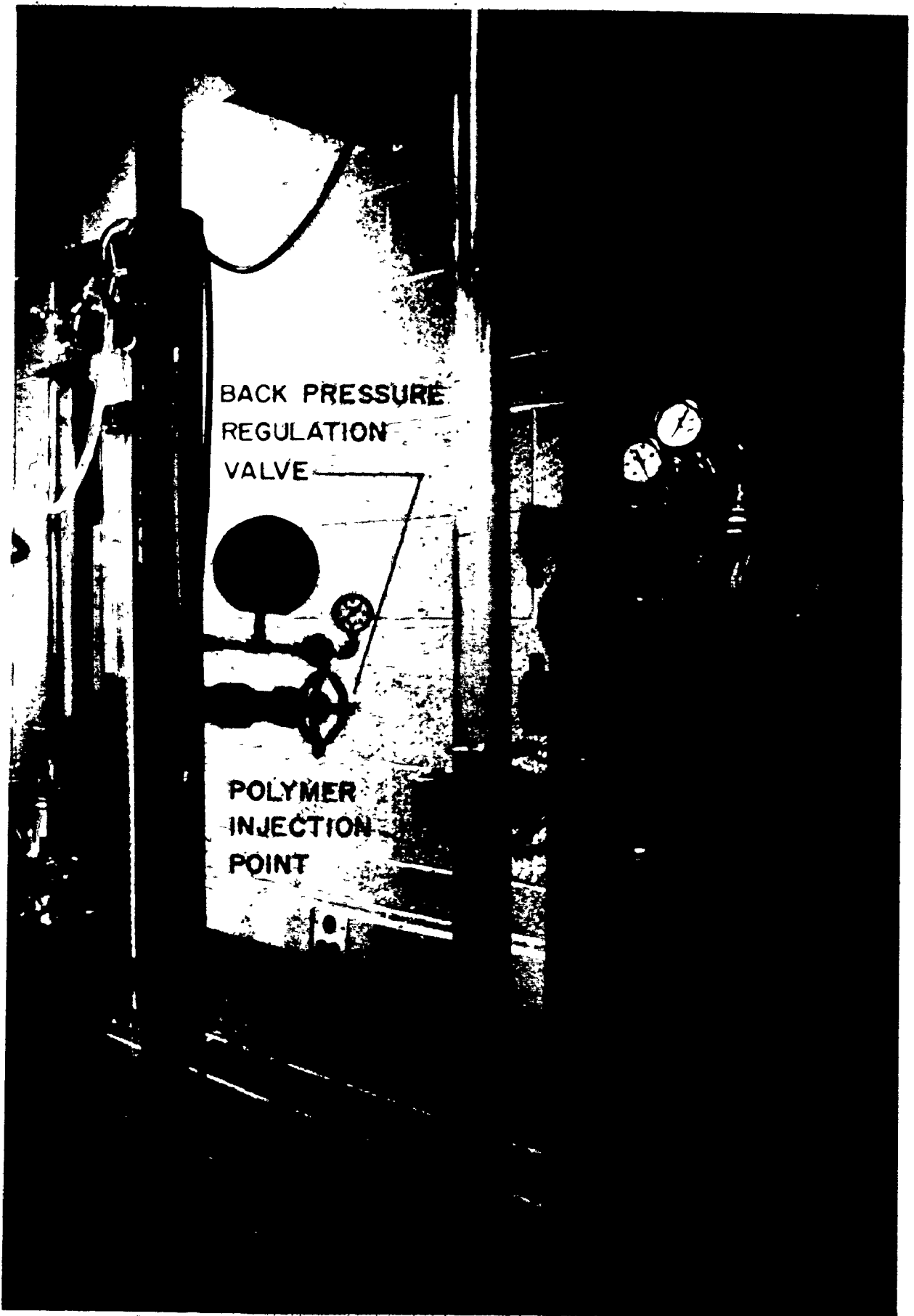
PLATE II POLYMER INJECTION & BACK PRESSURE REGULATION SYSTEMS.

It was found that a combination of a diffuser effect at the tubing (which opens up suddenly to a much larger section at the main flow system) and a long development length including the loop to the lower floor and entering the test section through the honeycomb filter is sufficient to provide a totally homogeneous solution in the test section (as indicated by rheological measurements of a sample fluid taken from the test section - this will be discussed further in section (d)).

The polymer solutions were prepared and stored in plastic bags in bins of about 70 litres capacity and the solution was pumped into the depressurised pressure vessel using a 3 arm Allspeed peristaltic pump powered by a 1 hp, 865 rpm Brooks motor and operating usually at around 200 rpm. This pump was used mainly to avoid mechanical degradation of the polymer since it produces very low flow rates and also since no parts of the pump are in direct contact with the fluid when it is in operation.

(c) The pressure measurement system

The pressure drop at the test section is measured by either one of two vertical U-tube manometers, one filled with oil (merian oil of S.G. 0.827) and the other with mercury. The two manometers are connected so that one may operate independently of the other between the same set of pressure taps at the test section as shown in Fig. 4.2. The manometer system is also provided with a drain so that fluid

FROM TEST SECTION

RESERVOIR

OIL MANOMETER

WATER OUT

WATER JACKET

WATER IN

MERCURY MANOMETER

TEST SAMPLE DRAINS

VALVE POSITIONS

(A) OIL MANOMETER (WITH DRAINS)

(B) MERCURY MANOMETER (WITH DRAINS)

(C) MERCURY MANOMETER (NO DRAINS)
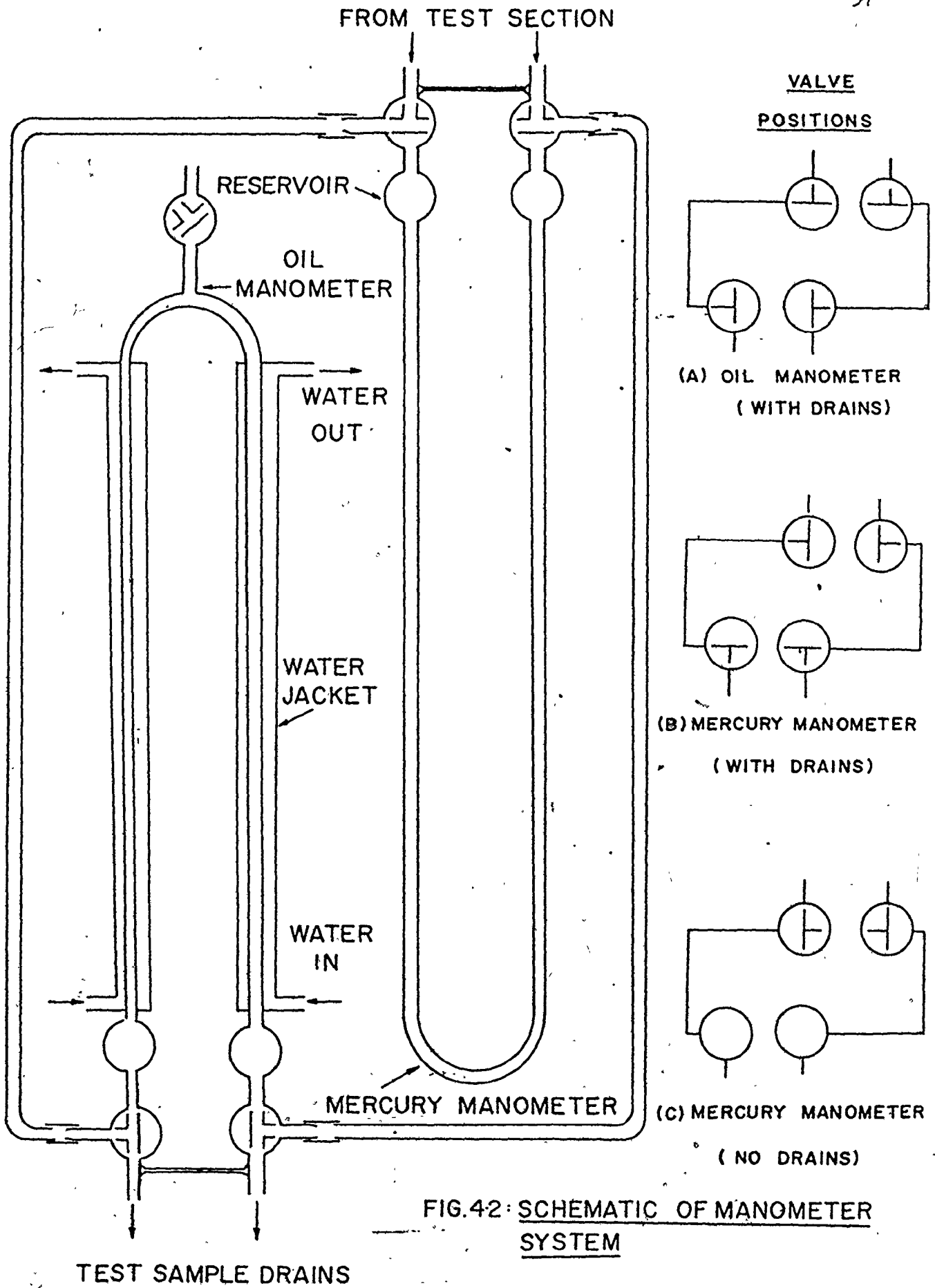
FIG. 4·2 SCHEMATIC OF MANOMETER SYSTEM

from the test section may be drained off for temperature
and rheological measurements. The oil manometer is also
fitted with a water jacket that ensures the temperature
of the oil to be identical to that of the fluid in the main
system. In order to avoid temperature gradient in the man-
ometer leads, a low flow rate was allowed to be discharged
through them before pressure measurements were taken. The
level in the U tubes is accurately measured using a cathe-
tometer.

(d)   The rheometer system

It is essential that the homogenity of the dis-
persion of the concentrated   aqueous polymer solution as
well as the degree of degradation, if any, be known through-
out the experiment. A simple but extremely reliable method
is to use a vertical tube (turbulent flow) rheometer.

Fig. 4.3 shows the construction of such an appar-
atus which works on the principle that the same volume of
fluid of different concentration of polymer additive takes
dissimilar times to pass through a narrow cross section
piping under identical pressure head provided in this case
by a 30 ft height of water. The volume of fluid is contained
in a funnel and drainage of this fluid through the narrow
2 mm capillary tubing is initiated by the opening of a $\frac{1}{2}$"
Ascoelectric solenoid valve at the exit end on the lower
floor level. The arrangement is shown in Plate III.

FIG. 4·3: SIMPLE GRAVITY RHEOMETER

LEVEL INDICATER

300 c.c. FUNNEL

2 mm. CAPILLARY TUBE

5/16" HOSE

3-WAY STOPCOCK

FLOOR 2

SOLENOID VALVE

FLOOR 1

S.W.L.
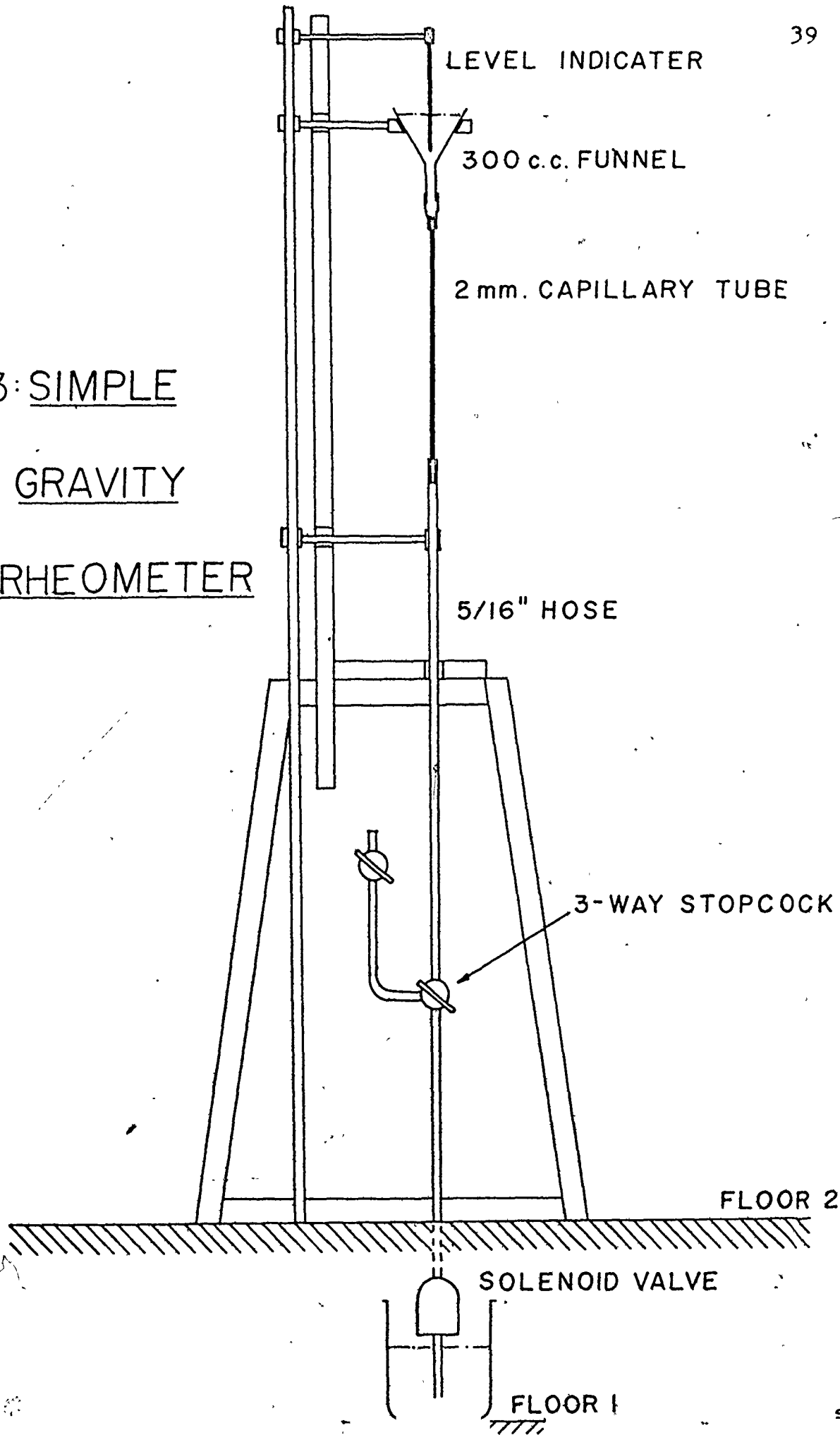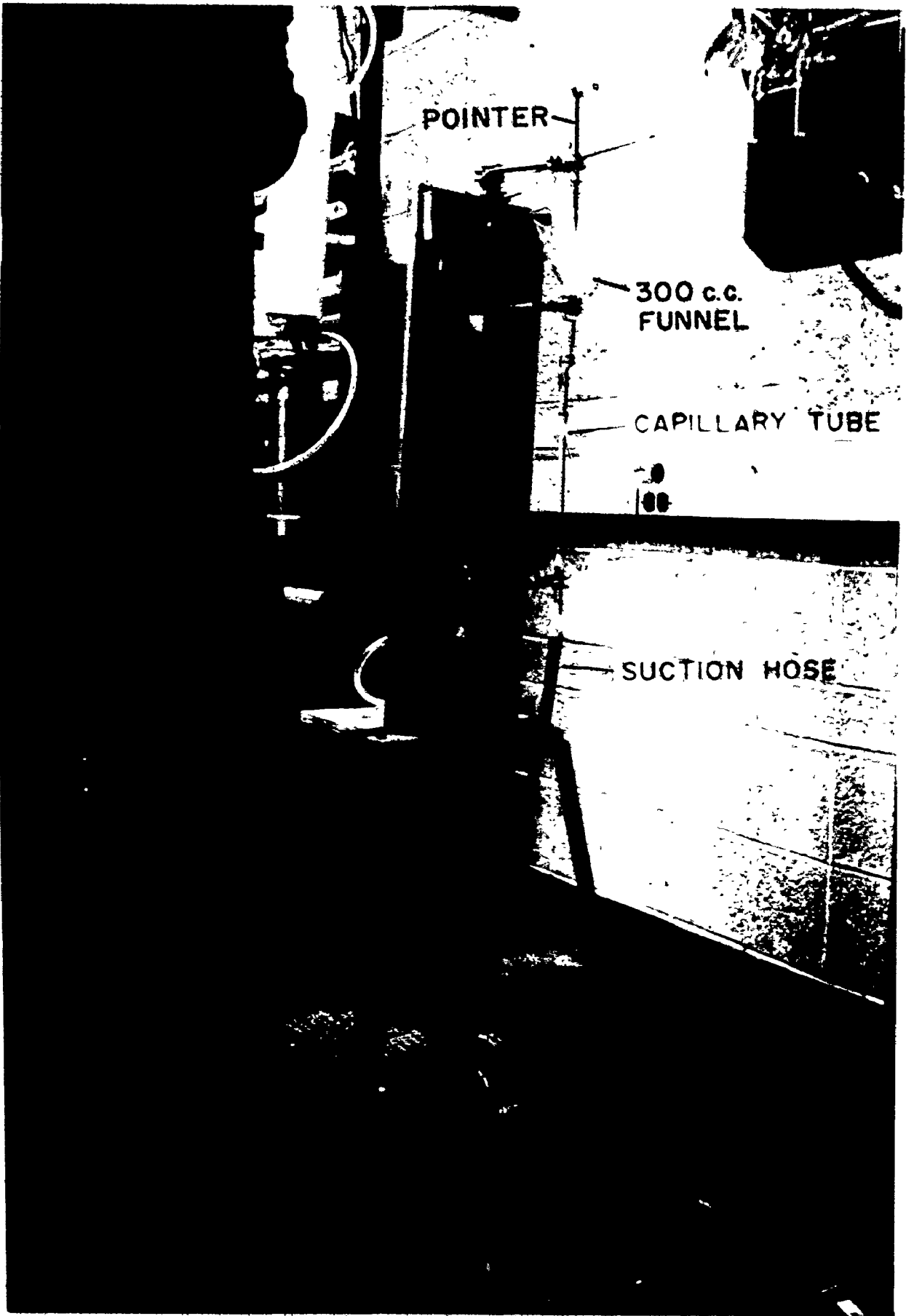
POINTER

300 c.c. FUNNEL

CAPILLARY TUBE

SUCTION HOSE

PLATE III: SIMPLE GRAVITY RHEOMETER

(e) The cylindrical bodies

Fig. 4.4 shows the type of cylindrical bodies used in this experiment. They are either aluminium or steel cylinders of specific gravity of respectively 2.7 and 7.8. The cylinder sections are either of an aspect ratio L/d equal to 1 or 2 and are connected to the desired lengths by screw threads at the ends of the sections.

Steel end caps are made by cutting spherical ball bearings into halves and welding them to a short section of cylinder. Cylinders are loosely attached to the metal screw cap in the apparatus using a nylon line and a swivel. This provides easy retrieval of the cylindrical bodies after they were used in the experiments.
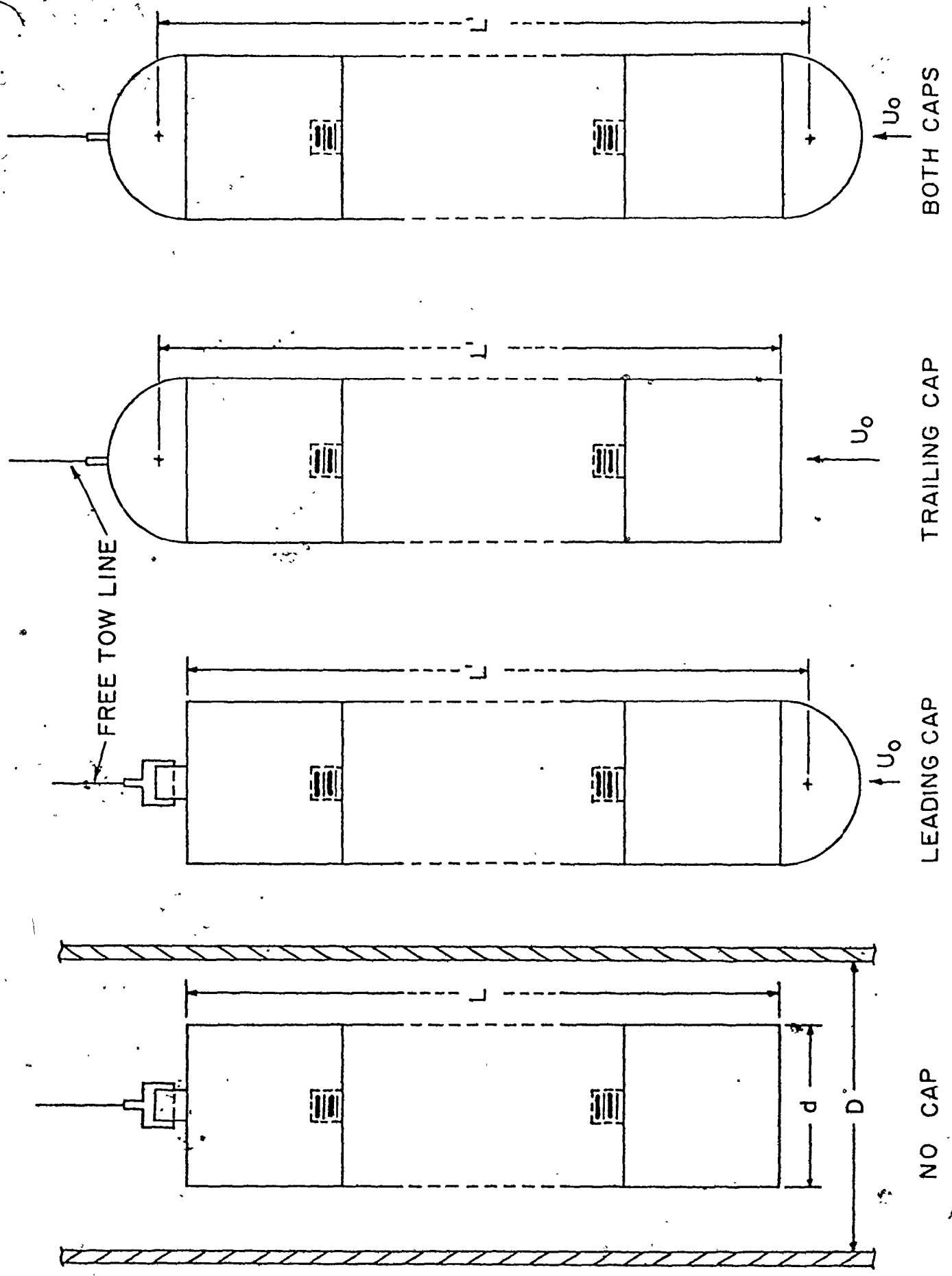
FIG. 4·4: ATTACHMENT OF CYLINDRICAL BODIES

V ' EXPERIMENTAL PROCEDURES

(a) Experiments using water as the carrier fluid

Experiments under this classification were done.
using both steel and aluminium cylinders but research on
the effects of the addition of end cap(s) were done only
with steel cylinders.

The procedure for blunt and modified cylindrical
bodies was the same. The flow of the water would be started
an hour prior to the actual testing to permit thermal stab-
ility. At the commencement of each experiment, some water
was drained through the manometer system from the test
section and its temperature was measured and recorded.

The surge tank level was adjusted so that it was
approximately half filled such that in the event of great
pressure variation, this level could move up or down the
tank without sucking air into the system or overflowing
into the air mains line.

The flow was then initiated and the flow rate
to maintain the cylindrical bodies hydrodynamically suspend-
ed in approximately the center of the test section was
recorded. Care had to be taken to ensure that the nylon
retrieval line was loose and that the bodies were not rot-
ating. The pressure drop across the test section was meas-
ured, depending on its magnitude, using either the oil or
the mercury filled manometer. Throughout such an experiment-
al run, a back pressure of 5 psi was applied to the test

section by slightly closing the control valve at the discharge (drain) pipe. Any fluctuation of the line pressure would be opposed by this applied back pressure. Another measurement was also made with no fluid flowing in the test section. This was necessary so that temperature variation during the course of the experiment may be accounted for.

The same procedure was repeated for all sizes and lengths of the steel and aluminium cylinders and for steel cylindrical bodies having end caps and also for the case of the test section without any bodies in it.

(b) Experiments with polymer solution

The polymer mixing procedure will first be described. The Reten 423 powder was pre-mixed with a small volume of methyl alcohol to produce a suspension that was added to a volume of water to give the required final concentration. This solution was allowed to stand for 24 hours during which time it was regularly stirred to allow for proper dispersion. The highly concentrated polymer solution was then pumped to the pressure vessel using the peristaltic pump and the vessel was charged to and maintained at about 70 psi using air pressure from the air mains line.

In operation, flow of the polymer and water solutions was adjusted using the control (gate) valves and the ratio of water to polymer from the vessel was controlled to conform to previously determined values (for the calibration,

see APPENDIX II). The arrival of the polymer at the test
section was easily noticable in that the hydrodynamically
suspended cylinder suddenly fell from its previously susp-
ended state with the nylon line loose showing that the drag
on the body was reduced. When this was observed, the flow
rate was increased to again suspend the cylinder and the
final pressure drop and flow rate was recorded as before.
A sample of the solution from the test section was obtained
by draining through the manometer lines and the sample was
then tested using the rheometer to determine the validity
of its concentration as compared to a previously obtained
calibration curve (see APPENDIX III).

The same procedure was repeated for all lengths
and diameters of the steel cylindrical bodies. The final
results are tabulated and shown in the APPENDIX.

(c) Rheometer Tests

The sample of polymer solution collected from
the test section in a procedure described in the previous
section has to be tested to establish its true concentrat-
ion. A small quantity of the sample (250 c.c.) was intro-
duced into the funnel and the time for this volume to drain
through the small bore tubing was recorded using a stop
watch. This measurement corresponds to the time between the
opening of the solenoid valve (activated by the foot operat-
ed switch) and the time for the level of the fluid to reach
the pointer (the position of the fluid before the 250 c.c.

volume was being introduced). The apparatus was flushed with a small sample of the fluid to be tested prior to an actual test to ensure that the particular sample fluid occupied the whole of the capillary test section.

The experiment was repeated at least twice to ensure reproducibility of the time measurements and if a difference of more than 0.2 seconds existed, the test procedure was repeated until good reproducibility was attained. The apparatus was cleansed after each series of test so that it may be ready for use for the next test.

VI   DISCUSSION OF RESULTS

The results obtained from the experiments on hydrodynamic suspension of cylinders will be discussed in three sections under the following headings : -

(1) The behaviour of cylinders of high density such as steel, and the effect of a change of density of the material of the cylinder.

(2) The effect of dilute aqueous polymer (Polyacryalmide) solutions as the carrier fluid compared with water and the possible variation with a change of its concentration in the solution.

(3) The effects of modifying the steel cylinders by the addition of end cap(s).

To make such comparisons, the results presented in this chapter are based principally on the length and diameter effects on some of the more pertinent flow parameters such as :

(a) The total pressure drop across the test section with or without the cylinders.

(b) The average flow velocities in the free stream or in the annulus between the cylinder and the pipe wall (i.e. local velocities).

(c) The "kinetic energy" associated with the flow as indicated by the square of the velocity term.

(d) The average drag coefficients based on the local and
free stream velocities.

(e) The hydraulic power dissipation for the flow in the
test section based on the flow rate and total pressure
drop across the test section.

However, before beginning the discussion, a not
so obvious aspect of the present experiment must be pointed
out. It must be borne in mind, when results are compared,
that the data were obtained for flows at different velocit-
ies and hence different Reynolds number. This is particul-
arly important for the case of cylindrical bodies of diff-
erent densities. The variation of the velocity and its
implications will be discussed in more details in this
chapter.

SECTION I : Steel cylinders and density effects

For any experiments', it is desirable to be able
to make comparisions with data from other sources, and in
this case, the work of McNown & Newlin[18] is used.

Fig. 6.1 is a plot of C_d^* against Reynolds number
and includes a limiting curve of Stokean flow which has
the form (after McNown & Newlin),

$$C_d^* = 24 \, / \, Re \tag{6.1}$$

The full lines which extend across the plot are actually
based on two relationships. The portion of the curves for
Reynolds number up to 400 which may be described by,

$$C_d^* = \frac{40}{Re} (\, 1 - \frac{d}{D} \,)^{-1.5} \tag{6.2}$$

and the portion which is practically "flat" extending bet-
ween Reynolds number of 10,000 and 1000,000 is described by

$$C_d^* = (\frac{d/D}{1 - (d/D)^2})^2 \tag{6.3}$$

The gap between the two portions of the curves are inter-
polated to give smooth curves across the transition zone.

Essentially, this plot shows that the present
experiments were done at such high Reynolds numbers that
the approximation equation of Oseen, (for Re up to 5)

$$C_d^* = (\frac{24}{Re}) (\, 1 + \frac{3}{16} \, Re \,) \tag{6.4}$$

LIMIT OF
STOKE'S RANGE

$c_d^* = 24/Re_d$.

c_d^*

10^3

10^2

10^1

10^0

10^{-1}

0.98

0.9

$d/D = 0.8$

0.6

0.4

0.0

$2 \triangle \triangle 3$

$6 \triangle 9^{12}$

$2 \square 3^{6} \square^{9} \square^{12}$

$2 \bigcirc 3^{6} \bigcirc^{12}$

$2 \diamondsuit 3^{6} \diamondsuit^{12}$

LEGEND

× △	$d/D = 0.864$
□	$d/D = 0.731$
○	$d/D = 0.624$
◇	$d/D = 0.434$

× serials indicate values of L/d
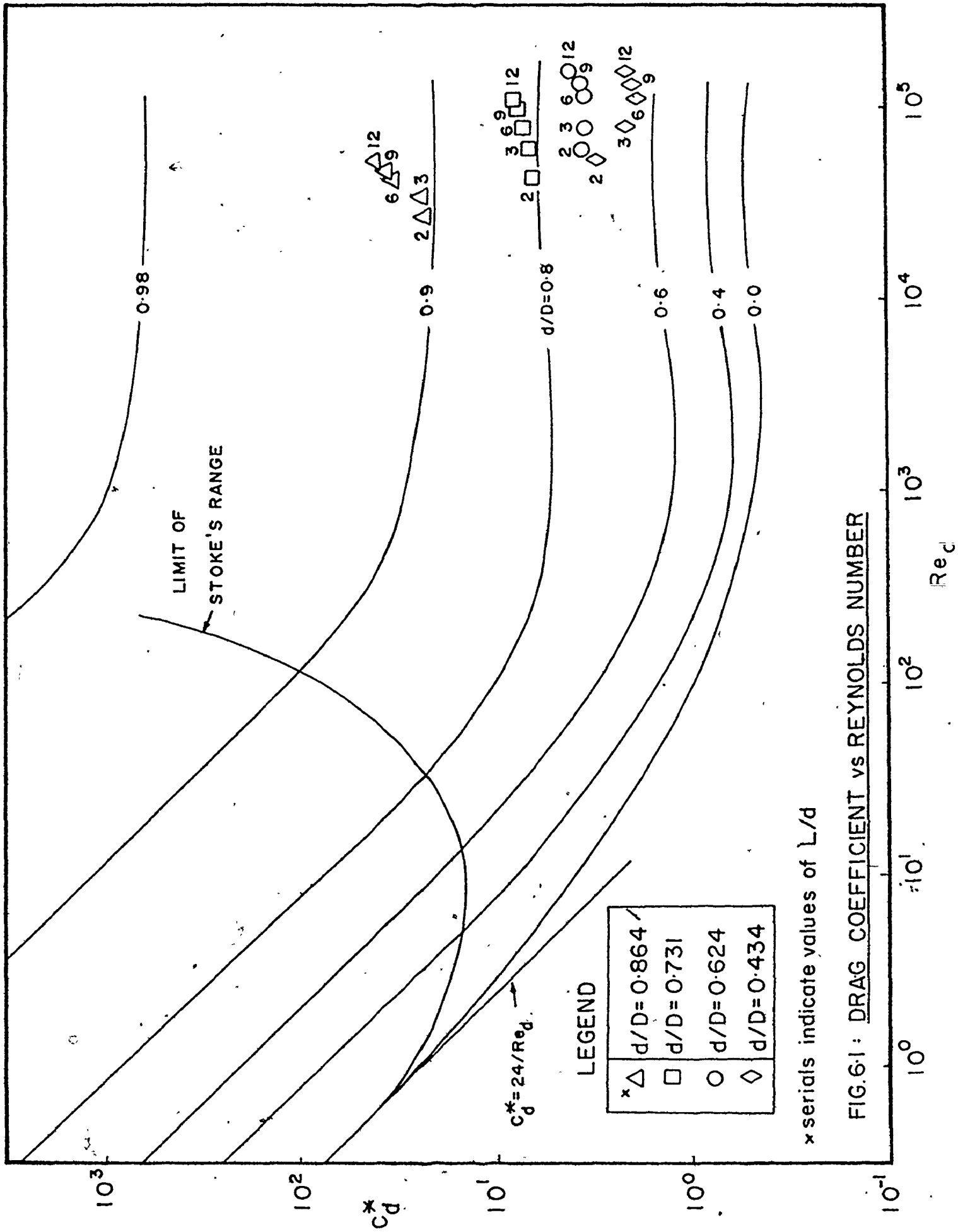
FIG.6·1 : <u>DRAG COEFFICIENT vs REYNOLDS NUMBER</u>

Re_d

10^0 10^1 10^2 10^3 10^4 10^5

or that of Abraham, (for Re up to 5000)

$$C_d^* = (\frac{24}{Re}) \, Re \rightarrow 0 \quad (1 + \frac{9.06}{Re^{0.5}})^2 \qquad (6.5)$$

do not apply.

The plot does indicate two characteristics.
First, that there is an obvious length effect particularly
at high diameter ratios. The fact that there is a high
total pressure drop associated with a high length to dia-
meter ratio indicates a greater contribution of the viscous
shear effect on the total pressure loss if a large circum-
ferential area is exposed to the flow.

The plot also show that there is little change
of C_d^* With the change of the aspect ratio L/d, but on the
contrary, the change of flow velocity required for the
cylinders is greatly affected by a variation of the L/d
ratio, particularly at low diameter ratios as Fig. 6.2
indicates.

There is, for instance, a 180% increase of the
required velocity at a diameter ratio of 0.624 for a
change of aspect ratio from 3 to 12. This means that the
skin friction at the pipe wall is not a major factor
affecting the pressure drop because there is also an
increase of as much as 400% in the circumferential area.
However, at a diameter ratio of 0.864, there is a 250% change
of C_d^* with the same variation of aspect ratio, but then,

FIG. 6·2 : PRESSURE vs VELOCITY

there is a total increase of 16 times in the surface area. The net effect is a reduction in the significance of the contribution by the base pressures on long cylinders with large diameter ratios. Indeed, for a case like this, the flow pattern is that of a flow in an annuluar space. Moreover, the results also suggest that a decrease of velocity is related to an increase of drag. This is thought to be associated with the nature of the boundary layer for the particular flow regime.

If curves are generated for the present diameter ratios using eqn. 6.3, it may be observed that there is a large deviation of the data from those curves for low diameter ratio. Indeed, McNown & Newlin themselves have found that eqn. 6.3 is good only for sphere diameter ratios greater than about 0.775. With cylinders, instead of spheres, it seems that the discrepancy between the data and eqn. 6.3 is so large that it is hardly applicable to the present analysis even if the diameter ratios are high. It must be said, however, that eqn. 6.3 was introduced for the flow of air past a spherical body and that it was not intended to describe the flow of a viscous fluid past a cylindrical body.

Returning to the pressure-velocity plot of Fig. 6.2, if the variation of pressure with velocity follows a smooth curve through the origin, then, for low diameter ratios, it seems that the data for aluminium and steel

cylinders almost follow the same curves. Indeed, the two separate curves suggest a continuous variation of pressure with velocity independent of the density of the material.

Perhaps, this suggests the existence of a small wall effects at low diameter ratios or that (in terms of a parameter so often used in sedimentation problems), the voidness ratio is large in this case. In fact, eqn. 6.3 suggest a form of this ratio because $(d/D)^2$ to $1 - (d/D)^2$ is the ratio of the size of the cylinder to the annular spacing between it and the pipe wall. This equation, however, fails to include the wall effects explicitly and in essence, holds only in a regime where the wall effects are negligible.

Fig. 6.3 shows the variation of pressure with diameter ratios. It shows that the variation of the pressure per length of the cylinder is almost constant regardless of the aspect ratio and is only different for different sizes of the cylinders. This of course means that at diameter ratios of 3 or more, the end effects are a minor contribution and as such, the cylinders may be regarded as infinite rods extending from the test section to the far field downstream. Such a postulation supports previous observations and will be discussed further in section III of this chapter.

Perhaps, it is the plot of Fig. 6.3 which suggests that the diameter and the density effects should be included in such a plot. Indeed, if the average pressure per length

FIG.6.3 : PRESSURE PER LENGTH vs AVERAGE VELOCITY

AVERAGE VALUE : $\Delta P_m/L$

mat'l \ d/D	0.864 0.731	0.624 0.434
STEEL	△ □ (0.44)(0.35)	◇ ○ (0.23)(0.3)
ALUMINIUM	▲ (0.11)	◓ (0.09)(.075) —

SERIALS INDICATE INCREASING VALUES OF L/d

$\Delta P_m/L$ (CM. HG.)/CM.

U_o (CM/SEC)
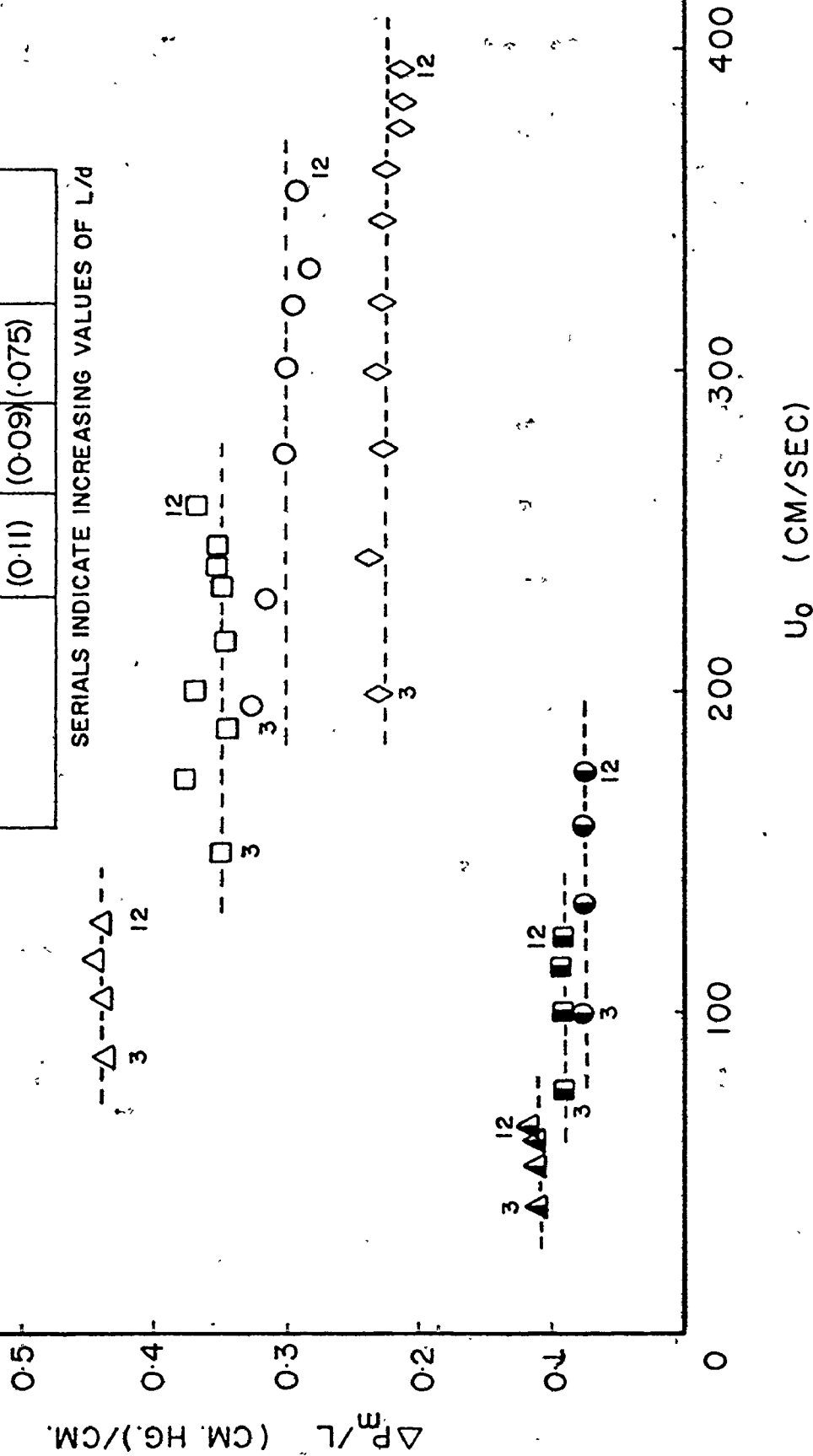
values in the plot are divided by the density and the diameter ratios, an average value of 0.987 and 0.987 psi/ft is obtained for steel and aluminium cylinders respectively. Even though this rather surprising result is obtained for only two materials, it does help to indicate the usefulness of correlating data on a per length basis – something which is not indicated from the Buckingham's Dimensional Analysis. This has a theoretical basis since eqn. 3.25 suggest that the pressure differential varies only with the length, diameter and the density.

In fact, if the present results are substantiated through further experimentation, then, a relationship of the form,

$$\frac{\triangle P_m}{g L \left(\frac{d}{D}\right) \left(\sigma - \rho\right)} \doteq 1 \qquad (6.6)$$

exists and a comparison with eqn. 3.25 gives the ratio

$$\frac{\triangle P_o}{\triangle P_m} = \left(1 - \frac{d}{D}\right) \qquad (6.7)$$

and as such, give the contribution of the wall friction to the total pressure loss and shows that the percentage loss of pressure head from skin friction is proportional to the voidness ratio of the cylinder-pipe system.

If the drag coefficients are plotted against the aspect ratio L/d as in Fig. 6.4 it seems that c_d^*
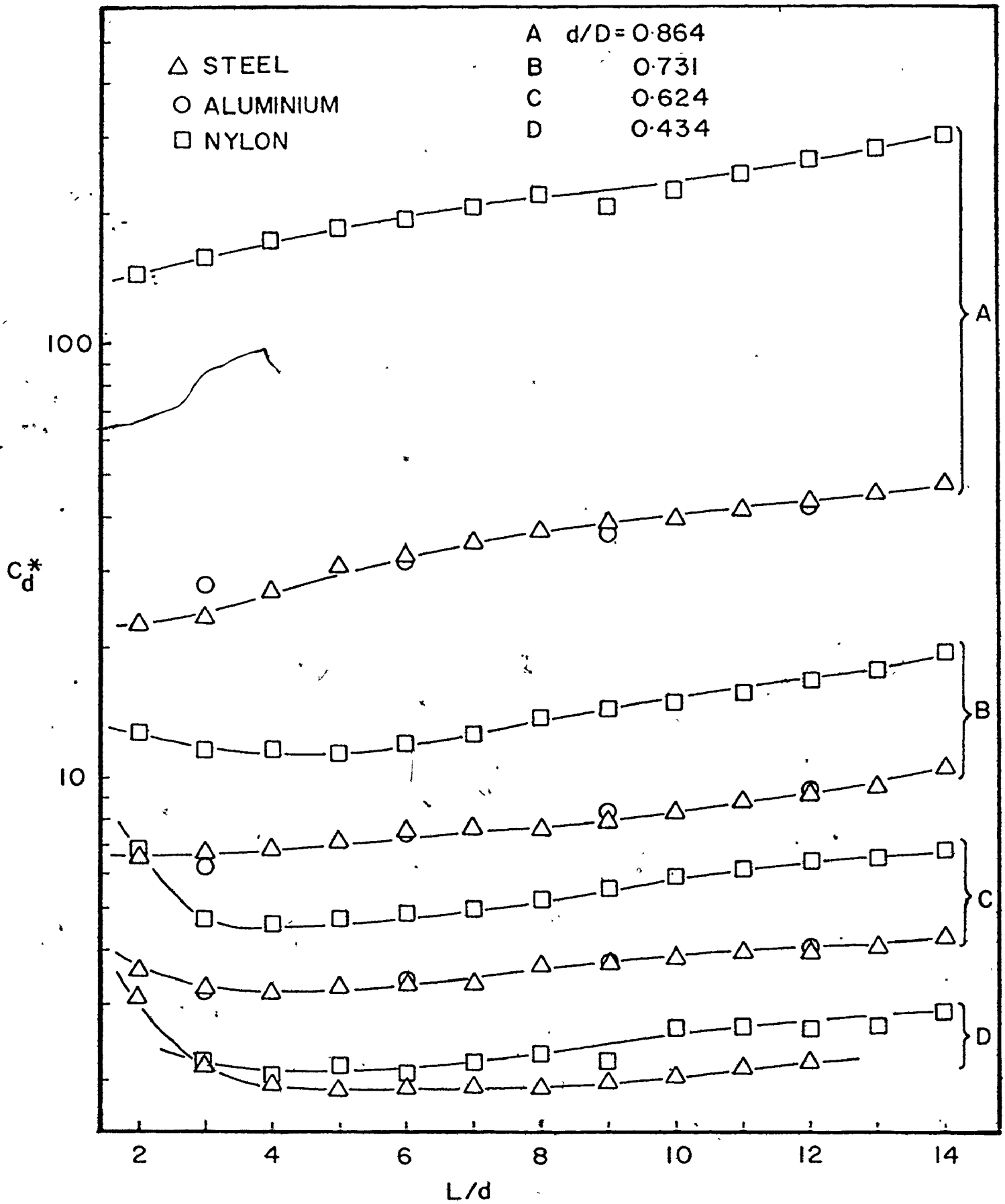
FIG. 6·4 : DRAG COEFFICIENT vs ASPECT RATIO

approaches a constant value at high L/d ratios and that
the high C_d^* values at low L/d values indicate a large end
effect.

Another interesting aspect indicated by this plot
is that there is little difference between the drag coeff-
icient for aluminium or steel cylinders which is, however,
not in agreement with the values for the nylon cylinders,
particularly for those at high L/d ratios. This result may
be misleading, but since,

$$C_d^* = \text{Drag} / \text{(area) (density) (velocity)}^2 \quad (6.8)$$

and the velocity for nylon cylinders are much less than
for steel and aluminium cylinders, the total drag force
may effectively be the same for all the materials consid-
ered.

The same argument applies to the plot of C_d^*
against L/d given in Fig. 6.5 which again shows that for
aspect ratios close to 14 or higher, the end effects are
practically invariant and that the only variation of C_d is
associated with the change of diameter ratios.

To eliminate the velocity effect, a plot of eqn.
3.26 is shown in Fig. 6.6. Here, the pressure function,
which is proportional to the drag force term in eqn. 6.8
is plotted against the diameter ratios whose variation is
related to the change of the velocity if all other effects
are held constant. It must also be said that the pressure

FIG.65 DRAG COEFFICIENT PER ASPECT RATIO vs ASPECT RATIO

MAT'L	SYM	A	B	C	D
NYLON	○	·904	·769	·642	·452
ALUMINIUM	△	·863	754	·617	—
STEEL	□	864	·731	·623	434

$\dfrac{C_d^*}{(L/d)}$

L/d

FIG.6·6: PRESSURE FUNCTION vs DIAMETER RATIO
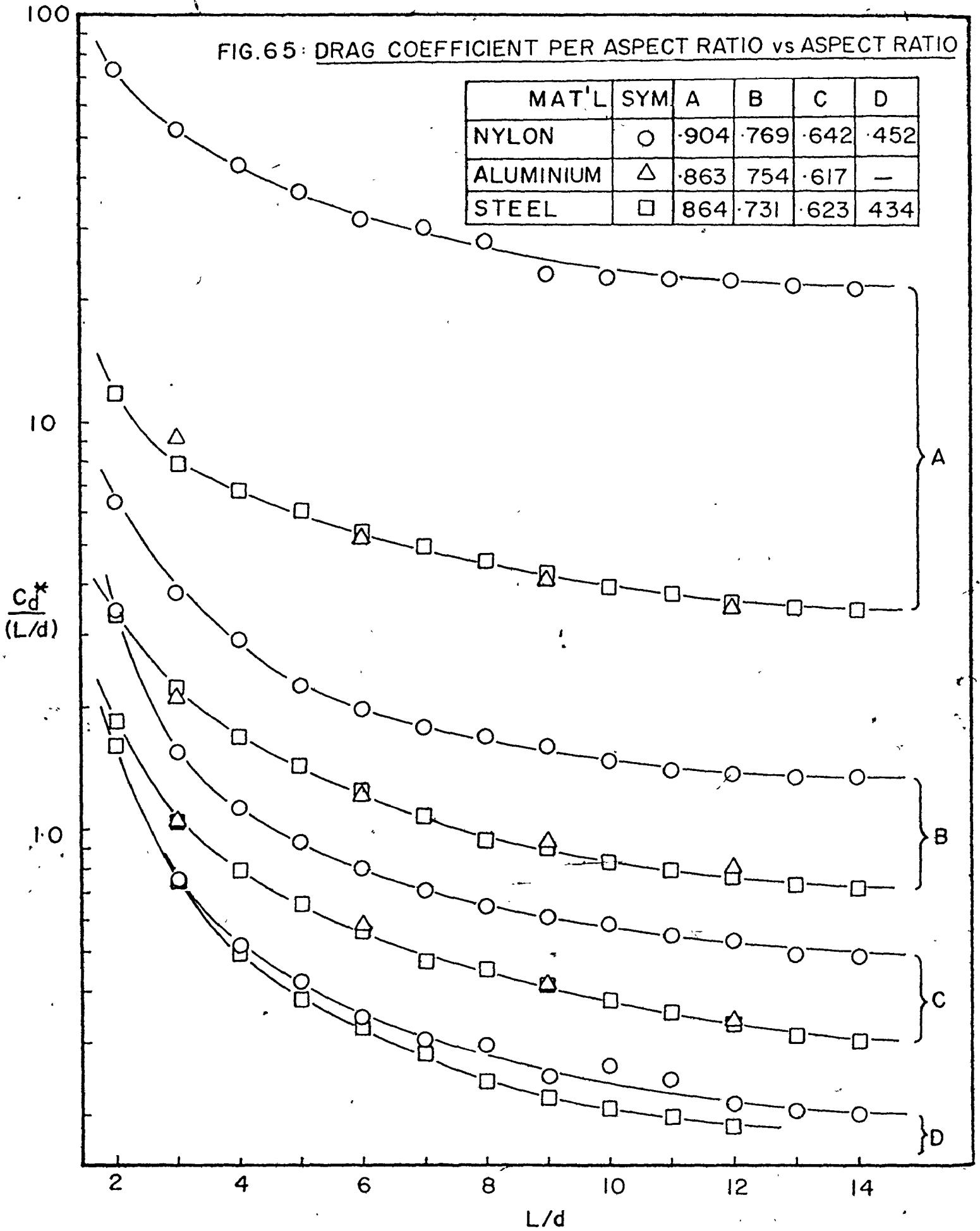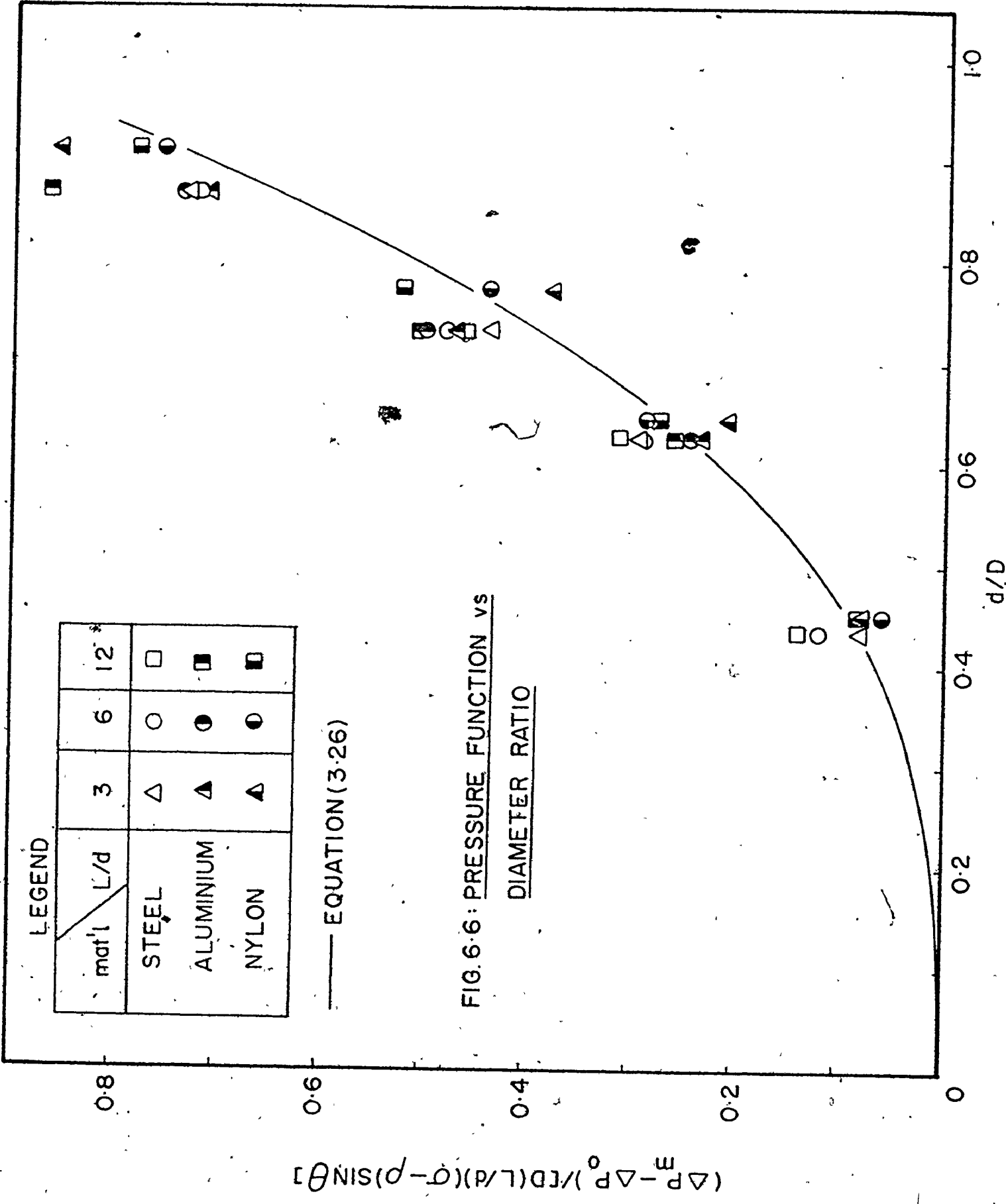
function represented by the abscissa, can be broken down
into the following form,

$$\Delta P_m - \Delta P_o = L \ (\ \sigma - \rho \ ) \ (\ \frac{d}{D} \ )^2 \qquad (3.25)$$

which is the relationship for the full curve in the plot.
A careful observation shows that there is a random scatter
of the data points and this is believed to have been
caused by errors in experimental measurements. Such a non-
systematic variation of the pressure function with diameter
ratios suggests the validity of using the parameters in
the form of eqn. 3.25 and that the wall effects are not
affecting results at high d/D ratios.

In fact, if the pressure function data are cor-
related by plotting the same parameters as in Fig. 6.6 on
a logarithmatic scale, we may obtain the relationship shown
in Fig. 6.7.

In general, the equations obtained from Fig. 6.7
show that an increasing length decreases the magnitude of
the power term, while the decrease of density gives a
decrease of the constant. This length effect can be explained
on the basis that the base pressure varies with the area
of the base surface so that an increase of length of the
cylinder may be considered as equivalent to a reduction
of the end effects as has been shown earlier. There is no
such variation associated with a change of density, indeed

FIG. 6·7: PRESSURE FUNCTION vs DIAMETER RATIO

$$\frac{(\Delta P_m - \Delta P_0)}{(L/d)D(\sigma - \rho)\sin\theta} = C'\left(\frac{d}{D}\right)^n$$

SYM	MAT'L	L/d	C'	n
◇	STEEL	3 (THEORETICAL)	1·00	3·00
□	STEEL	3	1·04	2·82
△	STEEL	6	1·09	2·66
○	STEEL	12	1·13	2·52
⬠	NYLON	3	0·77	2·95
⬡	ALUMINIUM	3	1·00	2·93

vertical axis: $(\Delta P_m - \Delta P_0)/[(L/d)D(\sigma - \rho)\sin\theta]$

horizontal axis: d/D
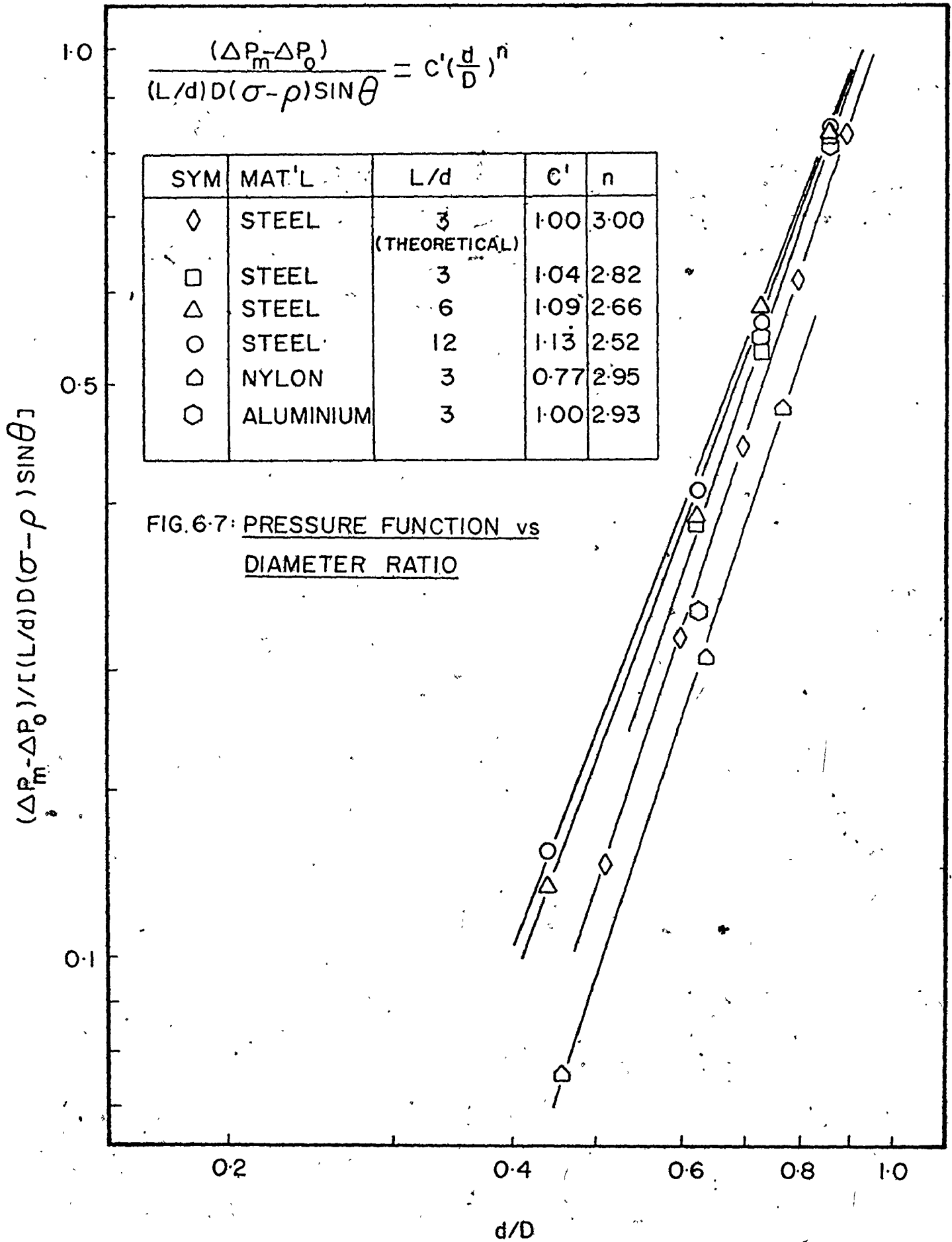
the variation is small enough, particularly with steel and aluminium cylinders, that they may be said to be invariant with density.

Fig. 6.8 shows the velocity function variation with diameter ratios. It must first be pointed out that the density effect is eliminated by having it in the denominator of the velocity function. This means that the abscissa represents some "kinetic energy" variation with size changes of the cylinders irrespective of the cylinder material.

If the velocity function is differentiated with respect to d/D and set to zero, the location of the maximum for the velocity function may be found to occur at d/D of 0.447. If the value of the velocity function is taken at this particular diameter ratio for a steel cylinder, we can obtain,

$$C_d \doteq 5 \left(\frac{d}{D} \right) \left(1 - \left(\frac{d}{D} \right)^2 \right)^2 \qquad (6.9)$$

Furthermore, at this value of d/D, C_d has a maximum of 1.45.

Indeed, if the drag coefficient based on free stream velocity is used in a form similar to eqn. 6.9, we have,

$$C_d^* = \left(\frac{2 L g}{U_1^2} \right) \left(\frac{\sigma - \rho}{\rho} \right) \left(1 - \left(\frac{d}{D} \right)^2 \right) \qquad (6.10)$$

Which may be compared to eqn. 6.3 proposed by McNown & Newlin that has the form,

FIG.6·8: VELOCITY FUNCTION vs DIAMETER RATIO
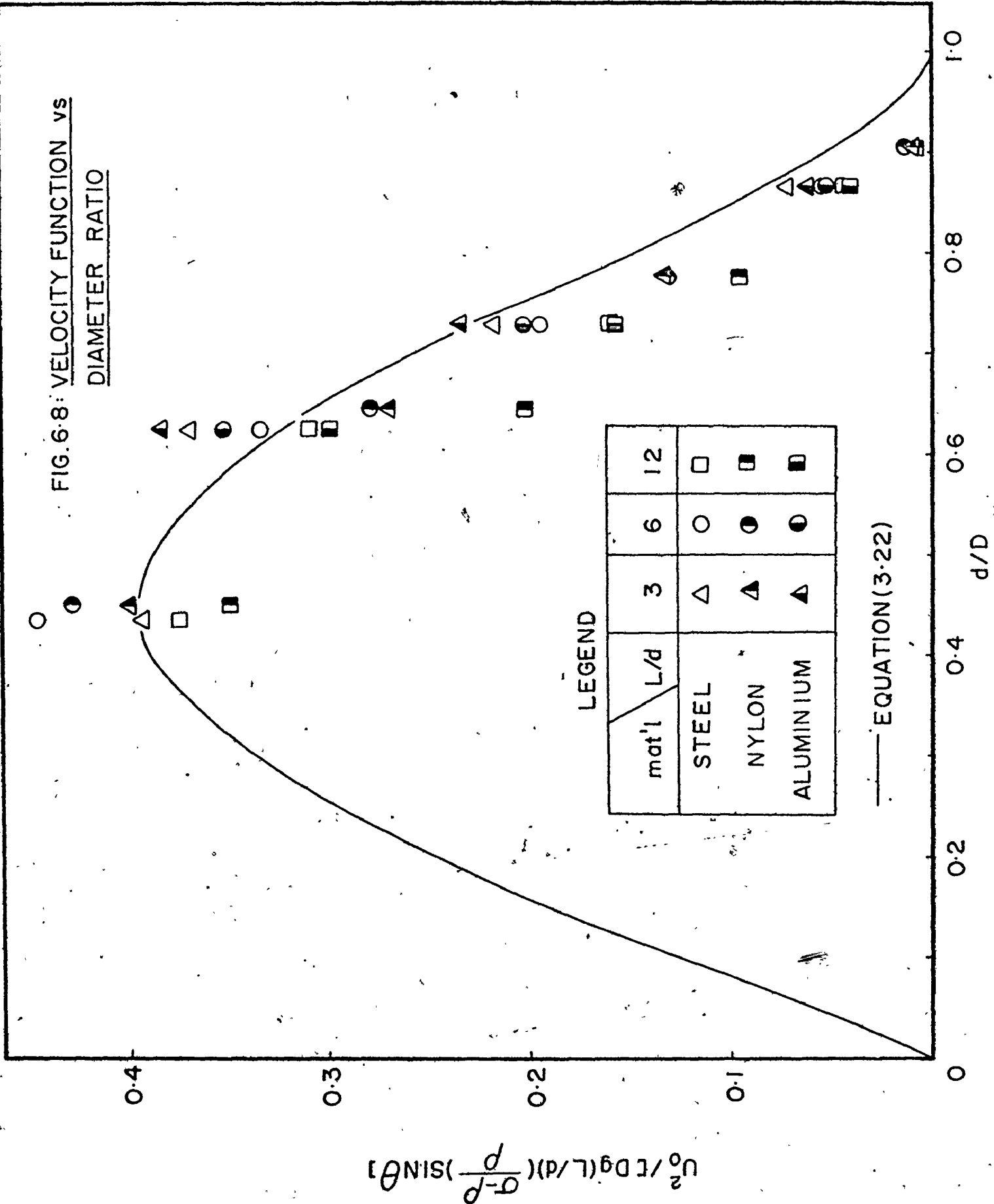
LEGEND

mat'l	L/d	3	6	12
STEEL		△	○	□
NYLON		◭	◐	◧
ALUMINIUM		◭	◐	◧

—— EQUATION (3·22)

$U_o^2 / [Dg(L/d)(\frac{\sigma - \rho}{\rho})SIN\theta]$

d/D

$$c_d^* = (\frac{d}{D} / 1 - (\frac{d}{D})^2)^2 \qquad\qquad (6.3)$$

As may be seen, eqn. 6.3 failed to account for the variation of density, viscosity as well as the flow velocity involved, so that perhaps the c_d^* relationship should involve more parameters such as,

$$c_d^* = f_1 (Re , L , \frac{d}{D} , \rho , \sigma - \rho) \qquad (6.11)$$

Finally, if the hydraulic "energy" is considered, a plot such as Fig. 6.9 may be made. Note that the density effect is eliminated by dividing the product of the pressure and flow rate by the specific gravity of the material. Yet, the plot shows that the hydraulic power requirement is greater for steel cylinders than for aluminium ones and in fact it increases as the L/d ratio increases. This can only be explained on the basis of a velocity difference since the pressure-flow rate product includes a velocity effect implicitly in the flow rate term, but the percentage variation of the pressure term does not occur at the same rate as the percentage variation of the velocity as a plot such as Fig. 6.2 indicates.

There is also a size effect present in this plot, and it seems to show a maximum power requirement at a diameter ratio of about 0.7 whereas (as will be shown later) the velocity attains a maximum at about d/D of 0.5. This can only result from a non-linear relationship between the pressure and the velocity terms.

FIG. 6·9: HYDRAULIC POWER INPUT vs DIAMETER RATIO

SECTION II : The effect of Polymer Additives

The experiments done in this category involve
blunt steel cylinders only and no investigation based on
density variation or modification of body shapes using end
cap(s) was done even though a comparison of the present
results with those of Aly[30] on nylon cylinders may be
possible,

The effect of polymer additives on the flow
system may be observed even without the presence of the
cylinders since the skin friction and therefore the press-
ure drop decreases with the presence of polymer additives
in a pipe flow. A similar effect on the measurements of
of the rotameters will be discussed later in the Appendix.

It was found that the percentage pressure drop
decreases as the concentration of the polymer is increased
from say 20 wppm (weight parts per million) to 100 wppm
and it is envisaged that this pressure drop will tend
towards a maximum and then decline as the concentration is
further increased to more than 100 wppm as Fig. 6.10
indicates. In fact, the skin friction factor may also be
plotted against the Reynolds number as in Fig. 6.11 using
the following definition for the skin friction factor,

$$\frac{\Delta P_o}{\rho} \left(\frac{g_c}{g} \right) = f_2 \left(\frac{L}{D} \right) \left(\frac{U_o^2}{2g} \right) \qquad (6.12)$$

FIG. 6·10: PRESSURE vs FLOW RATE
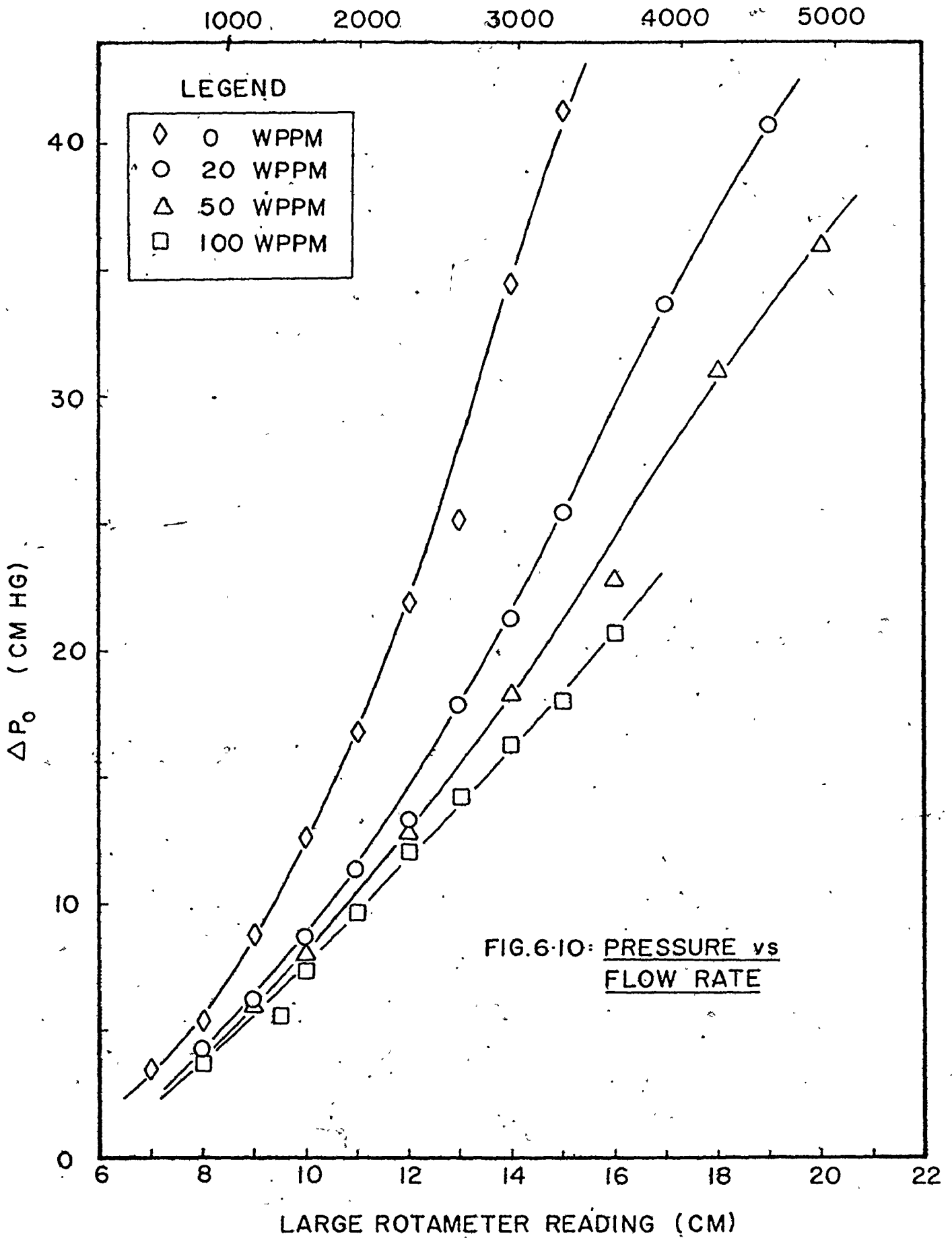
FIG. 6·11: MOODY PLOT,

5·122 CM. PEXIGLASS TUBE

$f = 0.3164 \, Re^{-0.25}$

$f = 64/Re$

$f = 5.6 \, Re^{-0.67}$, CASTRO ET AL

$f = 1.68 \, Re^{-0.55}$, VIRK ET AL

$f = Re^{-0.5}$, GILES ET AL

MAXIMUM DRAG
REDUCTION ASYMPTOTES
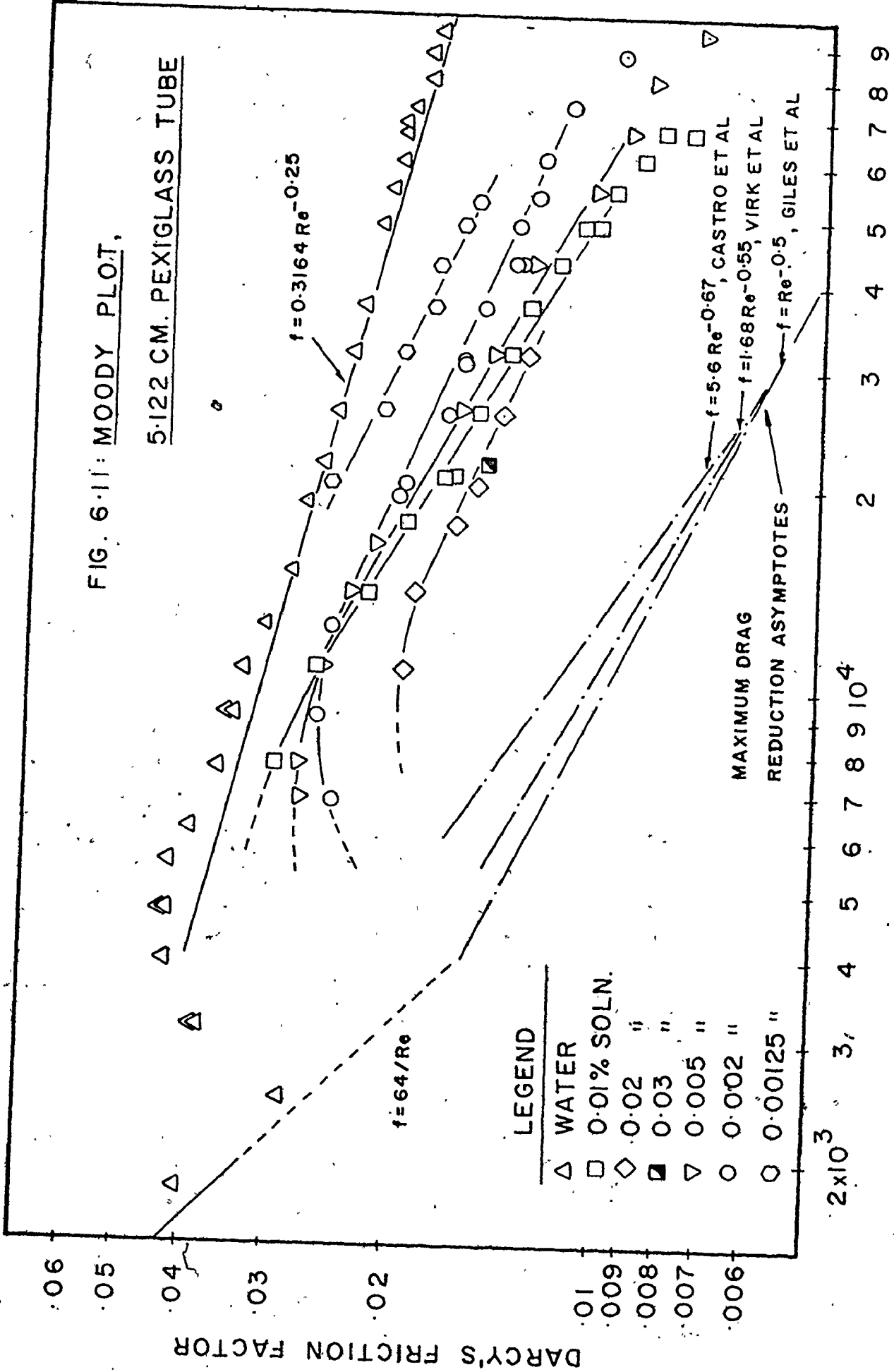
LEGEND

△	WATER
□	0·01% SOLN.
◇	0·02 "
◼	0·03 "
▷	0·005 "
⊙	0·002 "
○	0·00125 "

DARCY'S FRICTION FACTOR

·06
·05
·04
·03
·02
·010
·009
·008
·007
·006

2×10^3 3   4   5   6 7 8 9 10^4 2   3   4   5   6   7   8   9

REYNOLD'S NUMBER

The plot shows that the results of the present experiments using water closely resembles those of the Blausius equation for a smooth pipe which has the form,

$$f = 0.3164 \ (\ Re \ )^{-0.25} \qquad (6.13)$$

With the presence of a polymer additive at concentrations as low as 12.5 or 20 wppm, there is a drastic drop in the friction factor. But this drop decreases at a slower rate at higher concentrations of the order of 200 to 300 wppm. Note that this plot gives the polymer effects in the regime defined by the Reynolds number of between 7,000 to about 100,000 and for all intents and purposes, covers the entire range of flow for all the tests done in the present work.

It is also possible to compare the results of other researchers. The maximum drag asymptote of three other sources are shown in Fig. 6.11. In the regime that these three equations defines, the agreement among the equations is good and certainly the equation of Giles et al,

$$f = (\ Re \ )^{-0.5} \qquad (6.14)$$

seems to be of the simplest form as well as being the lowest friction factor asymptotes.

With an increase of the size of the pipe, the friction factor seem to tend more towards these asymptotes. Indeed, if the results of a similar experiment done by the

author on a vertical tube rheometer having a 0.16 cm. diameter (as compared to 5.1 cm. for the diameter of the test section used in this experiment) were plotted on the same graph, they lie closer to the asymptotes. This could only be explained on the basis that the boundary layer effects are much greater in a small tube than in a large one so that the percentage pressure loss observed in a pipe is equivalent to that of a smooth tube. The implication is that a larger "tube" (i.e. a pipe) has the same skin friction property as a smooth tube because of this boundary layer effect. It is then not surprising to see the present results tend towards the smooth pipe curve of eqn. 6.13.

If the drag coefficients for steel cylinders are plotted against the aspect ratio L/d as in Fig. 6.12, the curves resembles that of a density variation plot of Fig. 6.4. It seems that at a high diameter ratio, the presence of any concentration of polymer has much the same effectiveness in drag reduction and that there is only a slight advantage gained by increasing the concentration. This may suggest that at high diameter ratios, the narrow annular spacing restricts the flow so much that the velocity at this region is greatly accerlated and a fully turbulent flow exists that is not much affected by changes within the viscous layer. The increasingly high C_d^* value generally associated with an increase of diameter ratio
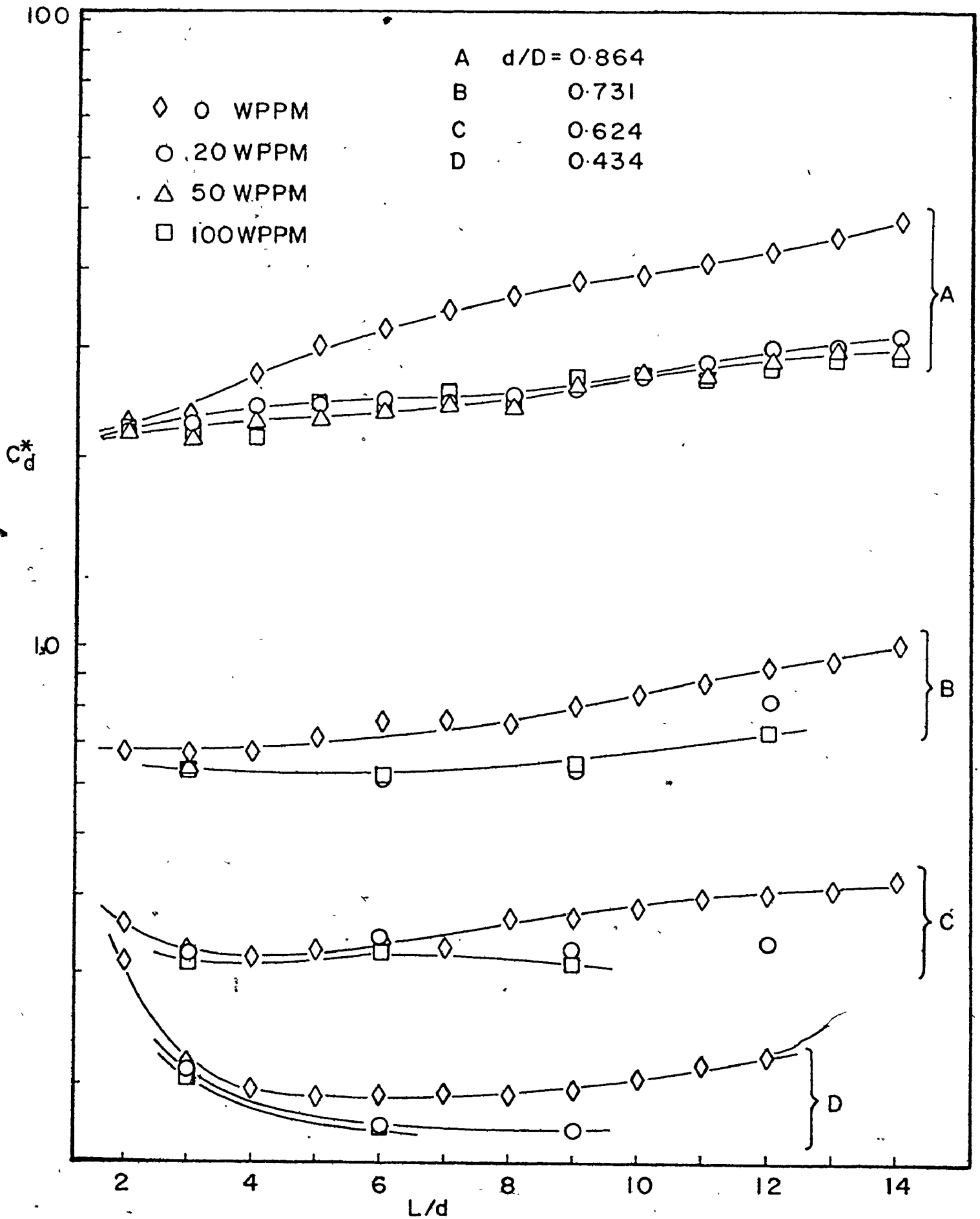
FIG.6·12: DRAG COEFFICIENT vs ASPECT RATIO

may be due to an increase of shear surface notwithstanding
a parallel increase of the base area on which the base
pressure act.

By comparison with Fig. 6.4, an increase of
density has the same effect as the addition of the polymer
and suggests that a polymer solution. like a system with
a heavier cylinder, increases the flow velocity required
to hydrodynamically suspend the cylinders. It also means
that the increased axial flow minimizes the effect of the
tangential velocity component which is instrumental in
causing rotation of the fluid and the cylinder.

The length effect may be minimised if $C_d^* / (L/d)$
is plotted against L/d and show that the curves slopes
rapidly towards a constant value for a given d/D as Fig.
6.13 indicates.

The effects of the polymer concentration is best
protrayed by a plot of "drag reduction" against polymer
concentraton as shown in Fig. 6.14. Such a plot does
suggest the existence of maximum "drag reduction" at around
20 to 40 wppm depending on the aspect ratio. Perhaps, the
plot also shows a greater drag reduction which is as high
as 35% at the high L/d ratio of 12. But since at these high
L/d ratios, the end effects is minimised particularly for
cylinders of high diameter ratios that were used (see pre-
vious discussion). This is so since the contribution of
the base pressure loss is less than that for viscous loss

FIG. 6·13 DRAG COEFFICIENT PER ASPECT RATIO vs ASPECT RATIO
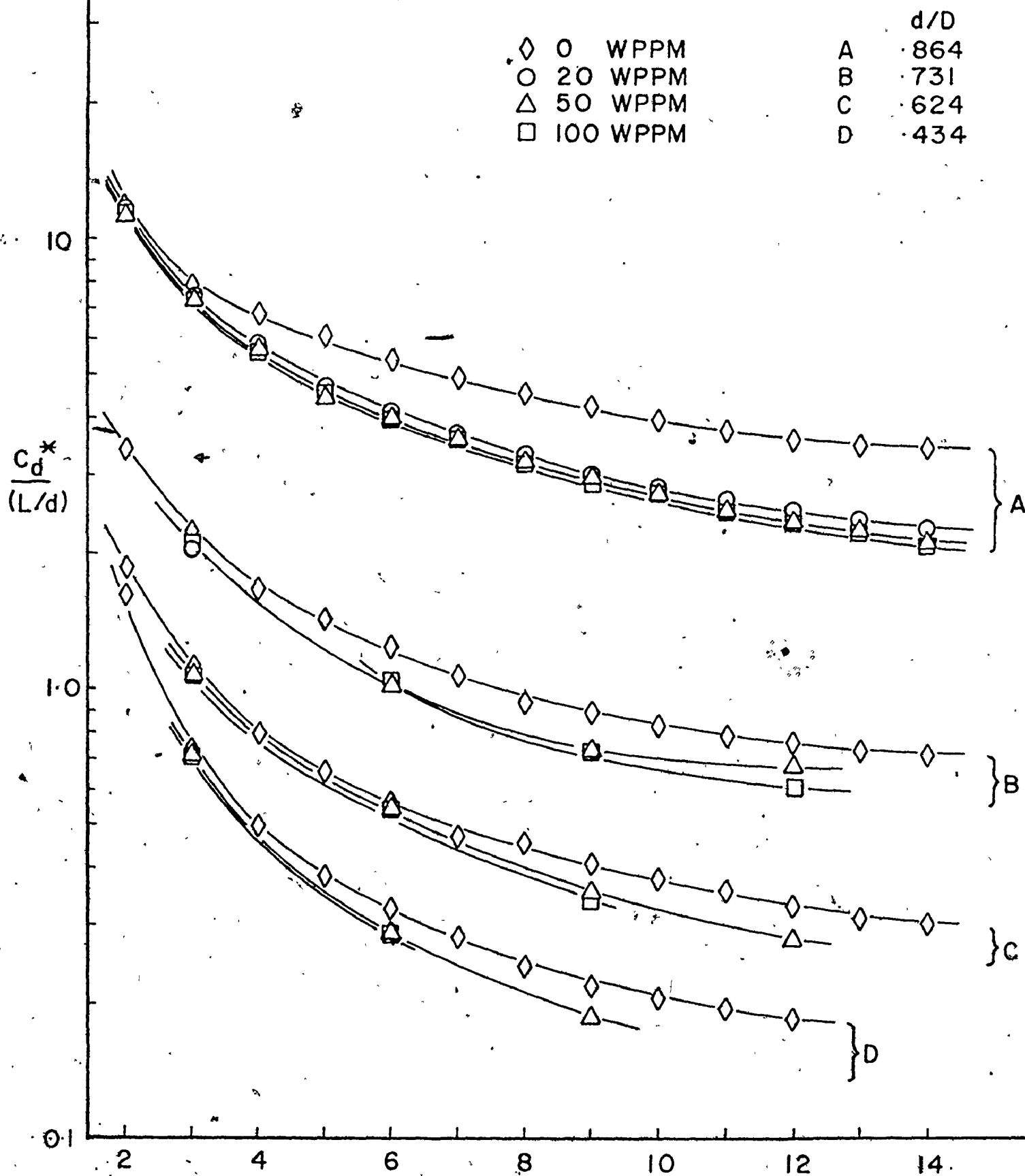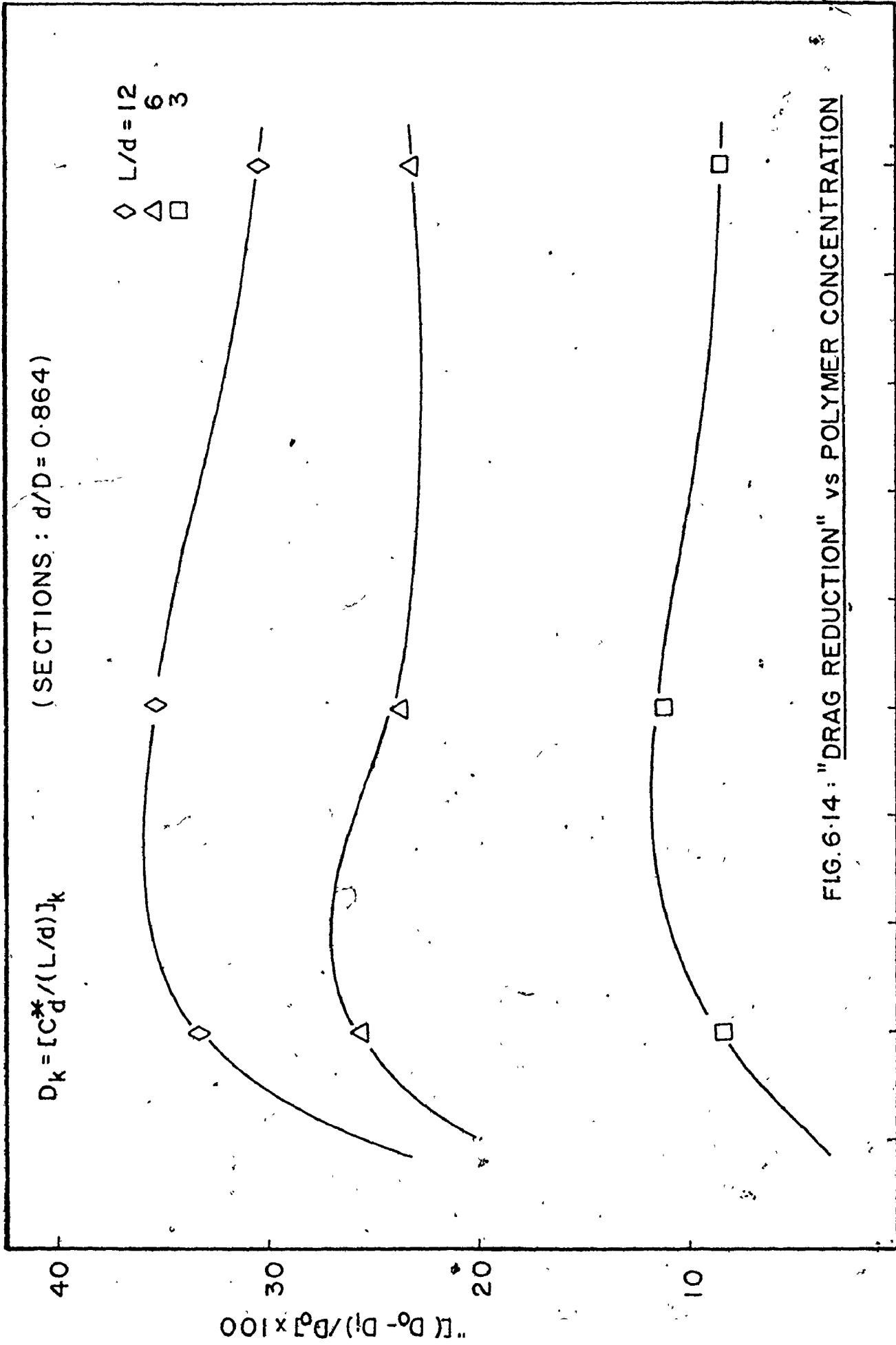
FIG.6.14: "DRAG REDUCTION" vs POLYMER CONCENTRATION

$D_k = [C_d^* / (L/d)]_k$

(SECTIONS : $d/D = 0.864$)

$L/d = 12$
6
3

$\lozenge$
$\triangle$
$\square$

y-axis: "$[(D_o - D_i)/D_o] \times 100$"

x-axis: CONCENTRATION (WPPM)

at such high diameter ratios apparently because of the areas
on which the force acts changes more rapidly for the shear
force component than correspondingly for that of the base
pressure component.

If the pressure drop is considered with respect
to the diameter ratios as in Fig. 6.15 which portrays a
steady increase of the pressure differential with diameter
ratios and with a decrease of polymer concentration.

On the basis of the pressure function plot of
Fig. 6.16, it may be said that there is no systematic
scatter of data points and that the relationship of eqn.
3.26 is obeyed regardless of the polymer concentration.

On a "kinetic energy" basis, Fig. 6.17 shows
that it is the presence of the polymer and not its concen-
tration that is vital to the improvement of flow velocity.
This is of course true for the range of polymer concentr-
ation investigated here. Here again, the data shows that
eqn. 3.22 is obeyed.

If the energy aspect is further investigated, a
plot of the hydraulic power verus diameter ratio must be
made. Fig. 6.19 shows an interesting point. At diameter
ratios less than about 0.75, there is a reduction of hydra-
ulic power requriement with the application of the polymer
additives. This may be caused by a reduced contribution
of the viscous loss term to the total loss term which is
essentially a pressure loss due to all the irregularities
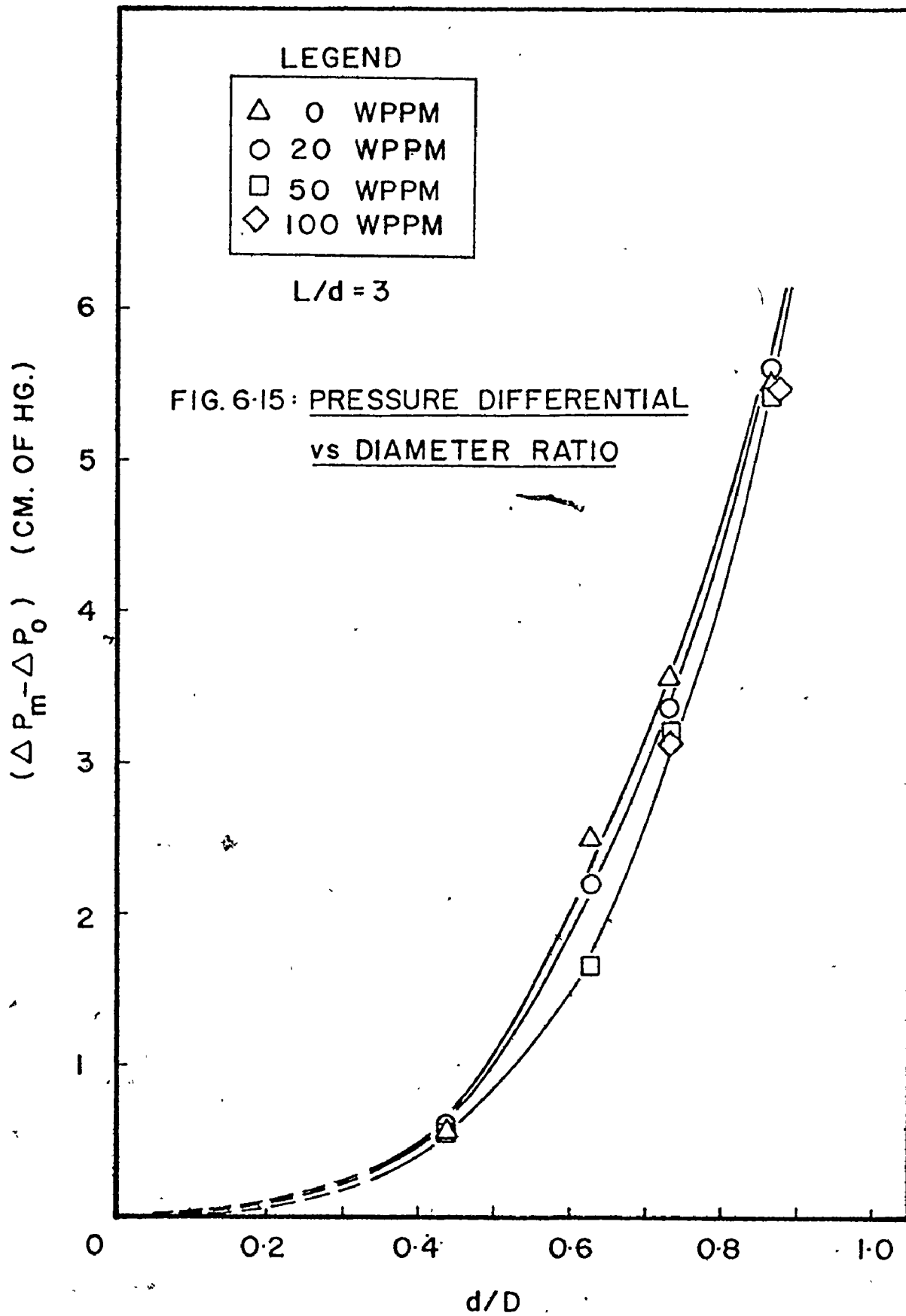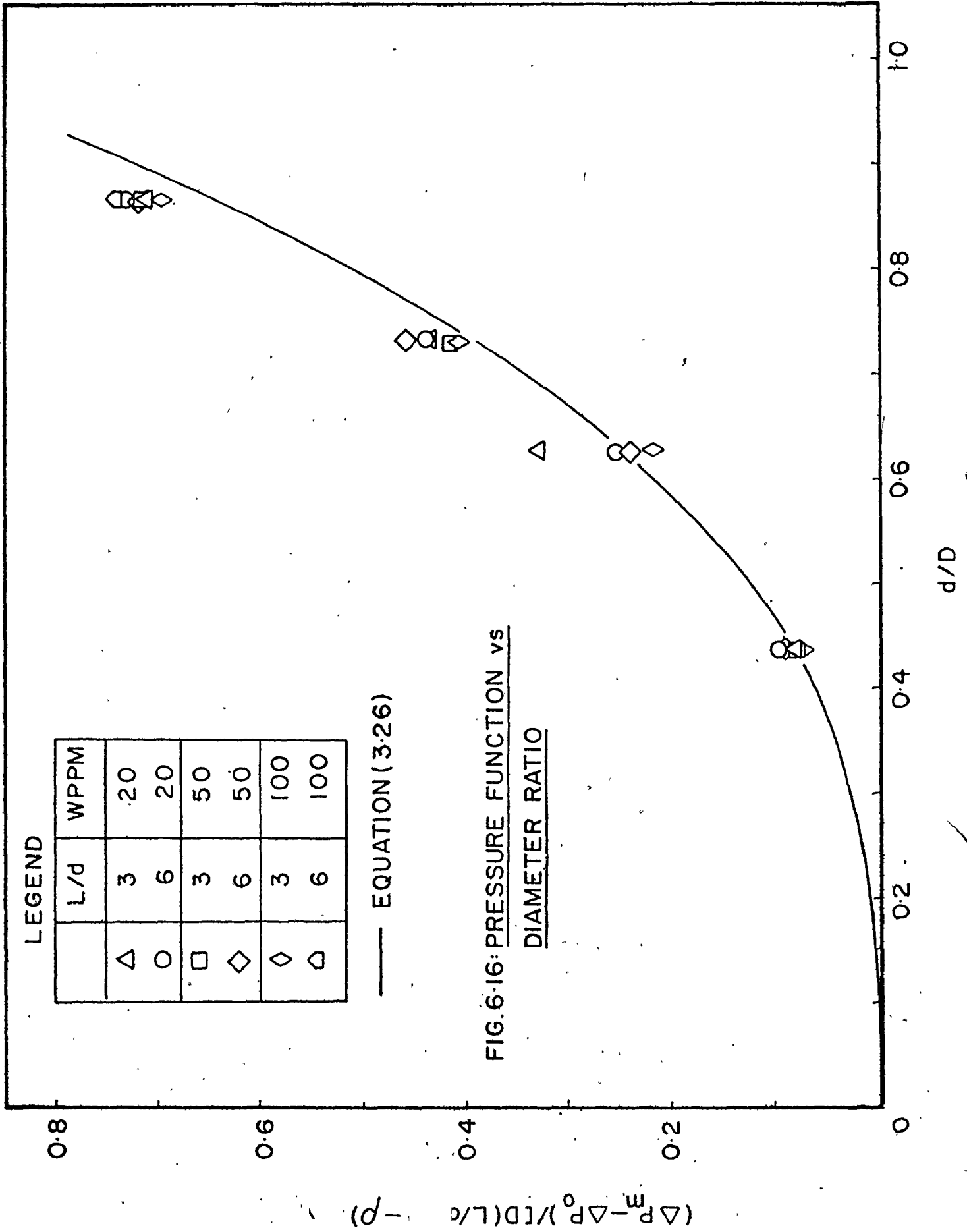
LEGEND

△   O   WPPM
O   20   WPPM
□   50   WPPM
◇   IOO   WPPM

$L/d = 3$

FIG. 6·15 : PRESSURE DIFFERENTIAL
vs DIAMETER RATIO

$(\Delta P_m - \Delta P_o)$ (CM. OF HG.)

d/D

FIG.6·16: PRESSURE FUNCTION vs DIAMETER RATIO

LEGEND

	L/d	WPPM
△	3	20
◯	6	20
☐	3	50
◇	6	50
◇	3	100
◁	6	100

—— EQUATION (3·26)

x-axis: d/D

y-axis: $(\Delta P_m - \Delta P_0)/[D(L/d - \rho)]$

17: FL

FIG.6·18: VELOCITY FUNCTION vs DIAMETER RATIO

LEGEND

WPPM L/d	3	6	12
20	△	○	□
50	◣	◑	◧
100	◤	◕	◩

— EQUATION(6·22)

$U_0'' / [\,\text{E Dg}(L/d)(\dfrac{\rho}{\rho})\text{SIN}\theta\,]$

d/D
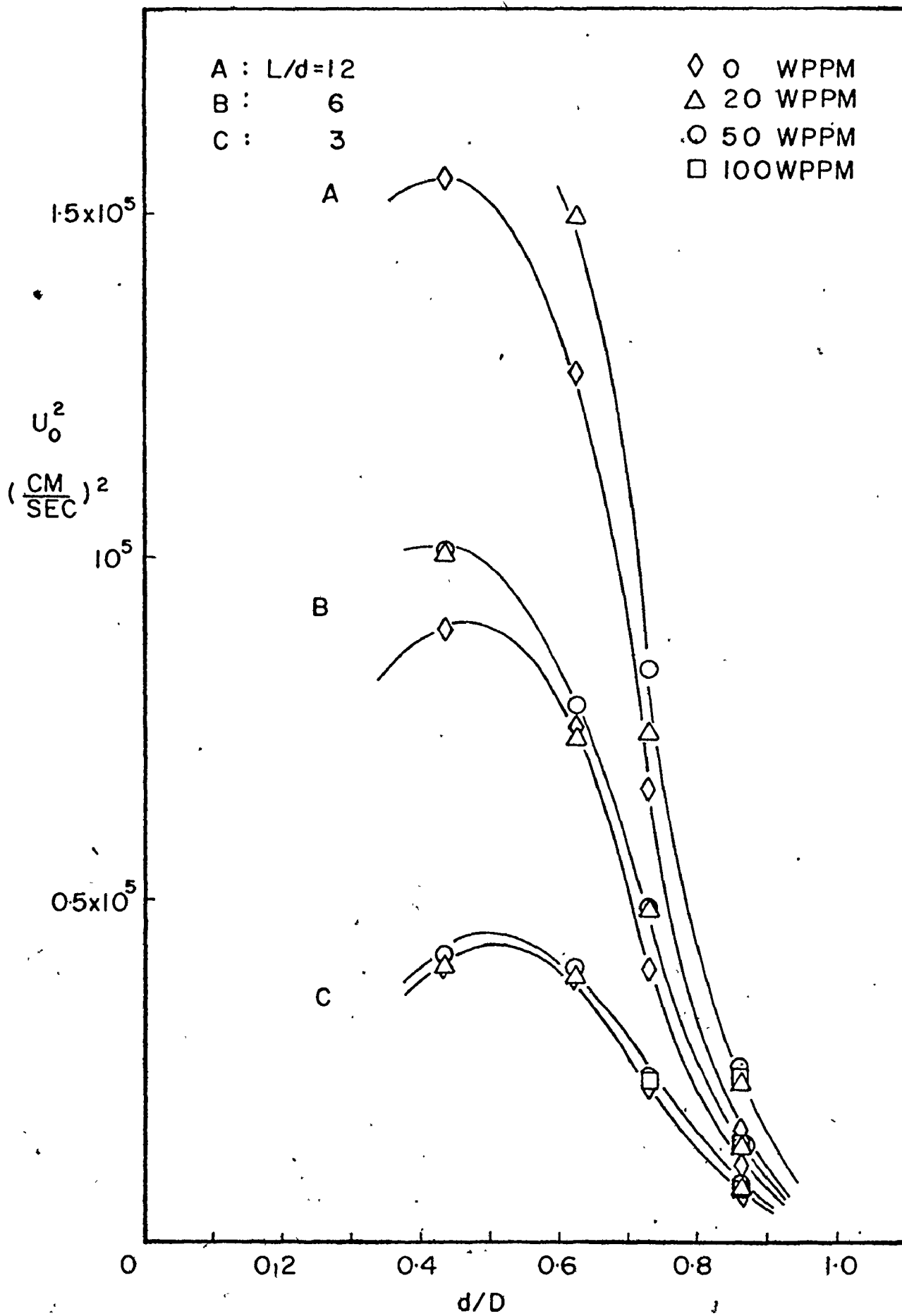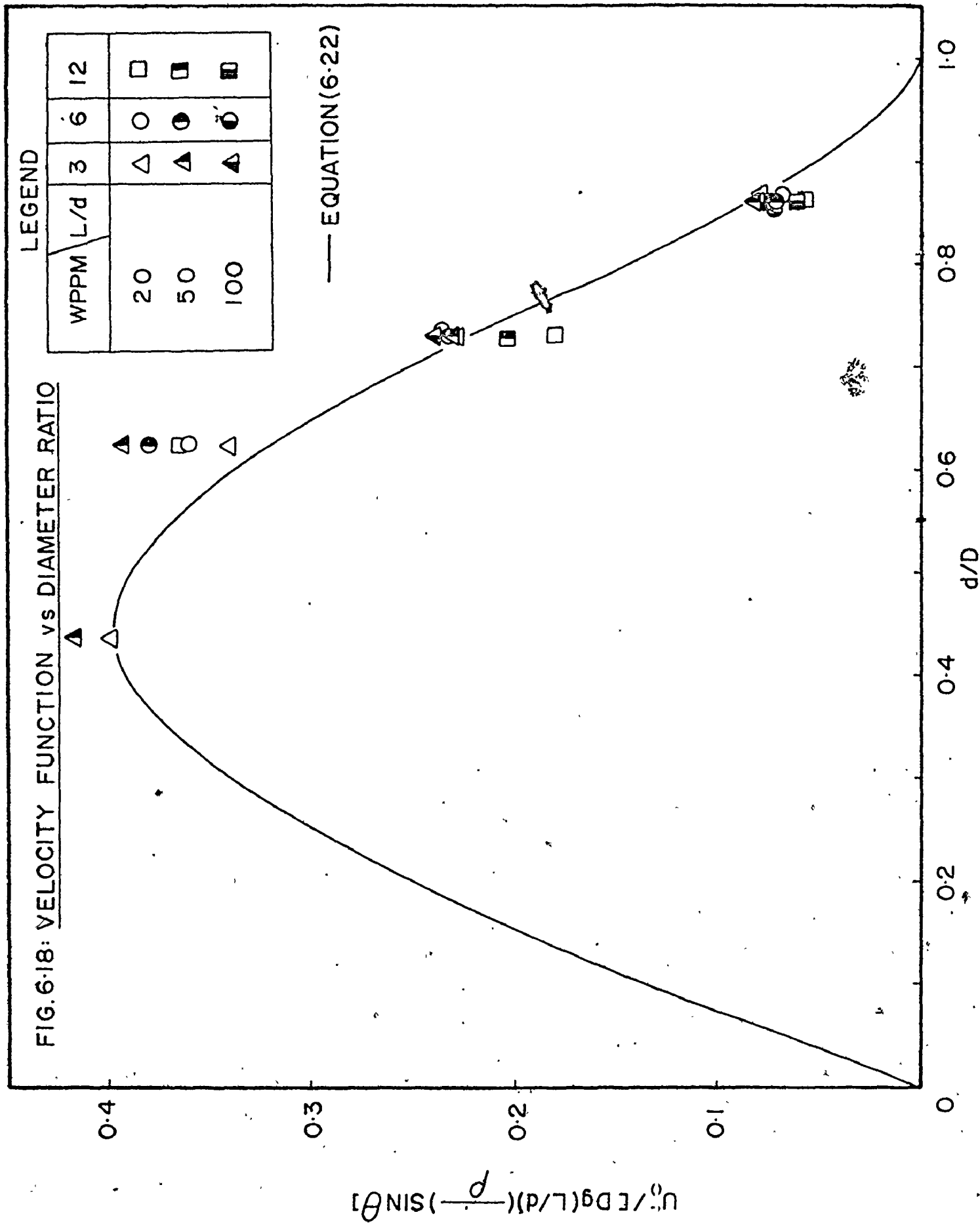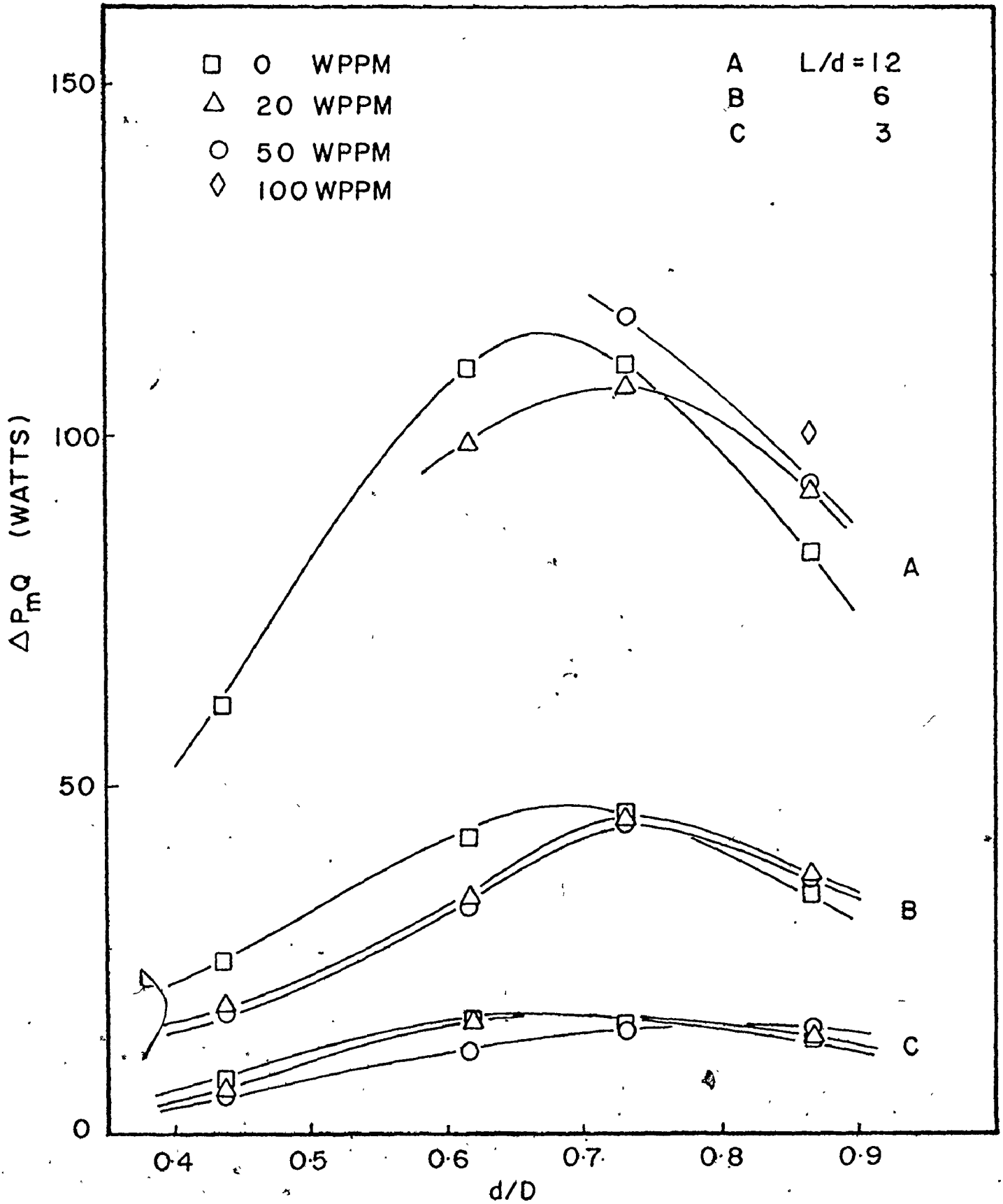
FIG. 6·19: HYDRAULIC POWER INPUT vs DIAMI

in the flow. It is at conditions where a large volume of
fluid exists in the annular spacing between the cylinder
and the pipe that the boundary layer improvements by pol-
ymer additives is obvious - a fact supported by the obser-
vation discussed earlier on velocity requirement.

There is however, a greater power requirement
at high polymer concentration for larger cylinder sections
compared to that for water as the carrier fluid. This of
course is related to the non-Newtonian nature of the aqueous
polymer solution. In fact, if the shear stress required to
produce the same shear rate for different concentrations
were measured using say, a cone and plate type viscometer,
it was found that the high concentration solutions requires
a higher shear stress than a low concentration solution.
The data for such a comparison may be available from another
work done by the author[36].

SECTION III : The effects of end cap(s)

Before embarking on discussions on this section,
it must be pointed out that the aspect ratio L'/d for those
cylinders modified by end cap(s) are based on an equivalent
length L' of a cylinder having the same volume as that of
the modified body. For a cylinder with one cap for instance,
we have,

$$(Volume)_{\substack{representative \\ cylinder}} = (Volume)_{\substack{blunt \\ cylinder}} + (Volume)_{cap}$$

i.e. $$L' = L + L/3$$

The choice of such a length is arbitary, but it
is hoped that it assumes a constant volume aspect for the
bodies and since the volume is the parameter that controls
the gravitational aspect of the body and to some extent,
the area of the shear surface, this definition has a good
basis.

The first thing to discuss under this section is
the drag coefficient and Fig. 6.20 to 6.24 give plots for
different diameter ratios of the length effect on the drag
as well as giving a comparison between blunt and 'stream-
lined' bodies (since the modification using end caps are
to improve the streamline of the bodies) of different
cylindrical shapes. The results indicate a reduction of
drag coefficient at sufficiently high L'/d ratios regard-

less of the size of the body or the use of caps. This seems
to occur at an aspect ratio of about 3 for a diameter ratio
of 0.864 but is increased to about 6 for the smaller ratio
of 0.624. Again, the inference is, for large bodies, there
is an abrupt change of geometry from the cylinder to the
end face (in the case of a cylinder with a leading end
cap) so that the base pressure is considerable. This base
pressure is caused by vortices and wake effects and for
long cylinders, this effect seem to be less decisive and
the viscous shear on the circumference becomes very much
the predominant factor with increasing aspect ratio. For
small cross sections, the loss at the trailing blunt end
is less significant because the flow is not very much
obstructed as it moves towards the cylindrical body. In
the limiting case of a long slender body, the effect of
the blunt end on the total loss term is minimal. However,
there is some optimal geometry at which a balance between
a sharp geometrical change and a large surface shear exist,
but this is dependent on the size of the body.
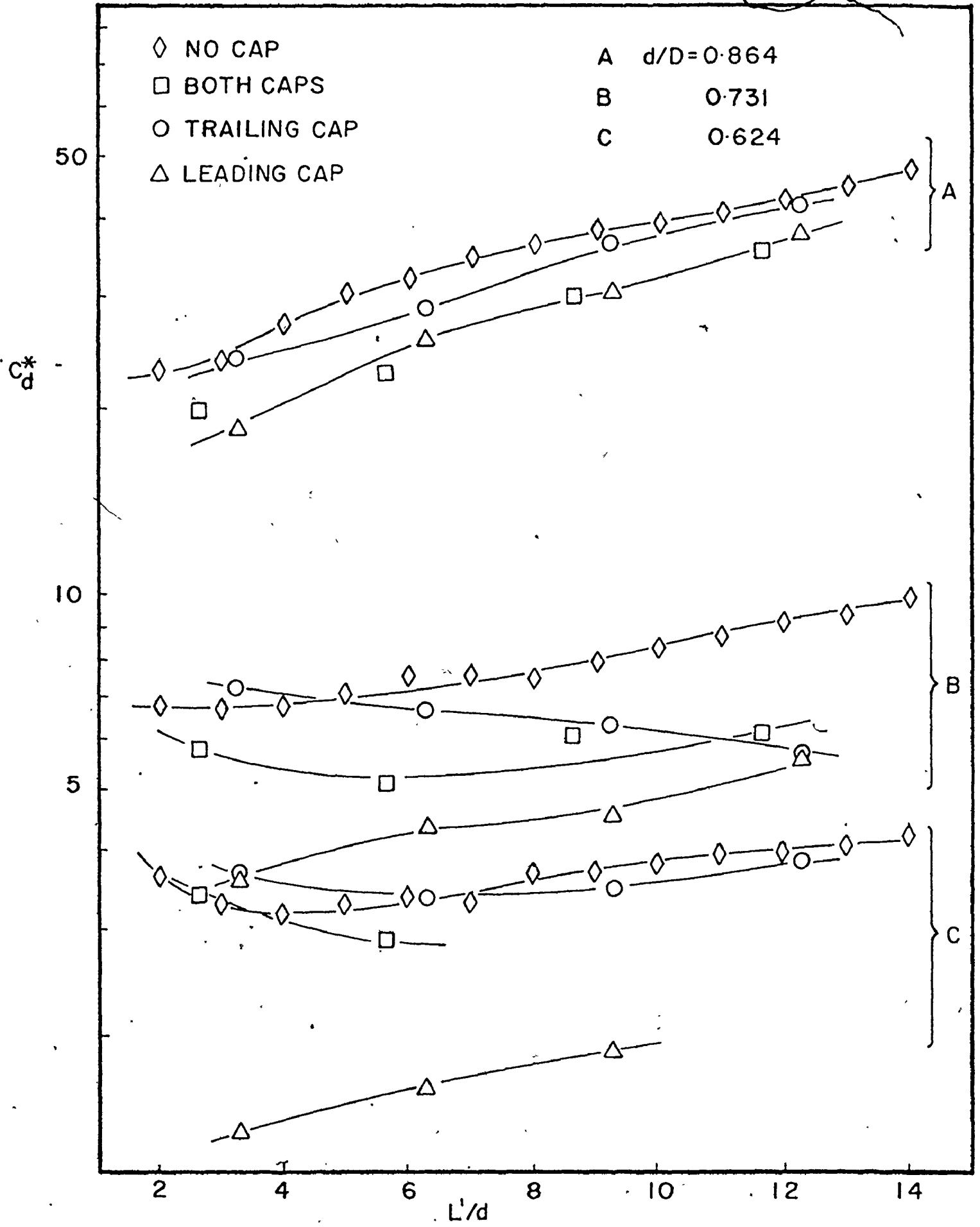
With a forebody (leading end cap) on the cylinder,
there is no sudden change of geometry at the leading end
and the boundary layer may extend further downstream from
the nose. Of course, since cylinders with semi-hemispherical
end caps are not the best streamlined shapes, there is still
considerable loss of pressure as the flow moves past the
nose of the body, but the magnitude of such a loss is much
smaller than that for a blunt cylinder.

FIG. 6·21 DRAG COEFFICIENT PER ASPECT RATIO vs ASPECT RATIO
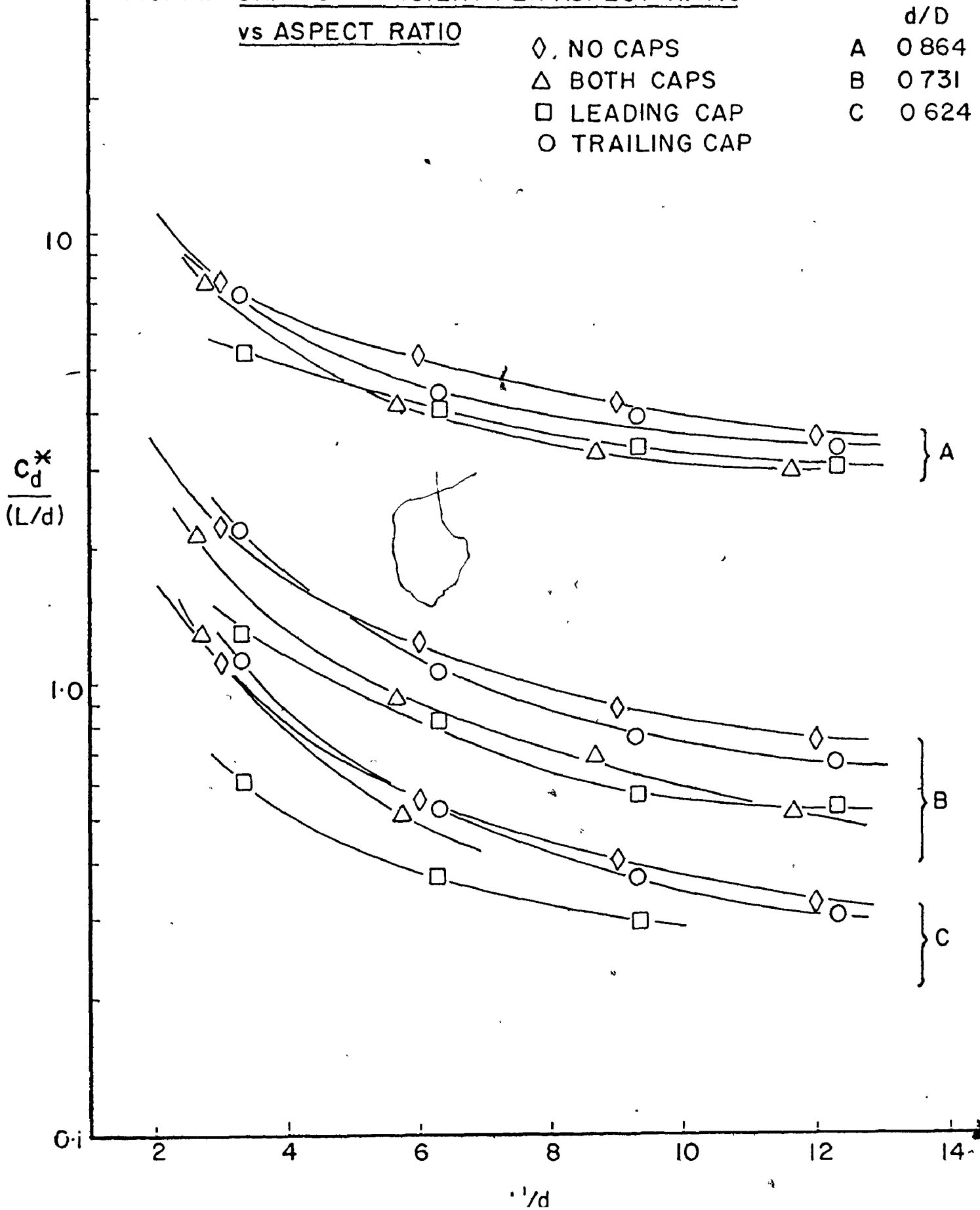
Another observation is that there is more drag
reduction associated with the addition of a forebody cap
than by having an afterbody cap - a not unexpected result.
However, the improvement of drag properties differs for
different shapes of the end caps and several possible
geometries are shown in Fig. 6.25b which is a collection
of results for experiments done in air.

With the addition of both forebody and after-
body end caps, however, there seems to be little change
in drag coefficient for cylinders with high diameter ratios
than for cylinders with single fore or afterbody caps. It
is thought that for these sizes, a smoothening of the body
shape has just about the same benefit as the loss that an
increase of shear surface would create. This fact helps to
establish the relative magnitude of the pressure and viscous
component of the drag coefficient pertaining to the caps
i.e. $(C_A)_P$ and $(C_A)_V$ as defined in chapter III of this
thesis so that even if the integration of the expression
in eqn. 3.8 is not possible, one can still estimate the
contribution from each term.

Indeed, plots such as Fig. 6.22 can be used to
evaluate the significance of each type of drag and friction
losses that are described in chapter III and no attempt is
made here to repeat the definitions of each loss term.
However, it may be shown that the effect of the cap(s) is
to change the value of C_d for a blunt cylinder as compared

FIG.6·22: DRAG COEFFICIENT vs ASPECT RATIO

LEGEND

d/D = 0·864

	BOTH CAPS
O	BOTH CAPS
◇	LEADING CAP
□	TRAILING CAP
△	NO CAP

TOTAL = PRESSURE + FRICTION (D)
DRAG = DRAG (A)

C = FORE (AFTER) BODY DRAG

B = BASE DRAG

L'/d

C_d
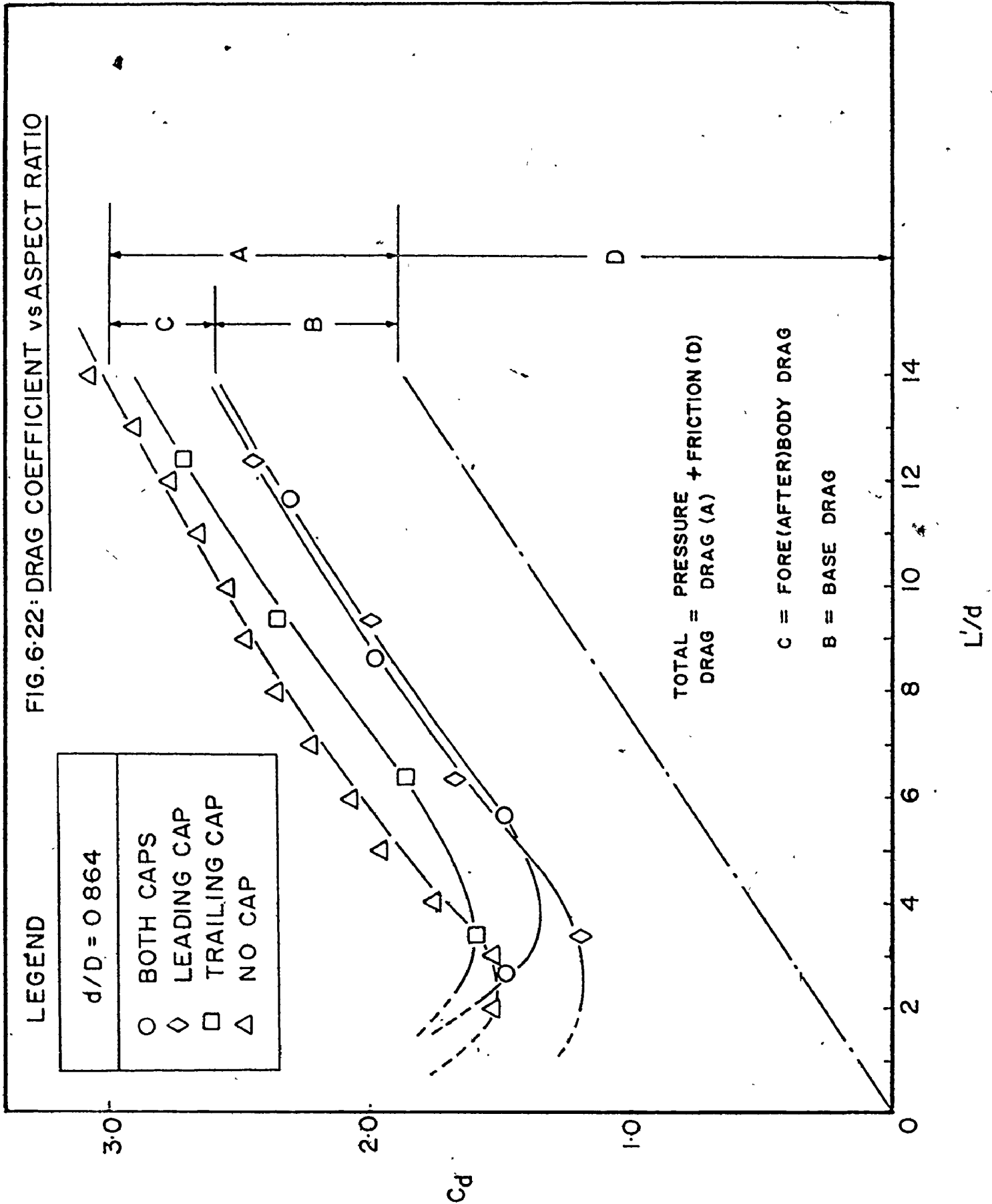
to that for a 'streamlined' body of different shapes. The
fact that this change is almost a constant for cylinders
of any diameter ratios over the entire aspect ratio range
suggest that one can associate a negative drag coefficient
to the end cap(s) when they are added to the cylinders to
create the 'streamlined' bodies. For instance, with diame-
ter ratio of 0.864, addition of the trailing and leading
end caps reduces C_d by 0.1 and 0.3 respectively. Of course,
the effects of both caps is by no means the sum of the
effects of each cap when used individually as a fore or
afterbody cap.

On the other hand, the frictional loss term is
not a conveniently measurable quantity in the experiment
conducted here nor is it directly assessable by mathematical
considerations. However, a friction line may be drawn on
these three plot from eqn. 3.22 to eqn. 3.24 because of
two assumptions. One, that the friction increases linearly
with the increase of the aspect ratio because more area is
exposed to   the flow as the length of the cylinder is
increased. Two, at the limiting case for an infinitely
long cylinder with L'/d approaches infinity, there is no
base drag associated with the ends and in this instance,
the curve for the blunt cylinder should converge with all
the other curves obtained from 'streamlining' the cylinders.
For the present plots, the friction line is drawn to converge
with an imaginary intersection of these lines and is effect-
ively a line parallel to these individual lines. This

FIG. 6·23: DRAG COEFFICIENT vs ASPECT RATIO

LEGEND

d/D = 0·731

O	BOTH CAPS
◇	LEADING CAP
□	TRAILING CAP
△	NO CAP

FRICTION

L'/d

Cd
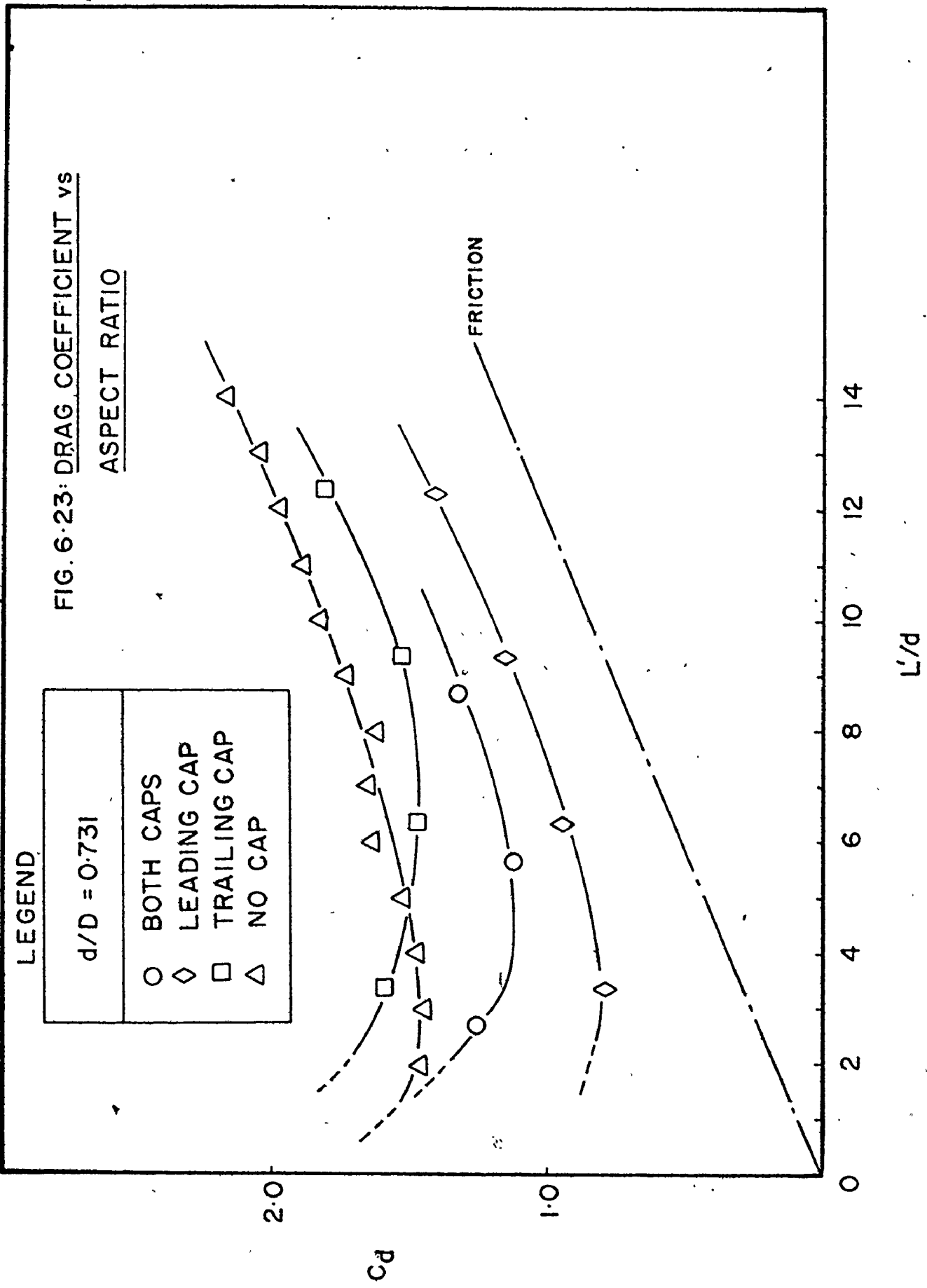
FIG. 6·24: DRAG COEFFICIENT vs ASPECT RATIO

LEGEND

d/D = 0·624

O	BOTH CAPS
◇	LEADING CAP
□	TRAILING CAP
△	NO CAP

FRICTION

C_d

L'/d
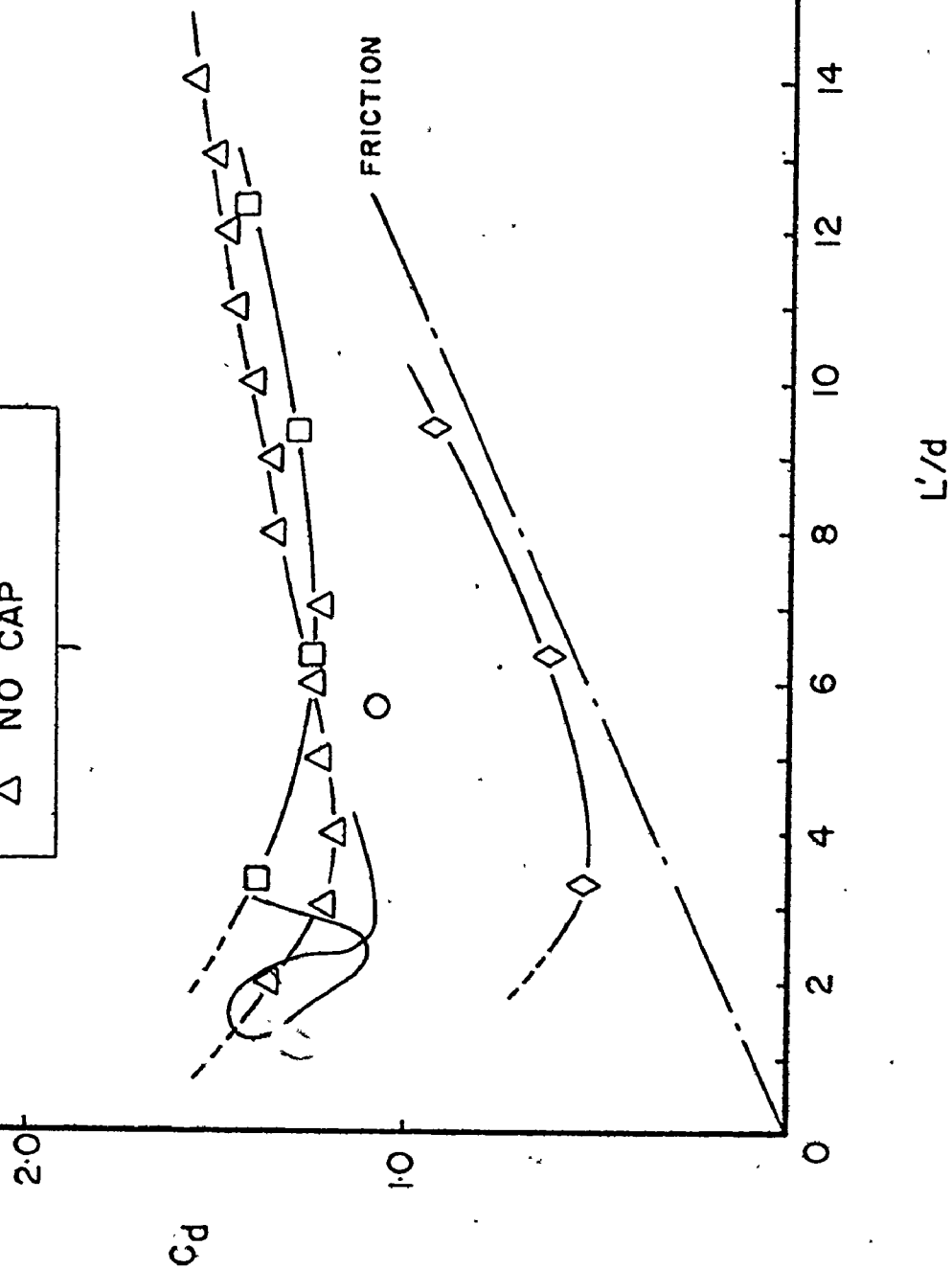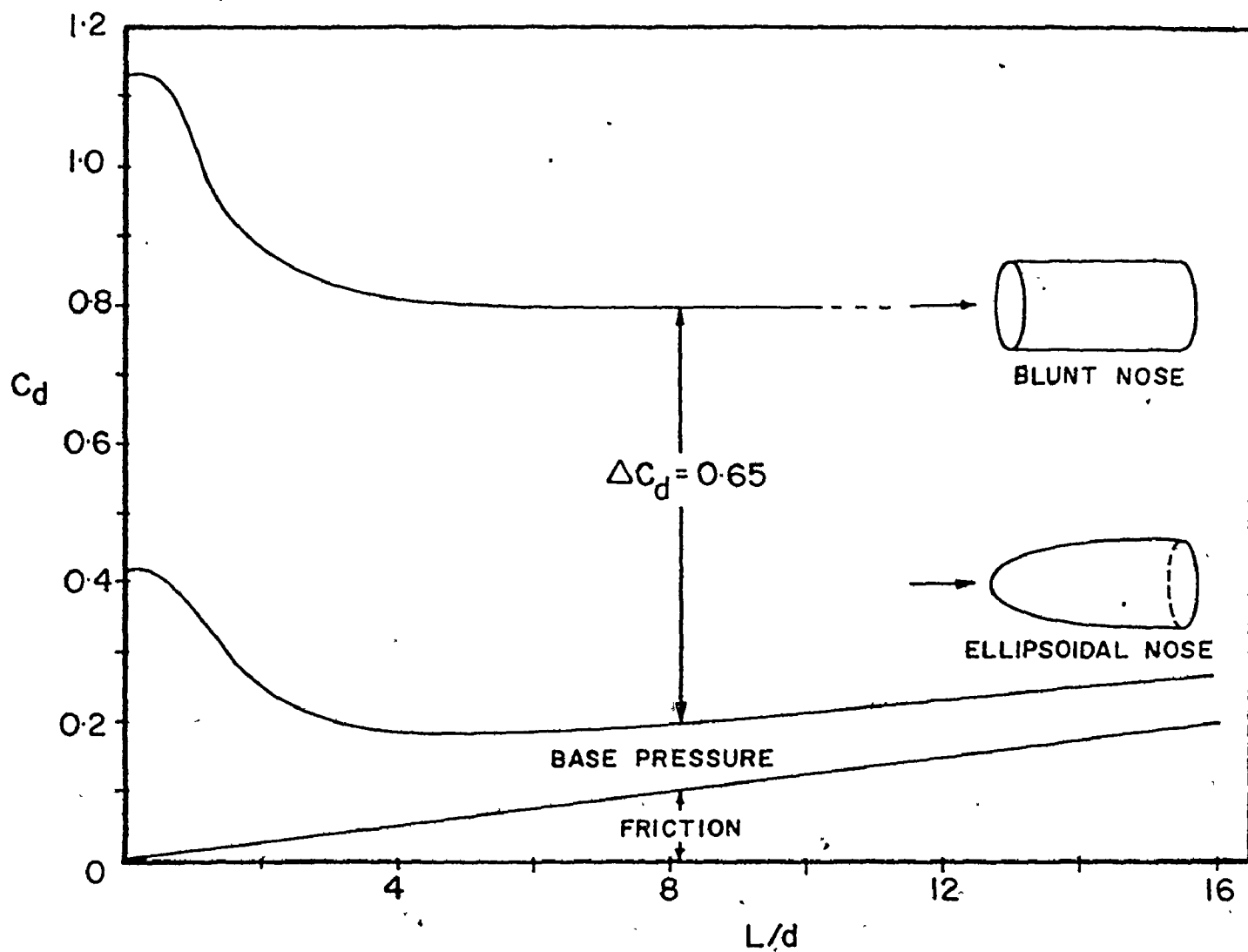
FIG.6·25a: <u>AXIAL FLOW OF CYLINDRICAL BODIES IN AIR (AFTER HOERNER)</u>
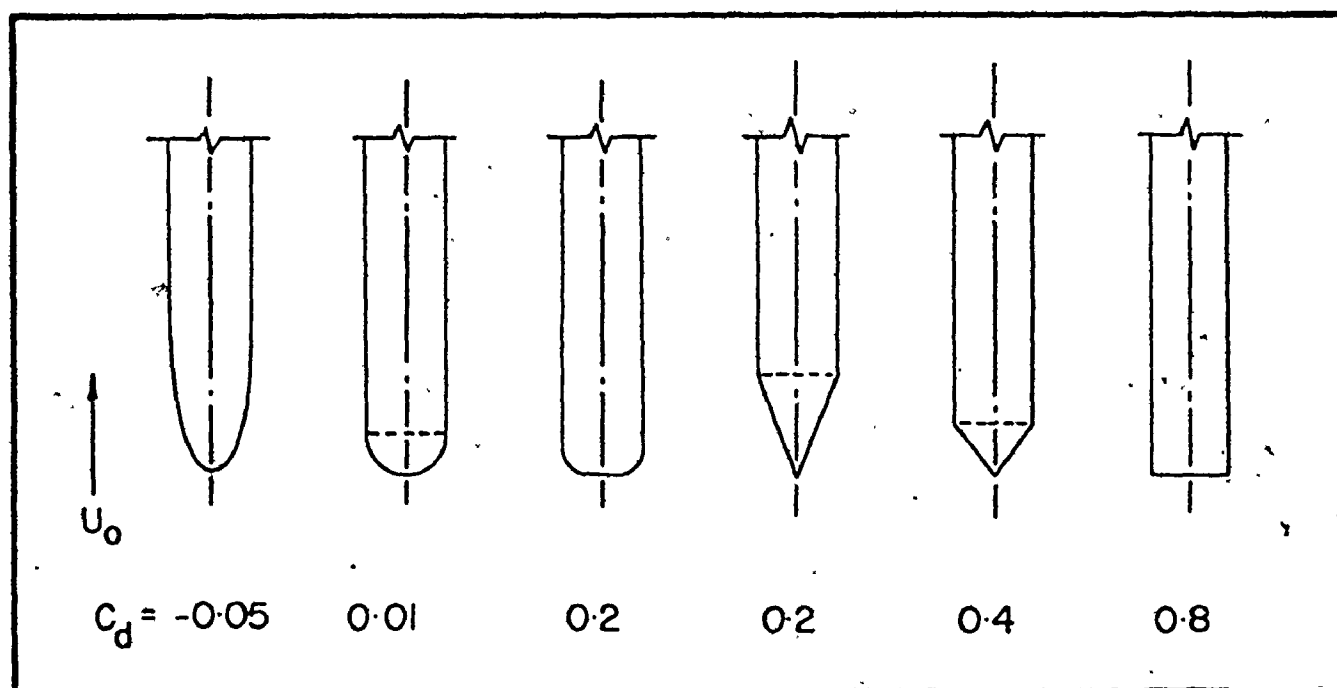
procedure is necessary since the limiting L'/d case has not been reached at the relatively small aspect ratios that were investigated in the present experiment.

If these results on drag coefficient are compared to those obtained from similar streamlined and blunt bodies in air such as those plots shown in Fig. 6.25a, a greater viscous effect is found to exist that imparts a steeper gradient to the C_d curves of the 'streamlined' and blunt bodies. This is essentially the main difference between experiments done in air and in water and is attributed to a difference in viscosity and compressibility of the two fluids. Note also that the drag coefficients obtained in water are slightly greater than those obtained in air.

If the contribution of each drag coefficient term associated with base pressure, friction losses etc are measured from the plots, eqn. 3.1 i.e.

$$\Delta P_{total} = \Delta P_{base} + \Delta P_{\substack{fore \; or \\ afterbody}} + \Delta P_{\substack{viscous \\ shear}} + \Delta P_{\substack{skin \\ friction}}$$

may be verified. This was done and is shown in Fig. 6.26 by taking the average percentage value of pressure change for each 'streamlined' body.

The result indicates that about half of the total drag results from the viscous shear on the surface of the cylinder and skin friction losses on the surface and that the presence of the afterbody caps could reduce the total drag by as much as 30%. There is also a decreasing drop

PRESSURE DRAG / TOTAL DRAG ×100 %

FRICTION / TOTAL DRAG ×100 %

◇ NO CAP
□ LEADING CAP
△ TRAILING CAP
○ BOTH CAPS

AFTERBODY DRAG / TOTAL DRAG ×100 %

d/D
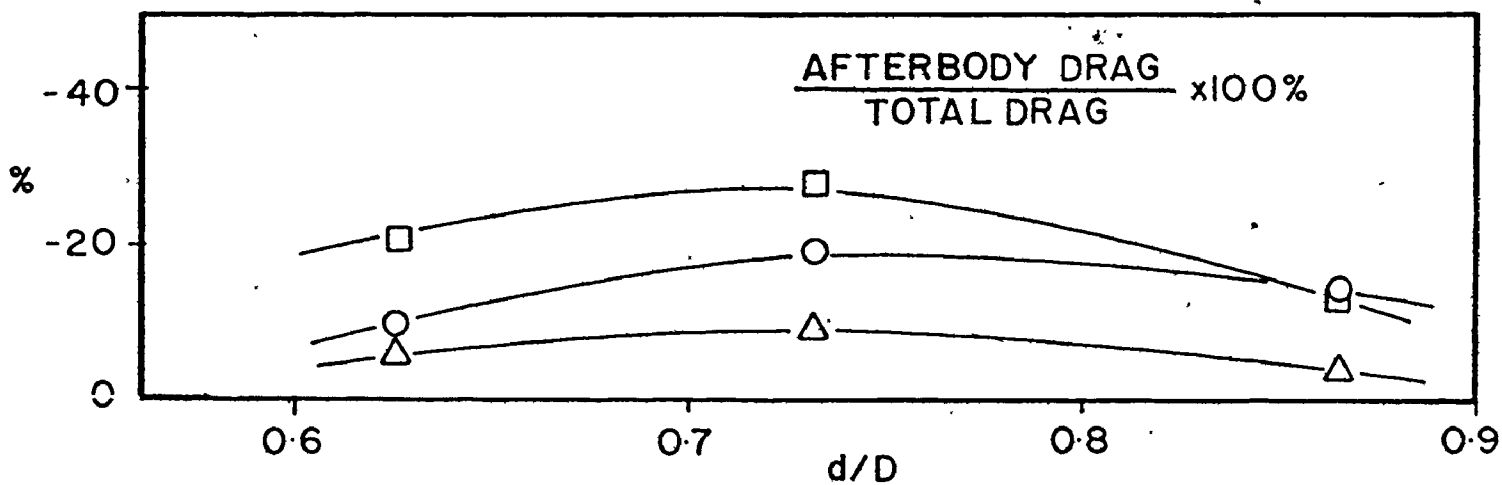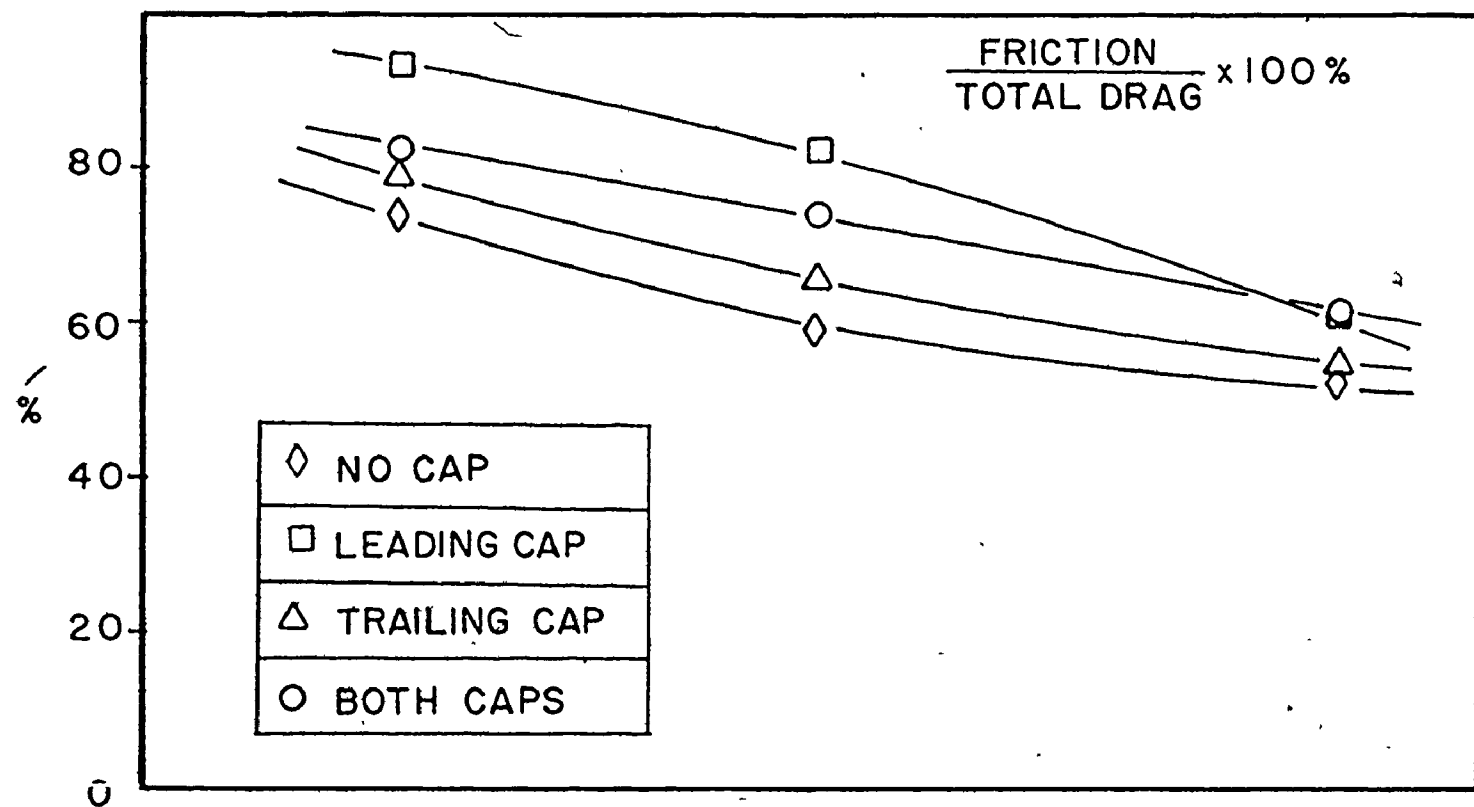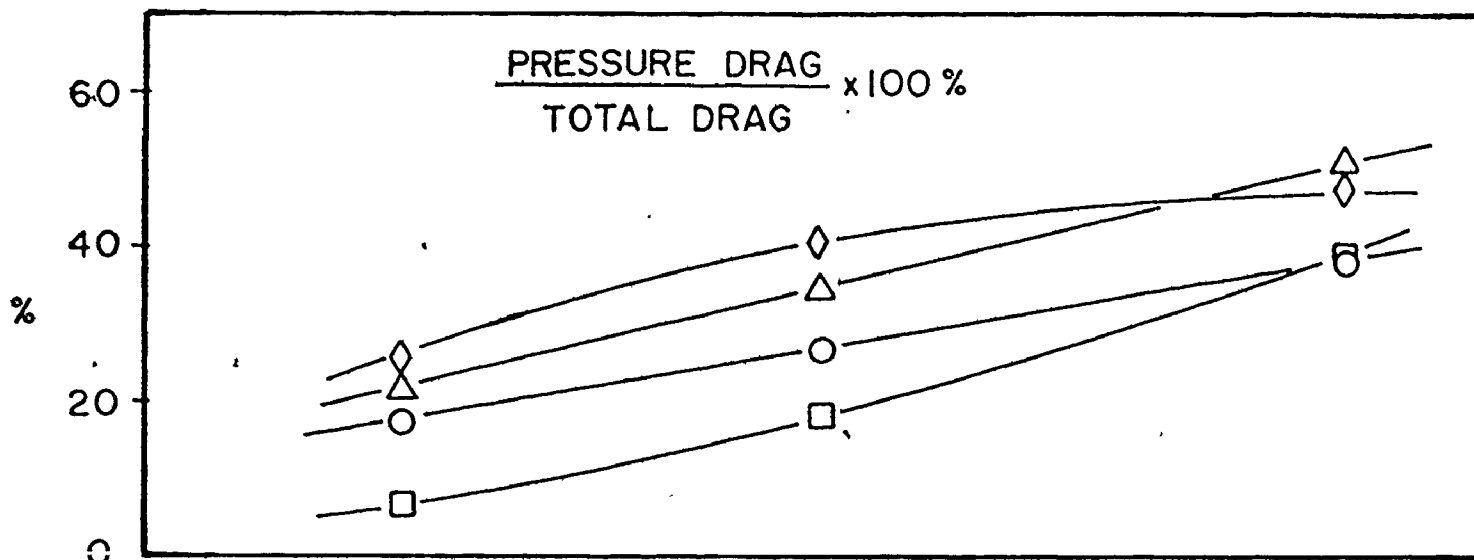
of the frictional effects as the diameter ratio increases.
The net effect is an increase of the pressure drag cont-
ribution as the size of the cylinder is increased. This
is understandable because at high diameter ratios, the flow
sees the cylinder as a more formidable obstruction.

If the pressure differentials are considered as
in Fig. 6.27, it seems that little pressure drop change
is associated with the use of caps. Indeed, there seems
to be a greater drop accompanying a forebody cap than for
the case of an afterbody cap which is normally the case of
aerodynamic flows.

If the pressure data are plotted in the form of
the pressure function versus the diameter ratios, as in Fig.
6.28, there seems to be more deviation from the $(d/D)^3$ line
than for the case of a density change or for polymer add-
ition which is shown in Fig. 6.6 or Fig. 6.16. This of
course suggests that L'/d is too low for the current usage
and that its definition, based on a constant volume, is
slightly inaccurate. But since the actual variation is
small, and since L'/d only exists in the first order in
the denominator of the pressure function, the effects of
not using an "exact" L'/d ratio may not be great.

There is also a considerable variation of vel-
ocity with a change of the diameter ratio of 'streamlined'
bodies (much in the same manner that a polymer solution
would create), and it seems that the velocity is greatest
for the case of a cylinder with a forebody cap. However,

LEGEND

△ NO CAP
□ TRAILING CAP
○ LEADING CAP

$L'/d = 3.33$

FIG. 6·27: PRESSURE DIFFERENTIAL vs DIAMETER RATIO
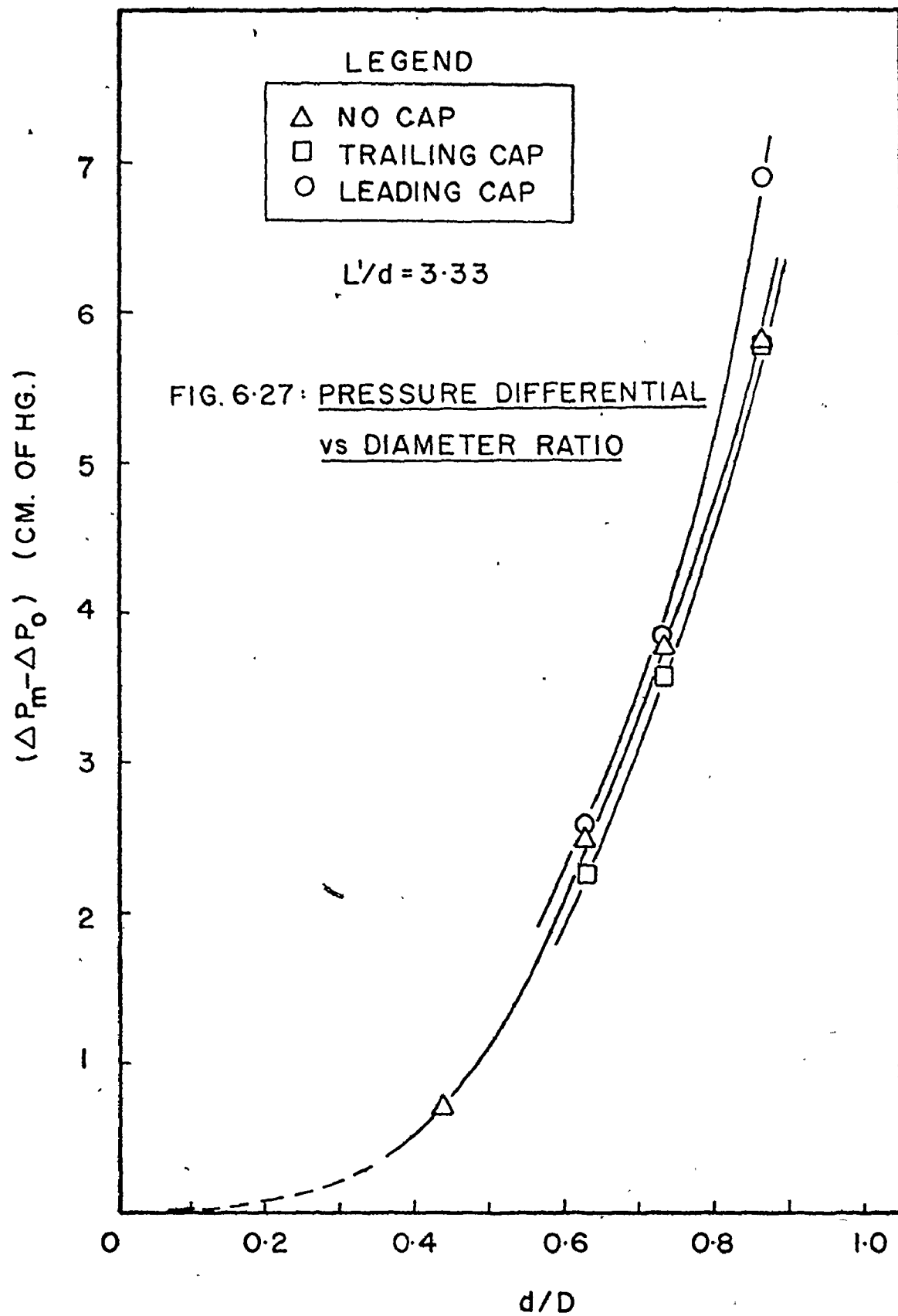
an examination of the energy plot of Fig. 6.31 indicates
that these bodies have a higher energy input. The inexact
choice of L'/d also gives a systematic variation in the
velocity coefficient plot and in fact much of the rather
obvious unsystematic scatter of the data is attributed to
this cause. This may be stated because the pressure funct-
ion of Fig. 6.28 and the velocity function of Fig. 6.30
have been found to hold for a change of density and the
use of polymer additives.

The hydraulic power input plot shown in Fig. 6.31
shows a less energy requirement for cylinders with an after-
body cap but this is also accompanied by a lower velocity
requirement as Fig. 6.29 indicates.

Indeed, the parameter of flow velocity has a far
reaching effect since in an actual pipeline problems, the
average bulk velocity of the fluid is only slightly greater
than the capsule velocity so that the choice of the capsule
shape has to be carefully considered since a capsule that
is transported at a slower speed requires a lesser power
input.

Fig. 6.32 shows the hydraulic power input plot
on a per mass (in still air) basis, and it clearly shows
the advantage of using a large diameter cylindrical body.
Whereas there seems to be a decreasing trend in the power
input as the diameter ratio is reduced to about 0.4,there

FIG.6·28:PRESSURE FUNCTION vs DIAMETER RATIO

LEGEND

CAP L'/d	3·3	6·3	12·3
BOTH CAPS	△	○	☐
TRAILING CAP	▲	◑	⊞
LEADING CAP	◢	●	▣

—— EQUATION(3·26)
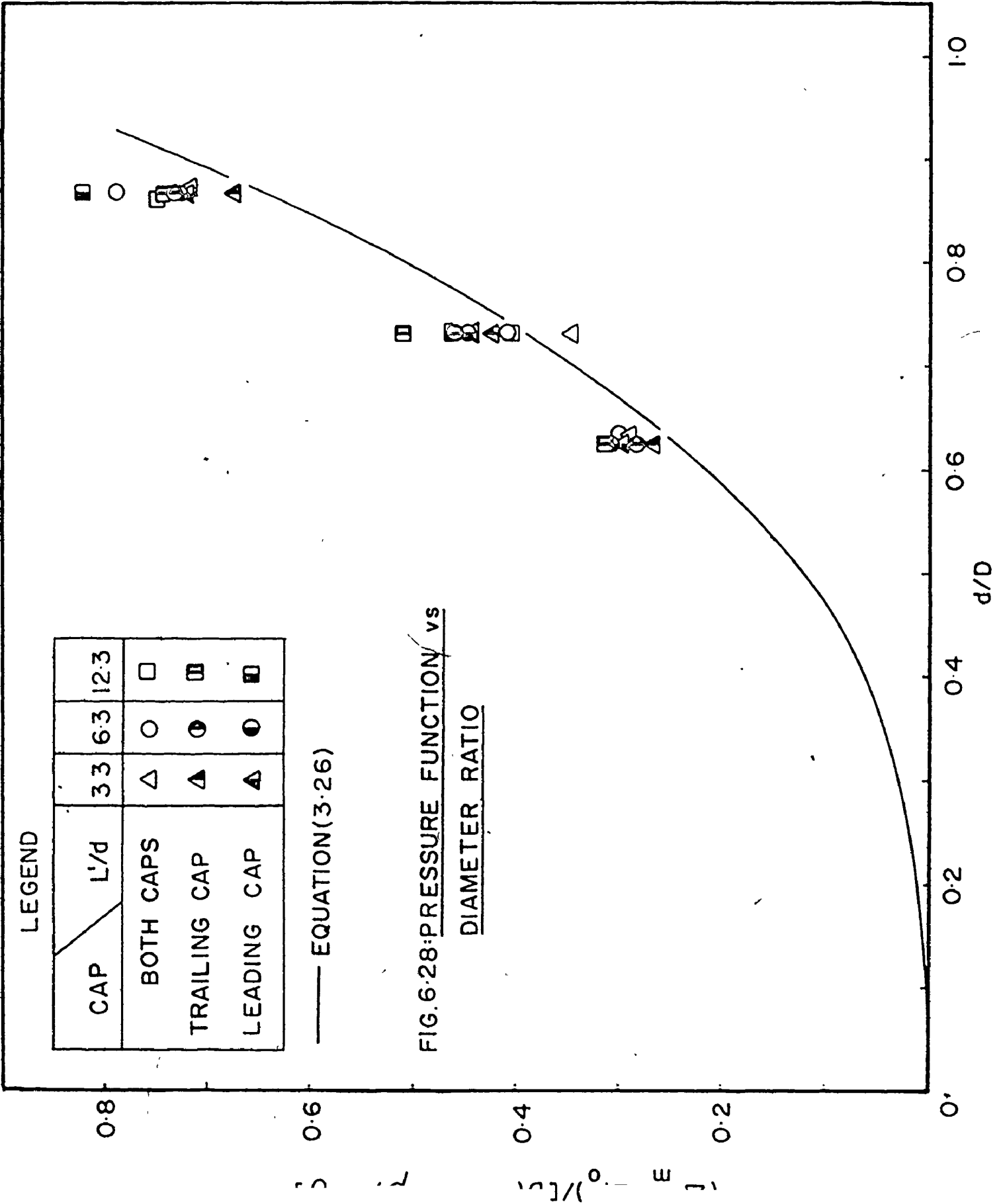
FIG. 6·29 : VELOCITY vs DIAMETER RATIO

FIG.6·30: VELOCITY FUNCTION vs DIAMETER RATIO

LEGEND

CAP	L'/d	33	63	12·3
BOTH CAPS		△	○	□
TRAILING CAP		▲	◑	▣
LEADING CAP		◀	●	�

—— EQUATION(3·22)

$U_0^2 / [C D g (L'/d)(\frac{\rho}{\rho}) \sin \theta]$

d/D
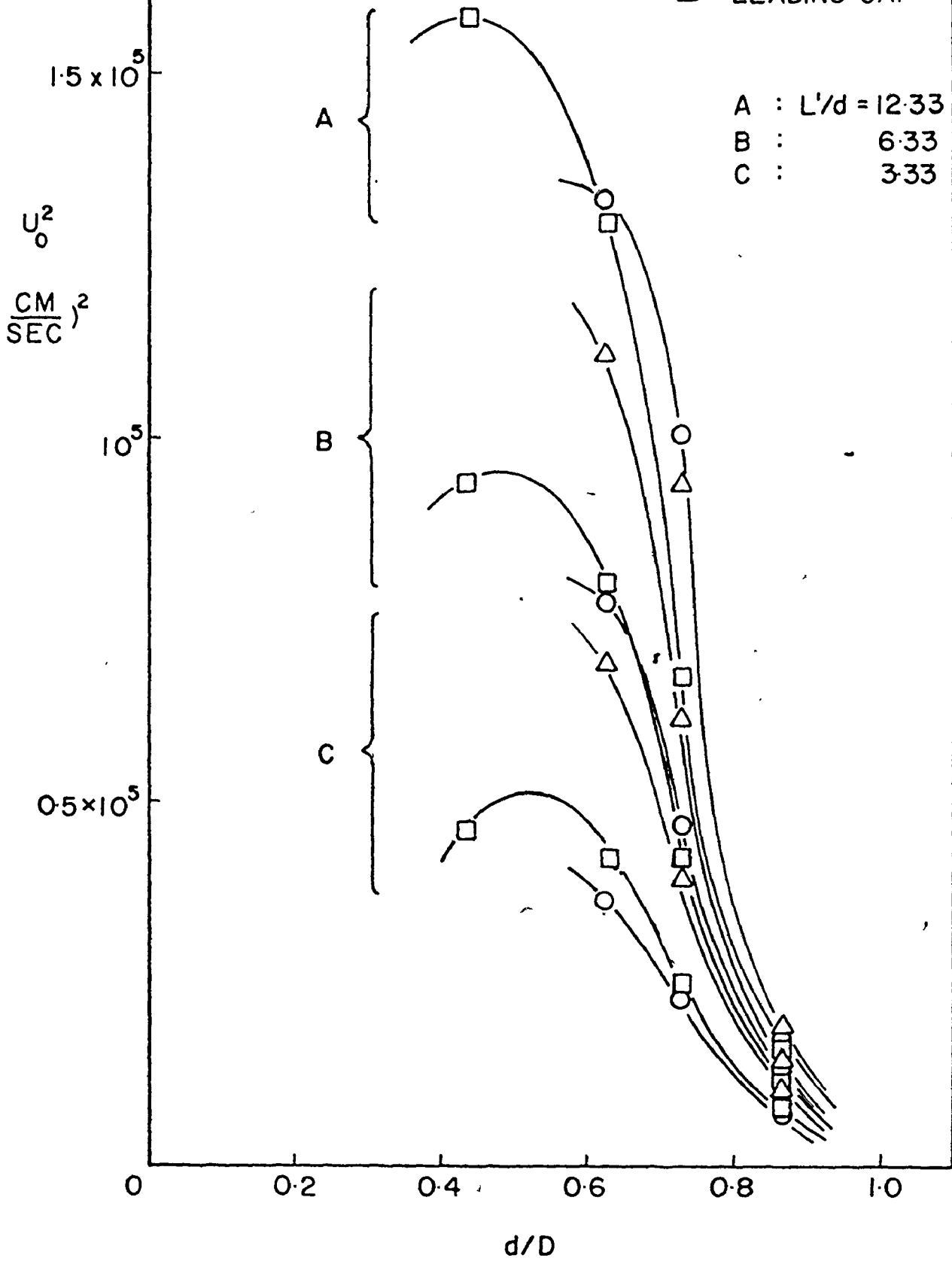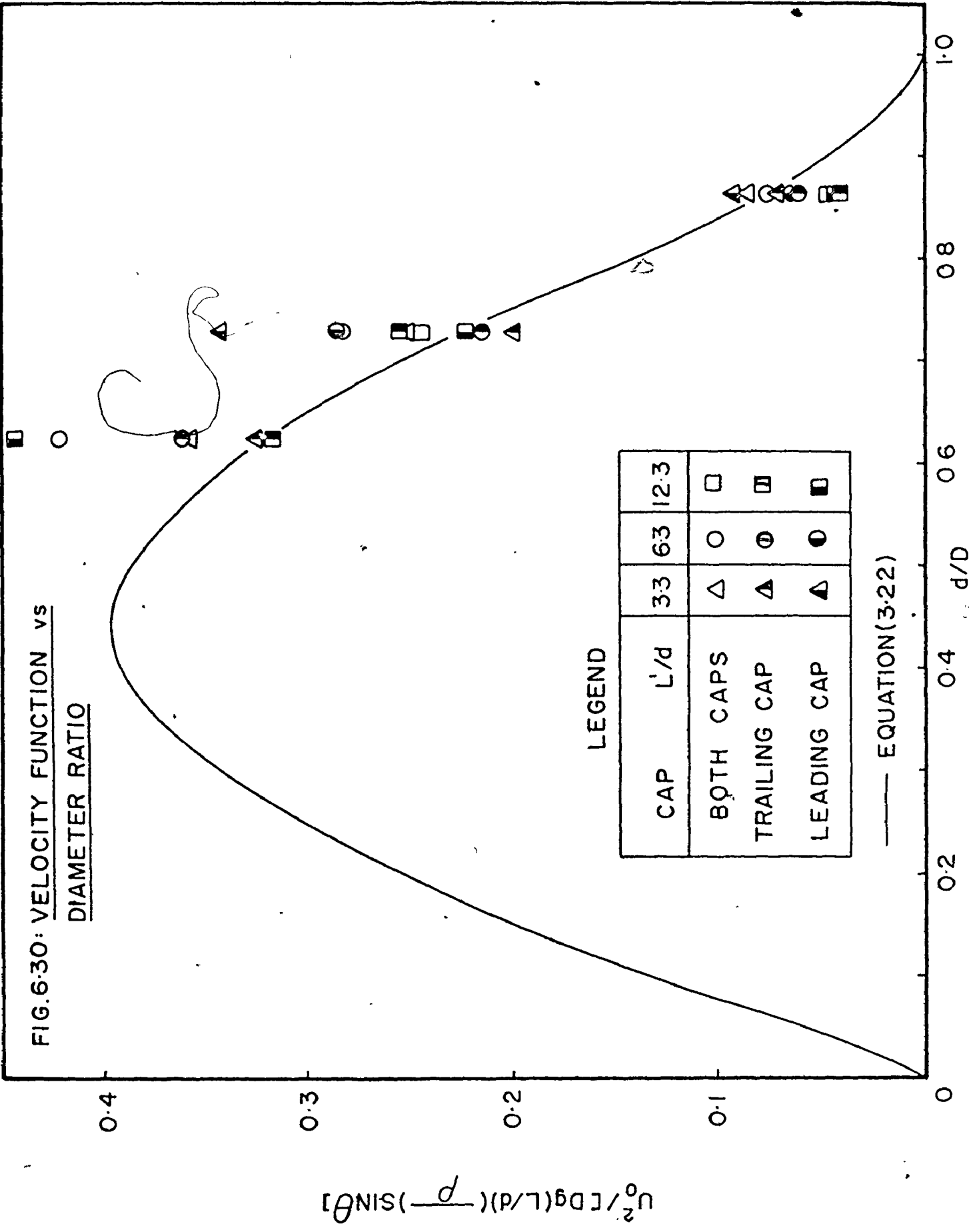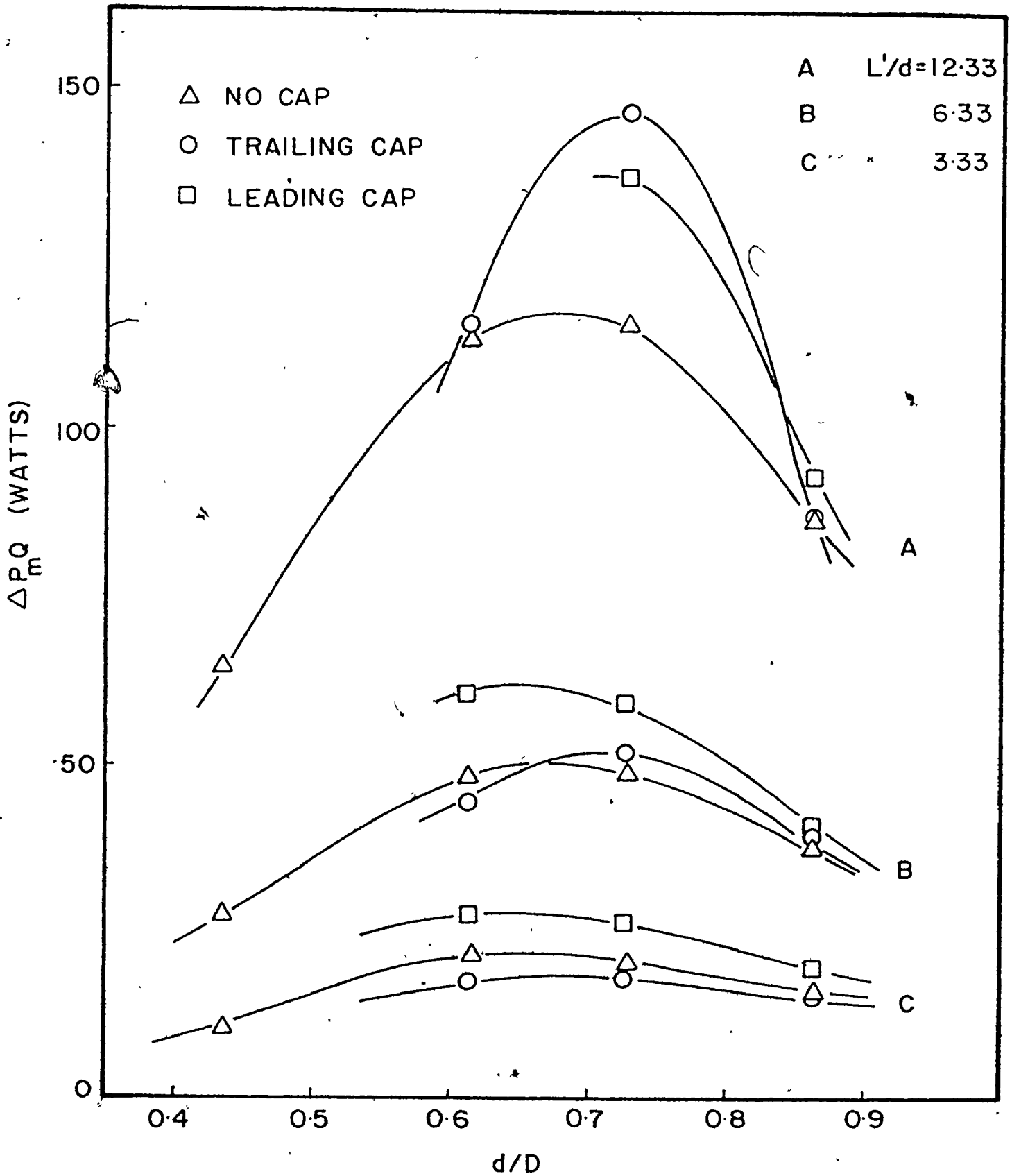
FIG: 6·31: HYDRAULIC POWER INPUT vs DIAMETER RATIO

FIG. 6·32 HYDRAULIC POWER INPUT PER MASS vs DIAMETER RATIO

seems to be an increase of power per mass with the exist-
ence of end caps for all diameter ratios and aspect ratios
except for the small aspect ratio of 3 presented in this
plot. The advantage of a lower power per mass requirement,
however, has to be carefully weighed against the disadvan-
tage of having a corresponding decrease in the transport
velocities of these capsules.

In fact, there is also a volume throughput
problem associated with these blunt and 'streamlined'
bodies if they are to simulate actual capsules used in
pipelines. 'Streamlined' capsules usually have less volume
per length if the capsules are connected in series, but
they require lower velocity requirements. The ultimate
choice will depend heavily on the desirability of a rapid
transportation and the limitation of available power
generation equipment that can deliver the necessary power.
However, these considerations are dependent on the require-
ment of Industry and further discussions will not be made
here.

VII   CONCLUSION

The results of the research presented in this thesis may be summarised in the following conclusions :-

(1)   For blunt cylindrical bodies hydrodynamically suspended in a pipeline, the drag coefficient per aspect ratio $C_d^*/(L/d)$ approaches a constant value at an aspect ratio L/d of approximately 14.

Increasing the density of the cylinder and the introduction of an aqueous polymer solution into the carrier fluid decreases the drag coefficient for all diameter ratios d/D investigated (i.e. d/D at 0.864, 0.732, 0.624, 0.434). However, this decrease of drag coefficient decreases rapidly as the density of the cylinder approaches that of aluminium (specific gravity = 2.7) or when the concentration of the polymer additive is near 20 wppm.

With cylindrical bodies modified by the addition of end cap(s), the L/d ratio required for a constant $C_d^*/(L/d)$ value is increased but there is a definite decrease of drag coefficient for cylinders having forebodies, both fore and afterbodies or afterbodies respectively while the possible amount of drag reduction attained in each case decreases for the geometries in that order.

(2) For blunt cylinders, the pressure gradient required
to hydrodynamically suspend the cylinders irrespective
of their length, size or density has been found to
obey the following relationship :

$$\Delta P_m = L \left(\frac{d}{D} \right) (\sigma - \rho)$$

(3) For all cylindrical bodies tested (with or without
end caps), the pressure differential $(\Delta P_m - \Delta P_o)$
is proportional to the length, the cross section and
the density of the cylinder, i.e.

$$\Delta P_m - \Delta P_o = L \left(\frac{d}{D} \right)^2 (\sigma - \rho)$$

or in the dimensionless form, the pressure function
is given as follows :

$$(\Delta P_m - \Delta P_o) / \left(\frac{L}{d} \right) D (\sigma - \rho) = c' \left(\frac{d}{D} \right)^n$$

where c' and n are constants that equal to 1 theoret-
ically. In the blunt cylindrical bodies investigated,
the constant n varies empirically with a change of
the aspect ratio while the constant c' changes with
a change of the cylinder density.
With the use of an aqueous polymer solution, the
variation of the pressure differential is negligible
while a change of its concentration has minimal effects.
On the other hand, the theoretical dimensionless pre-
ssure function equation is not strictly obeyed when

using cylinders modified by end cap(s). It is believed that the systematic variation observed may be due to an inexact representation of the L'/d ratio that was used in these analyses (note that the L'/d ratio is defined as the aspect ratio of a blunt cylinder having the same volume as the modified cylindrical bodies).

(4) For all cylindrical bodies with or without end caps, the square of the velocity is proportional to the density, the length of the cylinder, the density of of the carrier fluid and the annular spacing between the cylinder and the pipe wall, i.e.

$$U_o^2 = L \left(\frac{\sigma - \rho}{\rho} \right) \left(\frac{2g}{C_d} \right) \left(1 - \left(\frac{d}{D} \right)^2 \right)^2$$

or in a dimensionless form,

$$U_o^2 / \left(\frac{L}{d} \right) g D \left(\frac{\sigma - \rho}{\rho} \right) = \frac{2}{C_d} \left(\frac{d}{D} \right) \left(1 - \left(\frac{d}{D} \right)^2 \right)$$

This relationship has a maximum value at d/D ratio of 0.447 regardless of the shape of the cylindrical bodies but since C_d varies implicitly with d/D, C_d is strictly not constant so that the usefulness of the velocity equation is very much reduced. However, since U_o^2 is related to the kinetic energy, such a plot nonetheless is useful in evaluating the energy requirements for different bodies.

(5) The hydraulic energy required to hydrodynamically
suspend the cylindrical bodies increases with an
increase of the density and length of the cylinders
for a change of the diameter ratios, a maximum energy
requirement is observed for d/D equal to about 0.7.
With the addition of the aqueous polymer solution,
there is a reduction of the hydraulic power require-
ment for diameter ratio less than about 0.75 and
an increase for d/D greater than this diameter ratio.
These variations, however, differ little for a change
of concentration of the polymer additive. For bodies
modified with end caps, there is a reduction in the
power requirement at small aspect ratios but there
is generally an increase with the addition of after
or forebodies - in fact the increase is more pro-
nounced for cylinders with afterbodies. This indicates
that the improvement using end cap(s) is insuffic-
ient to offset the increased bulk mass and surface
area effects brought about by the existence of the
end cap(s).

(6) The required suspension velocities for low density
cylinders are generally lower than those for heav-
ier cylinders of the same diameter ratio. The velo-
city requirements for longer cylinders i.e. high
L/d ratios are greater than those of shorter cylinders.

Moreover, there is an 'optimum' diameter ratio at a d/D of about 0.45, when the velocity is a maximum for cylinders of all aspect ratios and densities investigated.

When an aqueous polymer solution is used, a higher flow suspension velocity for the cylinders is generally required. This results from less shear losses on the surface of the cylinder, thereby requiring the flow velocity to be attenuated.

An equivalent effect is achieved by having forebodies which avoids abrupt geometric changes at the nose of the bodies and hence a re-orientation of the streamlines. This has far reaching effects when separation at the leading edge of the blunt cylinders or possible back flows at the cylinder surfaces are considered. In the case of afterbodies, the sudden change in the geometry at the trailing end of the blunt cylinders which normally creates vortices is avoided and a much smaller turbulent wake is produced that effectively reduces the base drag but does little in alleviating the overall pressure drag losses.

(7)   All the improvements achieved by modifying the cylinders using end caps may be seen in a C_d versus L'/d plot. It appears that a sizable portion of the pressure drag (about 30%) may be removed by the add-

ition of the end cap(s). It is also found that more is gained by modifying the front (leading) end than the back (trailing) end of the cylinders. However, even with modification to the blunt cylinders using hemispherical end cap(s), the resulting shape is still not perfectly streamlined. It is therefore expected that residual pressure drag is bound to exist.

(8)   It may be said that, in an overall assessment, that the length effect on the performance of the cylindrical bodies is not crucial as long as the aspect ratio is greater than about 3. There is both advantage and disadvantage for an increase of the cylinder diameter ratio.

(9)   Finally, the addition of the aqueous polymer solutions is useful but the system is not too sensitive to the level of the concentration of the solution if more than about 20 wppm of the solution is present. The modification of the blunt cylinders is desirable and the addition of a forebody is most useful in the consideration of drag reduction, mass throughput and transportation velocity of the cylindrical bodies.

REFERENCES

1. Stokes G.G., Math. & Phy. Paper, (1901).

2. Newton R., Redberger P.J., Round G.F., C.J.Ch. E., 42, 168, (1964).

3. Charles M.E., C.J.Ch.E., 46, April, 1963.

4. Ellis H.S., C.J.Ch.E., 1, Feb.,1964.

5. Hodgson G.W., Charles M.E., C.J.Ch.E., 43, April, 1963.

6. Ellis H.S., C.J.Ch.E., 69, April, 1964.

7. Ellis H.S., Bolt L.H., C.J.Ch. E., 201, Oct., 1964.

8. Round G.F., Bolt L.H, C.J.Ch.E., 197, Aug., 1965.

9. Button B.L., Ma T.H., ASME, 74FE15, Feb., 1974.

10. Round G.F., Kruyer J., Ch. Eng. Sci., 22, 1133, 1967.

11. Kruyer J., Ellis H.S., C.J.Ch.E., 52, 215, April, 1974.

12. Round G.F. Kruyer J., Ch. Eng. Sci., 29, 397, 1974.

13. Hoerner S.F., FLUID DYNAMIC DRAG, (1958).

14. Toms B.A., Proceedings, Int. Rheological Congress, Holland, 1948, North Holland Publishing Co., Amsterdam, 1949.

15.   Gadd G.E., Encyclopedia of Polymer Science & Technology, <u>15</u>, (1971).

16.   White A., J. Eng. Sci., <u>8</u>, (1966).

17.   Hoyt J.W., Transaction of the ASME, 258, June, 1972.

18.   McNown J.S. & Newlin J.T., Proceedings, 1st. U.S. National Congress of Applied Mechanics, Chicago, 801, 1951.

19.   Jensen E.J., Bruce J.G. Proceedings, Hydrotransport I, University of Warwick, Coventry, 1970.

20.   White D.A., Nature, <u>216</u>, 994, (1967).

21.   Abdel-Alim A.H., Hamelec A.E., J. of Applied Polymer Sci., <u>17</u>, 3769, (1973).

22.   Brennen C., Gadd G.E., Nature, <u>215</u>, 1368, (1967).

23.   Virk P.S., Merrill E.W. et al, J. of Fluid Mechanics, 30, (1967).

24.   White D.A., Nature, <u>211</u>, 1390, (1966).

25.   White D.A., Nature, <u>212</u>, 277, (1966).

26.   White D.A., Nature, <u>216</u>, 994, (1967).

27.   Stow F.S., Elliot J.H., Polymer Letters, <u>8</u>, 611, (1970).

28.   Latto B., Round G.F., Anzenavs R., C.J.Ch.E., 51, 536, (1973).

29.   Anzenavs R., Master Thesis, McMaster U., 1972.

30.   Aly S.L., Master Thesis, McMaster U., 1974.

31.   Kruyer J., Ellis H.S., C.J.Ch.E., 52, 215, (1974).

32.   Chang P.K., SEPARATION OF FLOW, Pergamon Press, 1966.

33.   Vocadlo J.J., Sagoo M.S., ASME, 72MH10, June, 1972.

34.   McNown J.S., Lee H.M. et al, Proceedings of the VII International Congress for Applied Mechanics, London, 1948.

35.   Chapman D.R., NACA TR1051, July, (1950).

36.   Lee S.W., McMaster Report No. ME/73/FM/R/4.

37.   Charles M.E., Engineering Digest, 60, Oct., 1969.

APPENDIX I

CALIBRATION OF ROTAMETERS

The rotameter type of flow meters were exclusively used as flow measuring devices in this research. It was essential to initially calibrate the rotameters for use with both water and aqueous polymer solutions. With polymer solutions, only concentrations that were used in the experiments were selected for calibration.

The procedures used in the calibration involves measuring the flow rate of the fluid (passing through the rotameters) into a tank of known dimension. The tank most conveniently available was the aluminium reservoir in the main apparatus. This tank has the following dimensions :-

Length = 122 ± 0.05 cm.

Width = 60.7 ± 0.05 cm.

Height = $(h_1 - h_2)$ ± 0.1 cm.

Time   = $(t_1 - t_2)$ ± 0.05 sec.

Some typical results are shown in the following tables :

A1 : Small water rotameter calibration.

A2 : Large water rotameter calibration

A3 : Polymer rotameter calibration using 500 wppm solutions.

A4 : Polymer rotameter calibration using 2000 wppm solutions.

These tables are plotted as shown, respectively in Fig. AI.1, Fig. AI.2 and for the polymer calibration, AI.3.

Note that in these calibration experiments, the same set up of equipment as in an actual run of the apparatus was used so that the same kind of losses associated with pipe walls, fittings and other geometric head losses were included. This is particularly of importance in the calibration of the polymer rotameter since the flow measurements changes drastically with the use of polymer solutions.

Note also that the calibration of both of the large rotameters for water were found to be identical so that only one calibration is presented here.

FIG. AI·1:

CALIBRATION CURVE

SMALL WATER ROTAMETER

MAY, 1974.

FLOW RATE (C.C./SEC.)

READING (CM)

(IMP. GPM.)

FIG. AI·2:

CALIBRATION CURVE

LARGE WATER ROTAMETER

MAY, 1974.

FIG. AI·3: CALIBRATION CURVE

POLYMER ROTAMETER

MAY, 1974.

SOLUTION CONCENTRATION

□ 0·2 %

△ 0·05%

READING (CM.)
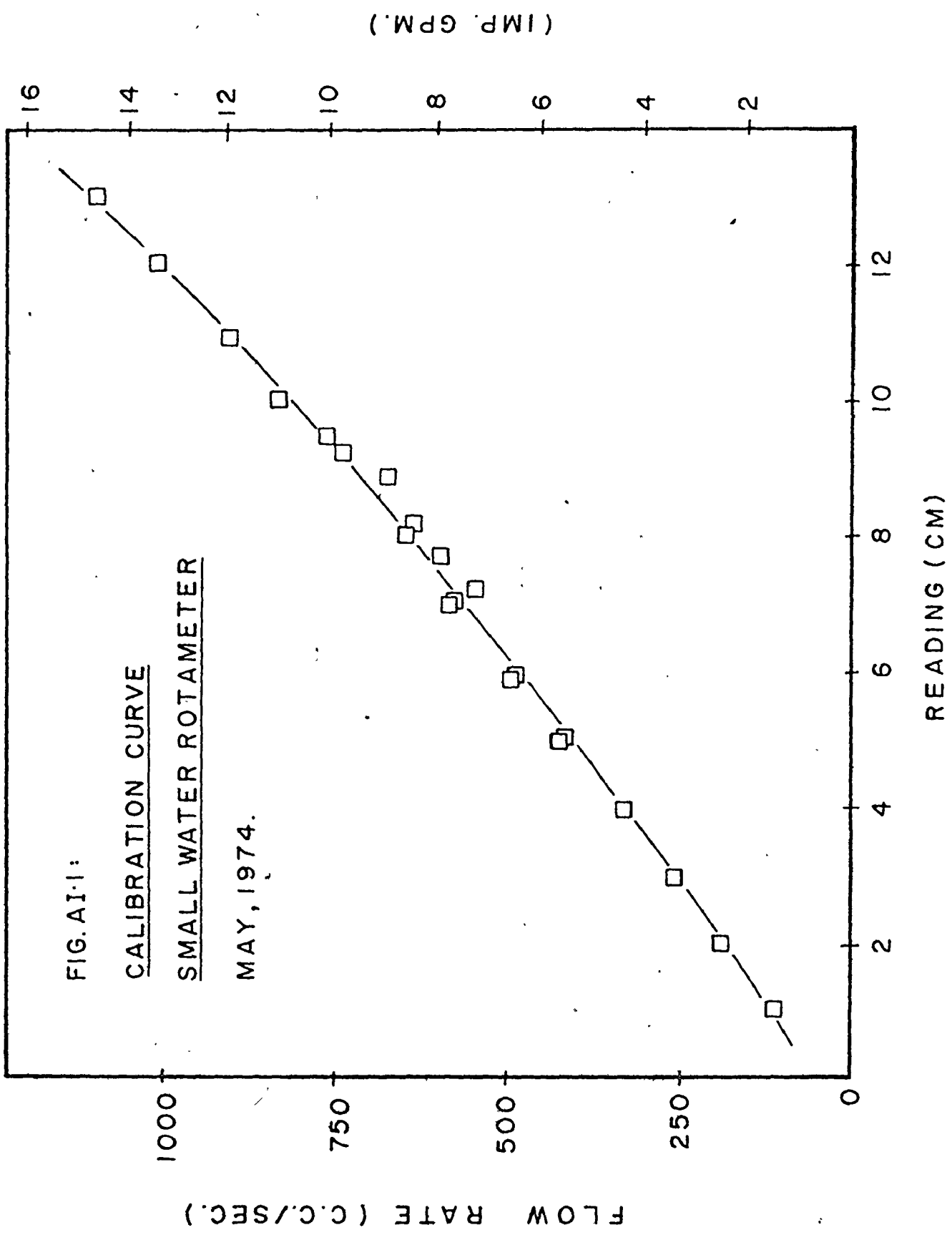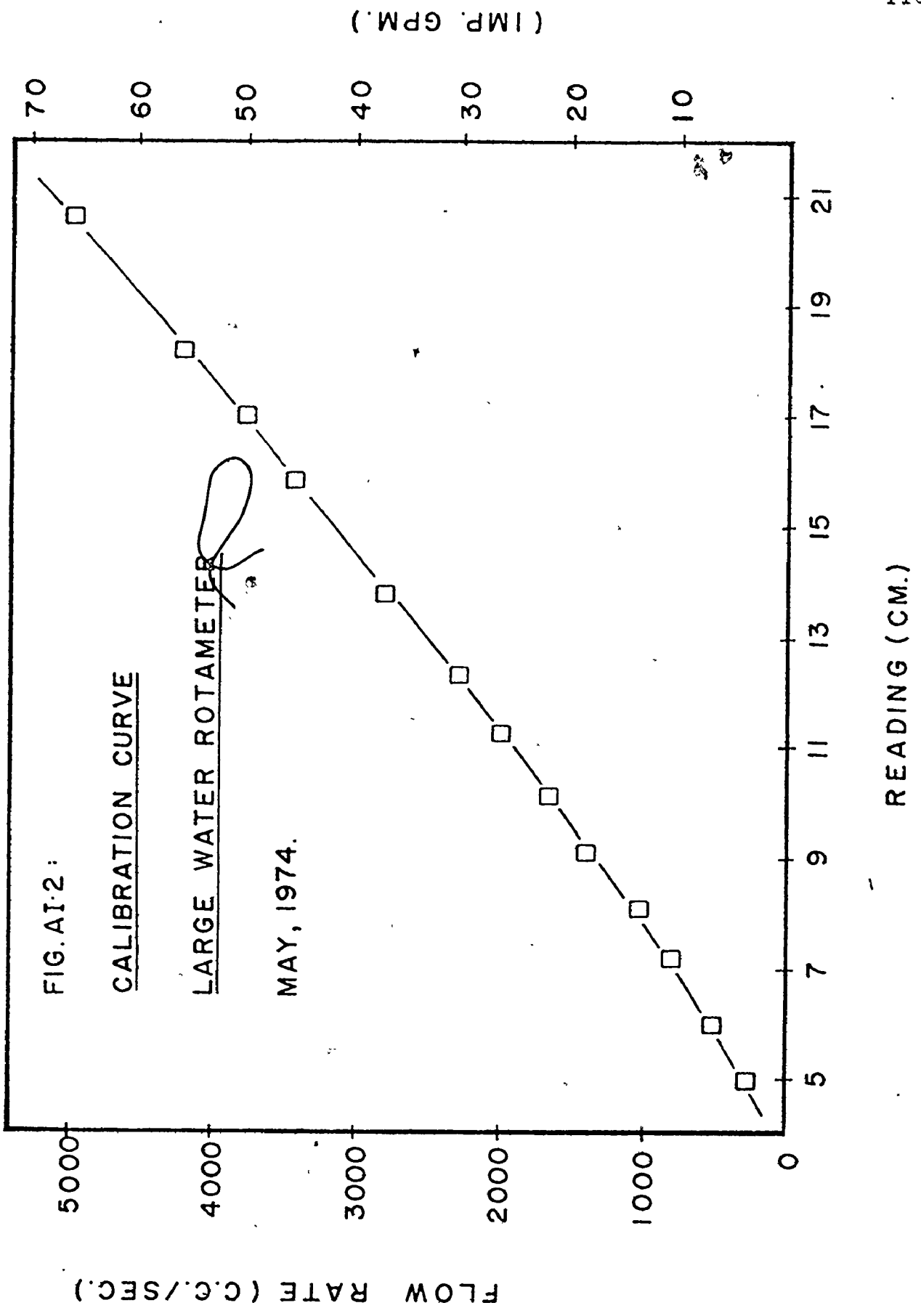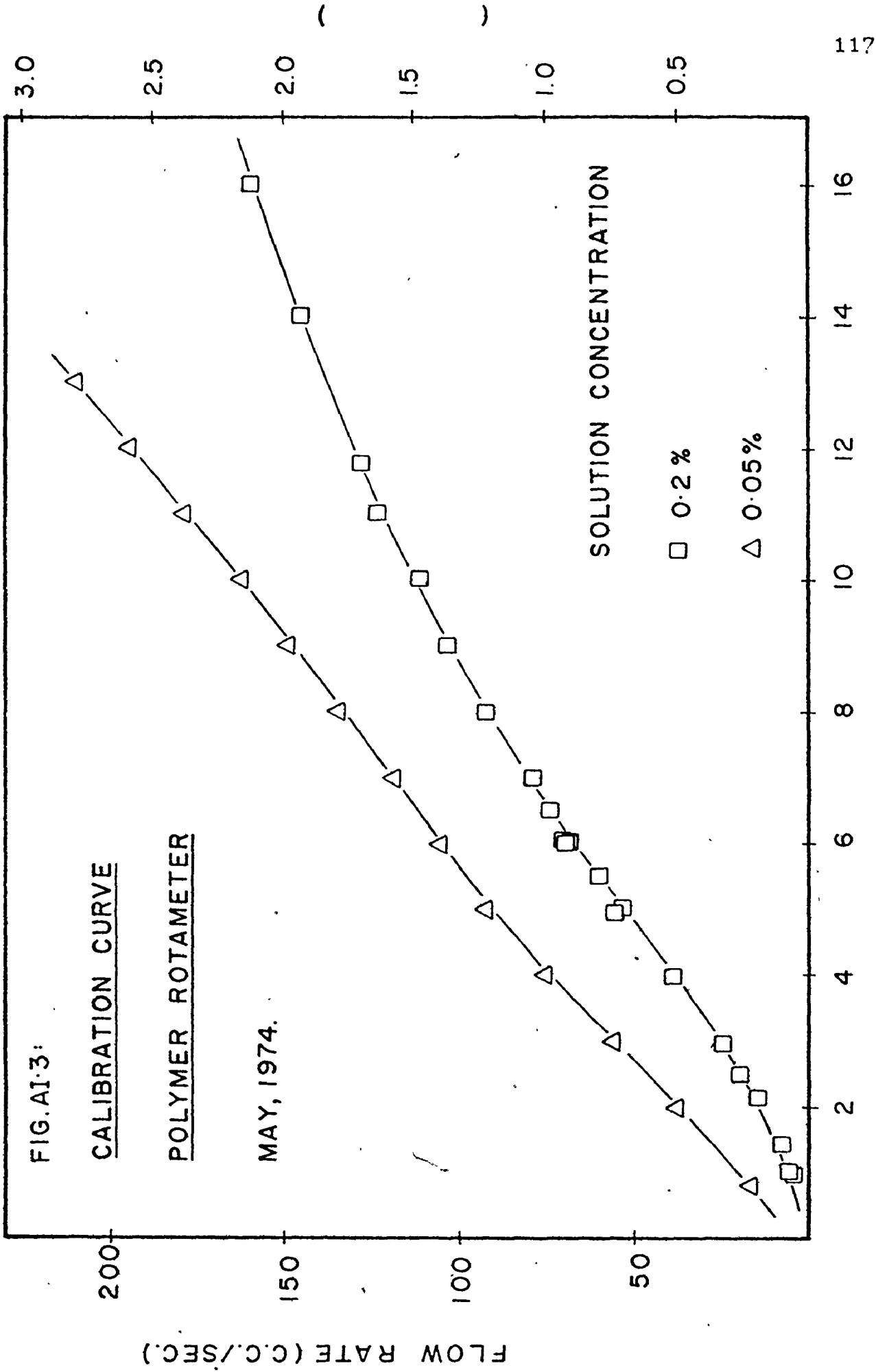
FLOW RATE (C.C./SEC.)

Table A1 : Calibration of small water rotameter

Reading (cm)	Time (sec)	(h_1-h_2) (cm)	Flow Rate (cc/sec)
13.0	40.65	6.0	1093.05
12.0	44.4	6.0	1000.73
10.0	44.95	5.0	823.74
9.45	49.05	5.0	754.90
9.2	50.65	5.0	731.04
8.85	44.45	4.0	666.40
8.15	47.15	4.0	628.24
8.05	58.00	5.0	638.40
7.7	50.45	4.0	578.15
7.2	55.35	4.0	535.17
7.0	52.10	4.0	568.55
6.95	45.00	3.5	575.98
5.95	60.95	4.0	468.00
5.85	53.15	3.5	487.66
4.95	53.35	3.0	416.42
4.95	54.2	3.0	409.89
3.95	69.15	3.0	321.28
2.95	73.65	2.5	251.37
2.0	61.05	1.5	181.95
1.0	73.80	1.0	100.34

Table A2 : Calibration of large water rotameter

Reading (cm)	Time (sec)	(h_1-h_2) (cm)	Flow Rate (cc/sec)
5.0	56.30	2.0	263.07
6.0	57.65	4.0	513.82
7.2	46.85	5.0	790.33
8.1	56.65	8.0	1045.78
9.1	49.75	9.0	1339.68
10.1	54.05	12.0	1644.12
11.25	44.65	12.0	1990.25
12.3	48.70	15.0	2280.92
13.8	31.7	12.0	2803.31
15.8	25.95	12.0	3424.40
17.0	19.85	10.0	3730.68
18.2	17.7	10.0	4183.84
20.6	22.45	15.0	4947.93
22.15	12.75	9.0	5227.34

Table A3 : Calibration of polymer rotameter using
500 wppm solutions.

Reading (cm)	Time (sec)	Mass (lbm)	Flow Rate	
			(Imp. GPM)	(cc/sec)
0.85	80.45	2.938	0.2191	16.6
2.0	64.85	5.438	0.5031	38.12
3.0	49.85	6.094	0.7349	55.68
4.0	45.15	7.438	0.9884	74.89
5.0	42.75	8.655	1.215	92.05
6.0	38.90	9.031	1.393	105.55
7.0	44.10	11.563	1.563	119.19
8.0	24.45	7.281	1.787	135.38
9.0	24.85	8.094	1.954	148.07
10.0	28.85	10.281	2.138	162.01
11.0	31.25	12.313	2.364	179.12
12.0	30.18	12.906	2.566	194.41
13.0	32.35	14.969	2.776	210.36

Table A4 : Calibration of Polymer rotameter using
2000 wppm solutions.

Reading (cm)	Time (sec)	Mass (lbm)	Flow Rate (Imp. GPM)	(cc/sec)
0.95	186.0	2.250	0.73	5.50
1.0	98.45	1.212	0.78	5.91
1.4	75.0	1.291	0.102	7.73
2.15	149.6	4.875	0.196	14.81
2.5	65.25	2.842	0.261	19.78
2.95	81.9	4.437	0.325	24.63
4.0	31.65	2.698	0.515	39.02
4.95	79.65	9.719	0.732	55.47
5.0	34.65	4.031	0.698	52.88
5.5	43.85	5.781	0.791	59.93
6.0	93.7	14.219	0.910	68.99
6.0	35.95	5.50	0.918	69.55
6.0	21.7	3.282	0.907	68.72
6.5	43.45	7.063	0.975	73.87
7.0	36.45	6.281	1.03	78.04
8.0	26.55	5.375	1.215	92.04
9.0	33.15	7.50	1.357	102.85
10.0	43.3	10.594	1.47	111.38
11.0	15.95	4.313	1.622	122.92
11.75	52.65	14.25	1.684	127.63
14.0	32.65	10.406	1.912	144.89
16.0	43.3	13.406	2.098	158.97

APPENDIX II

CROSS CALIBRATION OF POLYMER-WATER SYSTEM
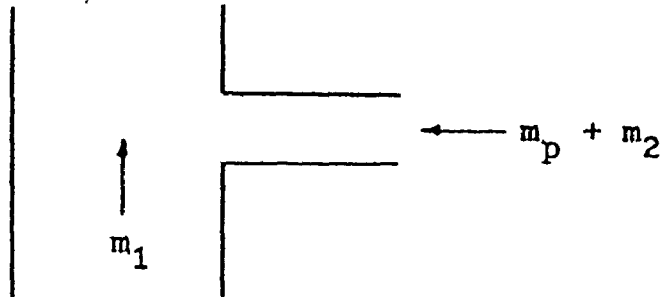
The preceeding figure shows a schematic of the junction of the polymer injection system where subscripts p, 1 and 2 represent the polymer, the mains water supply, and the water in the polymer solutions (as the solvent to the polymer) respectively. Now,

Stock solution concentration $= C_s = m_p / m_2$

Desired final concentration $= C_d = m_p / (m_1 + m_2)$

then, in a rate form, these relationships give,

$$\dot{m}_1 = \left(\frac{C_s - C_d}{C_d} \right) \dot{m}_2$$

for example, if $C_s = 2000$ wppm, and $C_d = 20$ wppm say, we have,

$$\dot{m}_1 = \left(\frac{2000-20}{20} \right) \dot{m}_2 = 99 \, \dot{m}_2$$

$$\dot{m}_2 = \dot{m}_1 / 99$$

This procedure was performed to produce the cross plots

for the rates $\dot{m}_1$ (desired final concentration) and $\dot{m}_2$ (the stock solution). For a stock solution of 500 wppm, the plot of Fig. AII.1 was generated while for a 2000 wppm stock solution, Fig. AII.2 was plotted.

Note that because of flow rate requirements, the small water rotameter is used for situations where small quantities of polymers were involved. To fully achieve this requirement, a lower concentration of the stock solution was used so that there is a larger flow rate passing through the rotameter that may be measured more accurately. For high flow rates of the polymer solutions, it is necessary to have a stock solution of higher concentration (so that re-fills are less frequent). This is the reason why two different concentrations of the stock solution were used in this experiment.
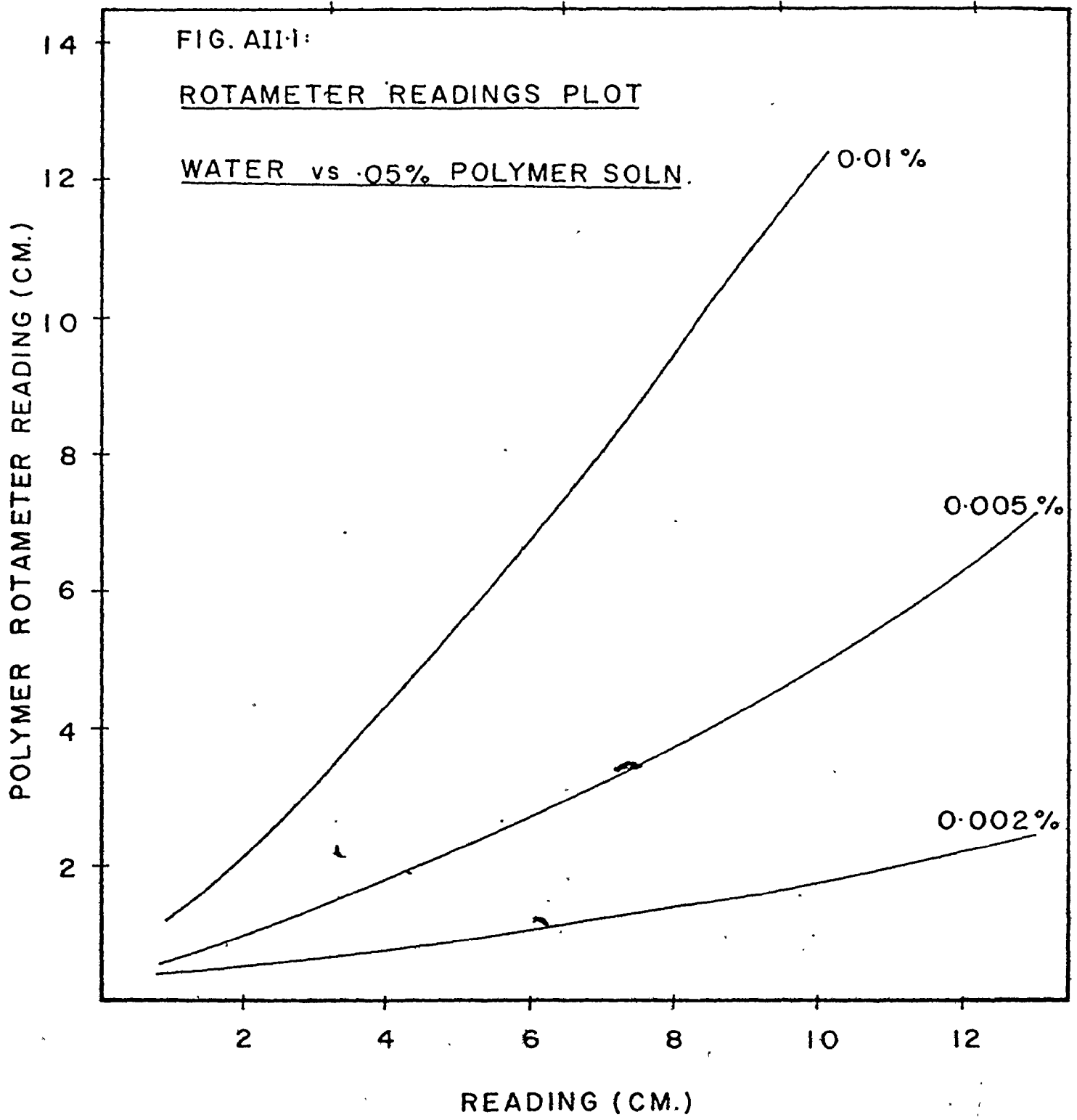
FIG. AII·I:

ROTAMETER READINGS PLOT

WATER vs ·05% POLYMER SOLN.

WATER FLOW RATE (C.C /SEC.)

FIG.AII·2·

ROTAMETER READINGS PLOT

WATER vs 0·2 % POLYMER

SOLN.

0·01 %

0·005%

0·002%

POLYMER ROTAMETER READING (CM.)

READING (CM.)
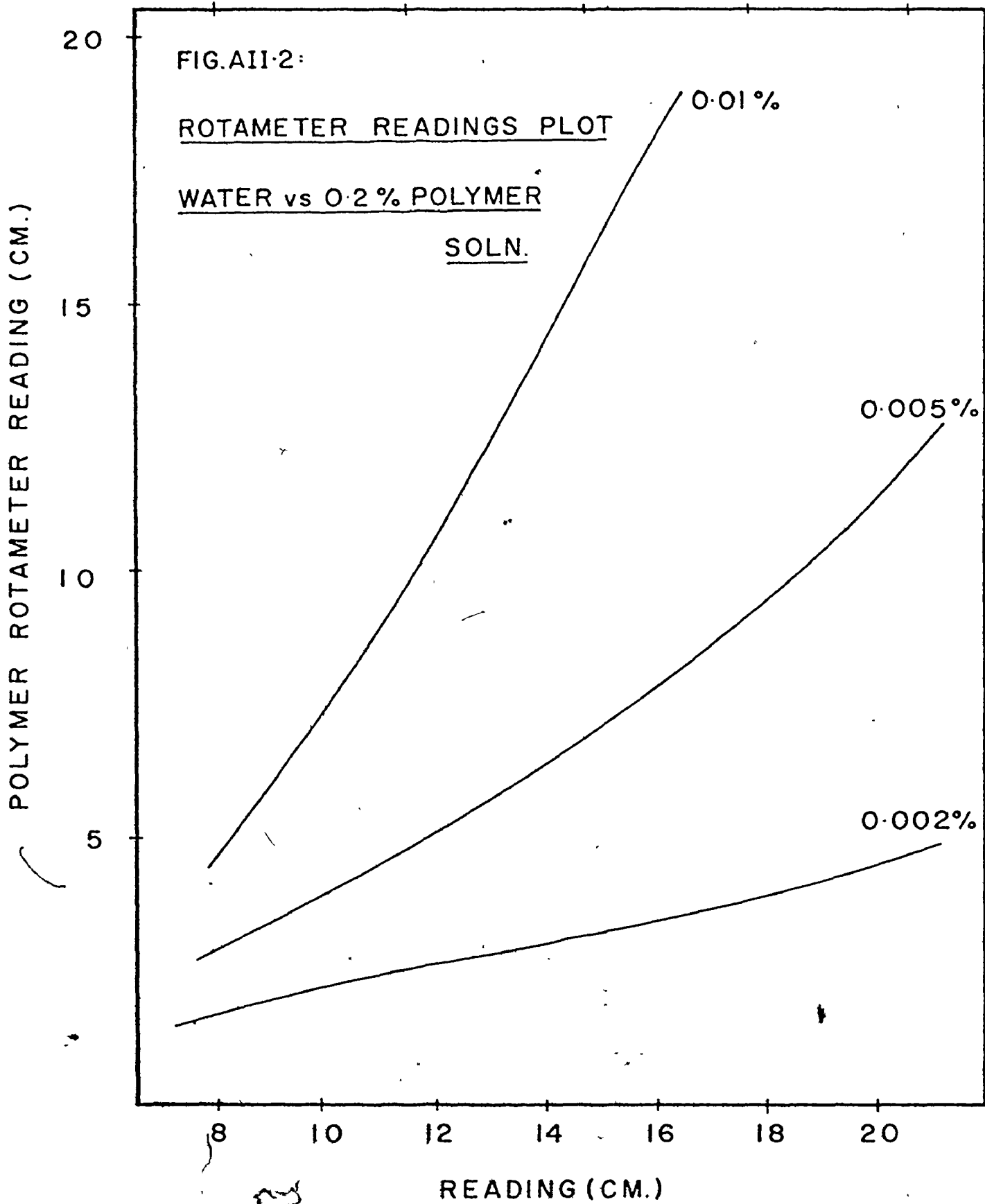
LARGE WATER ROTAMETER

APPENDIX III

CALIBRATION OF SIMPLE GRAVITY TYPE RHEOMETER

The simple gravity rheometer was described in Chapter IV. Bascially, it employs a constant suction head provided by a long vertical hose that is connected to the exit end of a capillary tube as shown in Fig. 4.3. The suction pressure thus provided is sufficient to draw the test fluid through the funnel at an approximately constant rate.

Since the level of the fluid at the upstream reservoir (funnel) varies only slightly at the beginning and end of the experiment, the differential head across the tube may be considered constant. The volume of the fluid being tested was the same for each run (250 c.c.), while the capillary has the same cross section and length. The theory of the rheometer is as follows, (for turbulent flow in the fluid),

$$C_f = T_o / (\rho \frac{U_o^2}{2g}) \tag{A.1}$$

but
$$T_o = \Delta P (\frac{1}{4} \pi d^2) / \pi dL$$
$$= \Delta P d / 4L \tag{A.2}$$

and since $U_o = L / t$ \hfill (A.3)

$$C_f = (\frac{g}{2} \Delta P \frac{d^2}{L^3}) \frac{t^2}{\rho}$$
$$= \text{Constant} (t^2 / \rho) \tag{A.4}$$

Eqn. A.4 is useful since $\triangle P$, g, d and L are constants and t^2 and ρ are characteristics depended on the fluid. Note that the specific weight of the test fluid depends on the concentration of the final polymer solution, but since this is a minute quantity (of the order of 10-100 wppm), the change in the specific weight is small and that ρ may be taken as a constant. Hence we may write eqn. A.4 as,

$$C_f = \text{Constant } (t^2) \tag{A.5}$$

Note that if we write,

$$C_f^{\frac{1}{2}} = \text{Constant } (t) \tag{A.6}$$

we may plot 't' against concentration and using eqn. A.6, may directly correlate the skin friction property as a variable of time which is readily measureable by a stop watch. If the quantities time and concentration are plotted, Fig. AIII.2 is obtained as a calibration for the fluid. Such a plot indicates a reduction of skin friction for concentrations up to about 200 wppm above which the viscosity of the fluid becomes predominent.

The calibration results are repeatable as the data on Table AIII.1 indicates and that if samples of fluids collected in an actual run of the apparatus were tested in this rheometer, the agreement is excellent proving the validity of the polymer mixing process. This is so since the stock concentration was as high as 2000 wppm and the dispersion process diluted it to say a 20 wppm solution

FIG.AIII·2:

DRAG DEVIATION - CONCENTRATION PLOT

SIMPLE GRAVITY VISCOMETER

RETEN 423 SOLUTION

PERCENT CONCENTRATION
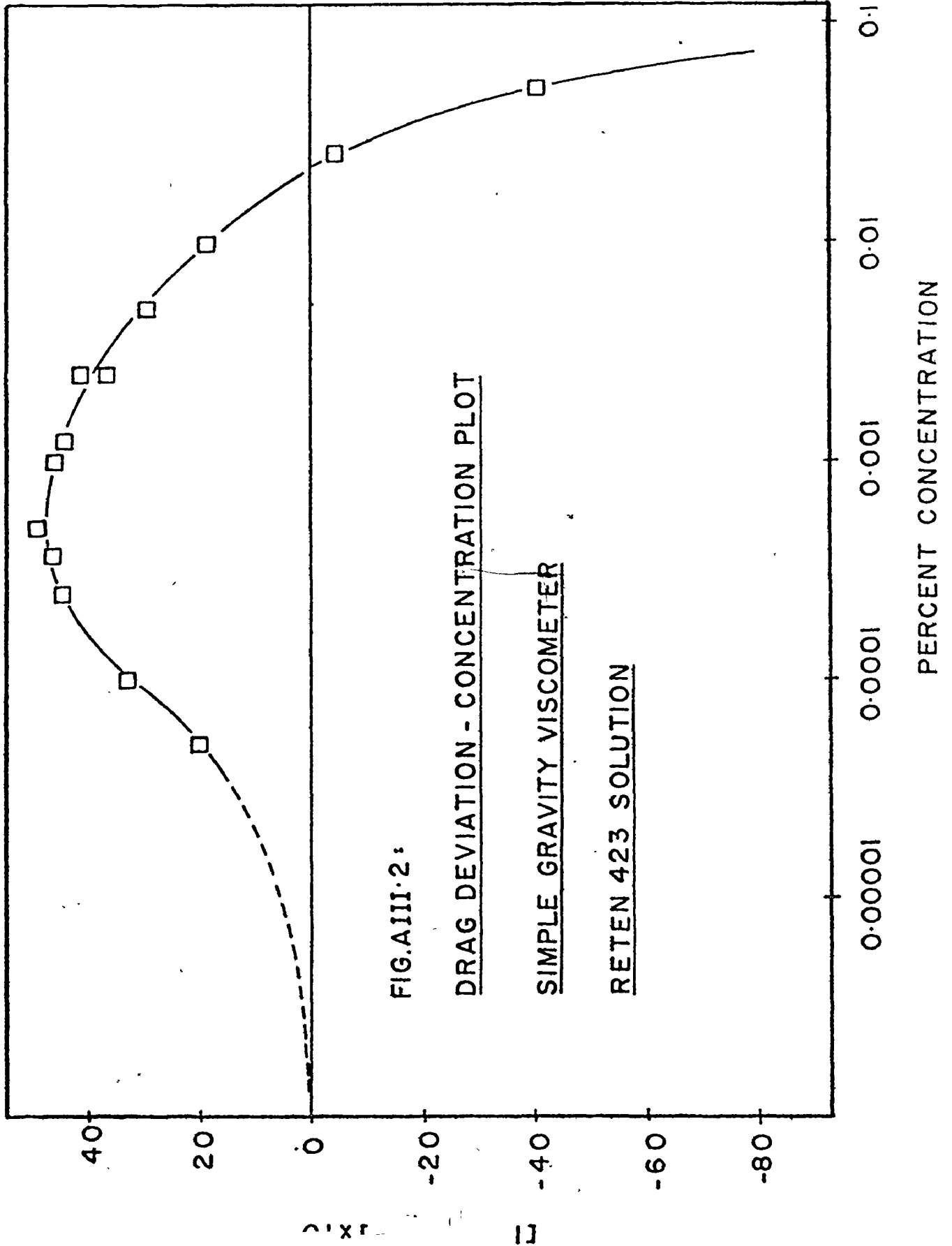
at the test section.

Another way of displaying the data obtained from the rheometer is to consider the reduction in skin friction by writing,

$$(C_f)_w - (C_f)_p \,/\, (C_f)_w = \text{reduction in skin friction}$$
$$= \frac{kt_w^2 - kt_p^2}{kt_w^2}$$
$$= 1 - t_p^2 \,/\, t_w^2 \qquad (A.\&)$$

where subscripts w and p stand for water and polymer solutions respectively. The parameter of eqn. A.7 was plotted against concentration as shown in Fig. AIII.3. The importance of such a plot is that it shows a maximum reduction in skin friction of about 45% at a concentration of around 5 wppm.

Finally, it may be said that the simple rheometer is very useful in establishing the concentration of a solution provided that we know its approximate magnitude since there are two possible concentrations for a given time measurement for concentrations less than 200 wppm. The problem is not serious unless one is working with a solution close to the maximum drag reduction condition shown in Fig. AIII.2, i.e. at about 8 wppm. For concentrations at least 20 wppm that was used in the present work, it is not difficult to establish the validity of the calibration chart since a 20 wppm is much different from say the 2 wppm solution that exists as the other possible solution for the same time measurement. Generally, a physical examination

of the solution is sufficient to differentiate between the two possibilities.

Also note that in the tables of values enclosed, that t stand for the time measurement taken for a sample fluid while t_o is associated with the time measurement for a water solution.

FIG AIII.1: TIME – CONCENTRATION PLOT

SIMPLE GRAVITY VISCOMETER

RETEN 423 SOLUTION

□ CALIBRATION
△ ACTUAL RUNS

PERCENT CONCENTRATION
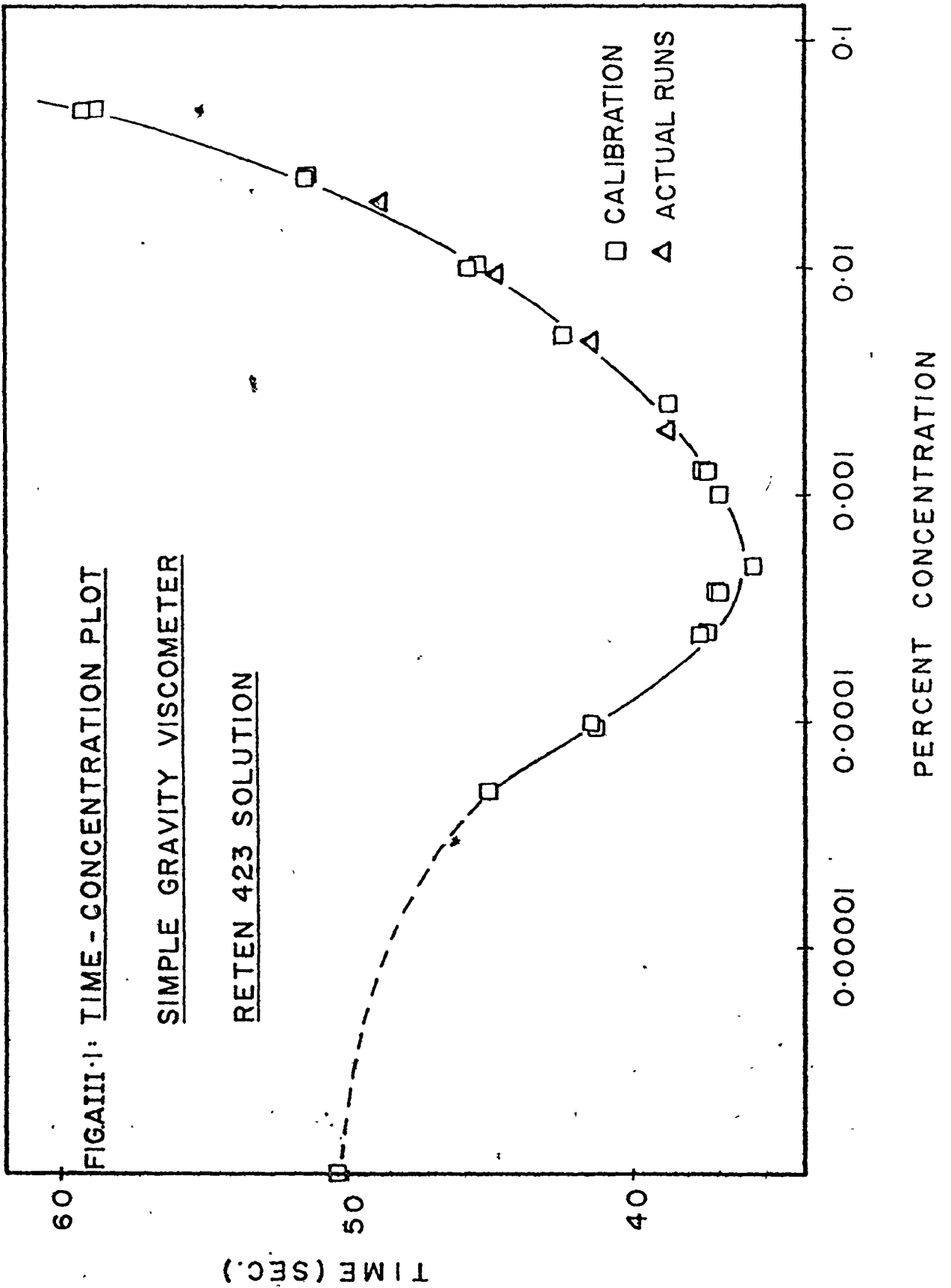
TIME (SEC.)

Table AIII.1 Calibration of simple gravity rheometer.

Concentration (wppm)	Time (sec)	Average time (sec)	$1 - (\frac{t}{t_o})^2$ (%)
0	50.2	50.2	0
0.5	45.0 45.0	45.0	20
1.0	41.4 41.25 41.0	41.22	33
1.875	39.8 40.1 40.2	40.33	36
2.5	37.8 37.5 37.8	37.7	44
3.75	36.8 37.1 37.25	37.05	46
5.0	35.75 35.8 35.75	35.77	49
7.5	37.3 37.1 37.2	37.2	45
10.0	36.9 36.9 36.8	36.86	46
12.5	37.3 37.7	37.5	44
25.0	40.3 40.3 40.1	40.23	36

(cont.)

Concentration (wppm)	Time (sec)	Average time (sec)	$1 - (\frac{t}{t_o})^2$ (%)
50.0	42.3 42.3 42.2	42.26	29
100	45.7 45.7 45.1	45.5	18
250	51.2 51.4 51.0	51.2	-4
500	59.4 59.2 58.8	59.4	-40
1000	84.0 86.1 85.0	85.0	-187
2000	144.9 145.6 148.6	146.4	-751

APPENDIX IV

MEASUREMENT OF THE INSIDE DIAMETER OF TEST SECTION

The test section used in the present apparatus has a rated diameter of 2" i.e. 5.08 cm., but since the validity of this value is vitally significant to all flow measurements, the exact I.D. of the test section must be determined.

To facilitate this, the volume of space between any two positions inside the test section must be found. The procedures involved improvising a bleed-off fitting in the lower portion of the test section and the lower pressure tap was used for this. At the start, the test section was partially filled, and the upper level was marked as accurately as possible before the water was drained to a container through the pressure tap. After the water level had dropped below a level of the test section which is thought to be of most significance (i.e. the central length of about 5'), the pressure tap was closed off and the level again marked. The volume of water collected was weighed while the length between the two marks was measured as accurately as possible. The procedures was repeated twice and the following results were obtained :

Volume (c.c.)	Length (cm.)	Average Diameter (cm.)
2000	96.85	5.1277
3000	145.90	5.1166

Mean Average Diameter = 5.122 cm.

APPENDIX V

DATA TABLES

The following notations were used in summarising the results as presented in the following tables :-

L/D $\quad$: $\quad$ L/d

L $\quad$: $\quad$ L

W $\quad$: $\quad$ Weight of cylinder - buoyancy on cylinder

PM $\quad$: $\quad$ $\triangle P_m$

PO $\quad$: $\quad$ $\triangle P_o$

Q $\quad$: $\quad$ Flow Rate

M $\quad$: $\quad$ Mass of cylinder in still air

VOL $\quad$: $\quad$ V

CD/(L/D) $\quad$: $\quad$ $c_d^* / (L/d)$

UO $\quad$: $\quad$ U_o

(UO)(W) $\quad$: $\quad$ $U_o W$

B/M $\quad$: $\quad$ $(\triangle P_m - \triangle P_o)(Q)/M$

C/M $\quad$: $\quad$ $\triangle P_m Q / M$

PRESS COEF $\quad$: $\quad$ $(\triangle P_m - \triangle P_o)/D(\sigma - \rho)$

VEL COEF $\quad$: $\quad$ $U_o^2 / Dg \left(\dfrac{\sigma - \rho}{\rho} \right)$

STEEL CYLINDER   (NO POLYMER - NO FLOW)

D/D=0.864

L/D	L(CM)	W(GMF)	PM(CM HG)	PO(CM HG)	Q(CC/SEC)	M(GM)	VOL(CC)
.2000E+01	.8850E+01	.9257E+03	.2794E+01	.1460E+00	.1450E+04	.1062E+04	.1361E+03
.2998E+01	.1327E+02	.1383E+04	.5802E+01	.2060E+00	.1780E+04	.1587E+04	.2040E+03
.3998E+01	.1769E+02	.1848E+04	.7333E+01	.2380E+00	.1920E+04	.2120E+04	.2720E+03
.4998E+01	.2211E+02	.2305E+04	.9529E+01	.2650E+00	.2030E+04	.2644E+04	.3399E+03
.5998E+01	.2654E+02	.2772E+04	.1166E+02	.2910E+00	.2160E+04	.3180E+04	.4781E+03
.6995E+01	.3096E+02	.3229E+04	.1394E+02	.3130E+00	.2250E+04	.3705E+04	.4760E+03
.7998E+01	.3539E+02	.3693E+04	.1545E+02	.3360E+00	.2390E+04	.4237E+04	.5442E+03
.8995E+01	.3981E+02	.4150E+04	.1781E+02	.3560E+00	.2420E+04	.4762E+04	.6121E+03
.9990E+01	.4421E+02	.4606E+04	.1970E+02	.3840E+00	.2520E+04	.5286E+04	.6798E+03
.1099E+02	.4862E+02	.5063E+04	.2131E+02	.4020E+00	.2580E+04	.5810E+04	.7477E+03
.1199E+02	.5305E+02	.5524E+04	.2336E+02	.4220E+00	.2640E+04	.6340E+04	.8158E+03
.1299E+02	.5746E+02	.5981E+04	.2581E+02	.4230E+00	.2680E+04	.6865E+04	.8837E+03
.1398E+02	.6186E+02	.6442E+03	.2708E+02	.4390E+00	.2700E+04	.1595E+04	.9512E+03

CTEEL CYLINDERS (NO POLYMER = 10 CTPC)

D/D=0.864

L/D	CD/(L/D)	(PM-PO) (CM HG)	(PM-PO)(Q) (WATTS)	(PM)(Q) (WATTS)	UO (CM/SEC)	(UO)(UO) (CM2/SEC2)	(UO)(W) (WATTS)
.2000E+01	.1193E+02	.2648E+01	.5119E+01	.5401E+01	.7037E+02	.4952E+04	.6388E+01
.2998E+01	.7886E+01	.5596E+01	.1328E+02	.1377E+02	.8638E+02	.7462E+04	.1171E+02
.3998E+01	.6791E+01	.7095E+01	.1816E+02	.1877E+02	.9318E+02	.8682E+04	.1588E+02
.4998E+01	.6064E+01	.9264E+01	.2507E+02	.2579E+02	.9851E+02	.9705E+04	.2226E+02
.5998E+01	.5366E+01	.1137E+02	.3274E+02	.3358E+02	.1048E+03	.1099E+05	.2350E+02
.6995E+01	.4939E+01	.1363E+02	.4087E+02	.4181E+02	.1092E+03	.1192E+05	.3459E+02
.7998E+01	.4568E+01	.1512E+02	.4716E+02	.4821E+02	.1136E+03	.1290E+05	.4113E+02.
.8995E+01	.4267E+01	.1745E+02	.5631E+02	.5747E+02	.1174E+03	.1379E+05	.4780E+02
.9990E+01	.3933E+01	.1932E+02	.6490E+02	.6619E+02	.1223E+03	.1496E+05	.5524E+02
.1099E+02	.3750E+01	.2091E+02	.7191E+02	.7330E+02	.1252E+03	.1558E+05	.6216E+02
.1199E+02	.3582E+01	.2294E+02	.8074E+02	.8223E+02	.1281E+03	.1641E+05	.6941E+02
.1299E+02	.3474E+01	.2539E+02	.9071E+02	.9222E+02	.1301E+03	.1692E+05	.7629E+02
.1398E+02	.3424E+00	.2664E+02	.9591E+02	.9749E+02	.1310E+03	.1717E+05	.8277E+01

STEEL CYLINDERS (NO POLYMER - NO GAPS)

D/D=0.864

L/D	B/M(WATTS/GM)	C/M(WATTS/GM)	B/V (WATTS/VOL)	C/V(WATTS/VOL)	PRESS COEF	VEL COEF
.2000E+01	.4821E-02	.5087E-02	.3761E-01	.3969E-01	.1033E+01	.1449E+00
.2998E+01	.8370E-02	.8678E-02	.6510E-01	.6750E-01	.2191E+01	.2192E+00
.3998E+01	.8569E-02	.8856E-02	.6676E-01	.6900E-01	.2773E+01	.2545E+00
.4998E+01	.9481E-02	.9752E-02	.7375E-01	.7586E-01	.3627E+01	.2850E+00
.5998E+01	.1030E-01	.1056E-01	.8022E-01	.8228E-01	.4443E+01	.3221E+00
.6995E+01	.1103E-01	.1128E-01	.8586E-01	.8783E-01	.5331E+01	.3499E+00
.7998E+01	.1113E-01	.1138E-01	.8666E-01	.8859E-01	.5913E+01	.3783E+00
.8995E+01	.1183E-01	.1207E-01	.9199E-01	.9388E-01	.6833E+01	.4050E+00
.9990E+01	.1228E-01	.1252E-01	.9547E-01	.9736E-01	.7568E+01	.4395E+00
.1099E+02	.1238E-01	.1261E-01	.9618E-01	.9803E-01	.8195E+01	.4609E+00
.1199E+02	.1274E-01	.1297E-01	.9898E-01	.1008E+00	.8991E+01	.4825E+00
.1299E+02	.1321E-01	.1343E-01	.1027E+00	.1044E+00	.9955E+01	.4975E+00
.1398E+02	.6012E-01	.6111E-01	.1008E+00	.1025E+00	.1044E+03	.5047E+01

B IS (PM-PO)(Q)
C IS (PM)(Q)

D/D=0.731

L/D	L(CM)	W(GMF)	PM(CM HG)	PO(CM HG)	Q(CC/SEC)	M(GM)	VOL(CC)
.1992E+01	.7460E+01	.5585E+03	.2530E+01	.3790E+00	.2500E+04	.6407E+03	.8217E+02
.2981E+01	.1117E+02	.8380E+03	.3894E+01	.5660E+00	.3080E+04	.9610E+03	.1230E+03
.3993E+01	.1496E+02	.1125E+04	.5720E+01	.7300E+00	.3550E+04	.1290E+04	.1647E+03
.4983E+01	.1866E+02	.1403E+04	.6390E+01	.8240E+00	.3670E+04	.1608E+04	.2055E+03
.5997E+01	.2246E+02	.1693E+04	.8339E+01	.9060E+00	.4120E+04	.1941E+04	.2474E+03
.6987E+01	.2617E+02	.1971E+04	.9033E+01	.9660E+00	.4430E+04	.2259E+04	.2382E+03
.8007E+01	.2999E+02	.2261E+04	.1053E+02	.1098E+01	.4780E+04	.2531E+04	.3307E+03
.8996E+01	.3368E+02	.2539E+04	.1192E+02	.1139E+01	.4910E+04	.2910E+04	.3710E+03
.1001E+02	.3748E+02	.2830E+04	.1307E+02	.1175E+01	.5060E+04	.3243E+04	.4120E+03
.1100E+02	.4119E+02	.3108E+04	.1394E+02	.1208E+01	.5200E+04	.3562E+04	.4537E+03
.1201E+02	.4499E+02	.3398E+04	.1552E+02	.1230E+01	.5300E+04	.3894E+04	.4956E+03
.1300E+02	.4870E+02	.3676E+04	.1716E+02	.1247E+01	.5420E+04	.4213E+04	.5364E+03
.1402E+02	.5249E+02	.3966E+04	.1779E+02	.1254E+01	.5460E+04	.4544E+04	.5782E+03

STEEL CYLINDERS (NO POLYMER - NO GAPS?)

D/D=0.731

L/D	CD/(L/D)	(PM-PO) (CM HG)	(PM-PO)(Q) (WATTS)	(PM)(Q) (WATTS)	UO (CM/SEC)	(UO)(UO) (CM2/SEC2)	(UO)(W) (WATTS)
.1992E+01	.3393E+01	.2151E+01	.7169E+01	.8433E+01	.1213E+03	.1472E+05	.6645E+01
.2981E+01	.2241E+01	.3328E+01	.1367E+02	.1599E+02	.1495E+03	.2234E+05	.1229E+02
.3993E+01	.1690E+01	.4990E+01	.2362E+02	.2707E+02	.1723E+03	.2968E+05	.1900E+02
.4983E+01	.1422E+01	.5566E+01	.2872E+02	.3797E+02	.1878E+03	.3577E+05	.2584E+02
.5997E+01	.1258E+01	.7433E+01	.4083E+02	.4581E+02	.1999E+03	.3998E+05	.3320E+02
.6987E+01	.1087E+01	.8067E+01	.4765E+02	.5335E+02	.2150E+03	.4622E+05	.4156E+02
.8007E+01	.9348E+00	.9436E+01	.6013E+02	.6713E+02	.2320E+03	.5381E+05	.5144E+02
.8996E+01	.8858E+00	.1078E+02	.7059E+02	.7804E+02	.2383E+03	.5678E+05	.5933E+02
.1001E+02	.8353E+00	.1169E+02	.8023E+02	.8816E+02	.2456E+03	.6030E+05	.6815E+02
.1100E+02	.7905E+00	.1273E+02	.8827E+02	.9664E+02	.2524E+03	.6368E+05	.7691E+02
.1201E+02	.7617E+00	.1429E+02	.1010E+03	.1097E+03	.2572E+03	.6616E+05	.8572E+02
.1300E+02	.7279E+00	.1592E+02	.1150E+03	.1240E+03	.2630E+03	.6918E+05	.9483E+02
.1402E+02	.7178E+00	.1654E+02	.1204E+03	.1295E+03	.2650E+03	.7021E+05	.1030E+03

STEEL CYLINDERS (NO POLYMER - NO CAPS)

D/D=0.731

L/D	B/M(WATTS/GM)	C/M(WATTS/GM)	B/V (WATTS/VOL)	C/V(WATTS/VOL)	PRESS COEF	VEL COEF
.1992E+01	.1119E-01	.1316E-01	.8725E-01	.1026E+00	.8400E+00	.4311E+00
.2981E+01	.1422E-01	.1664E-01	.1111E+00	.1300E+00	.1296E+01	.6578E+00
.3993E+01	.1831E-01	.2099E-01	.1434E+00	.1643E+00	.1940E+01	.8654E+00
.4983E+01	.1786E-01	.2050E-01	.1397E+00	.1604E+00	.2165E+01	.1029E+01
.5997E+01	.2104E-01	.2360E-01	.1650E+00	.1851E+00	.2883E+01	.1163E+01
.6987E+01	.2109E-01	.2361E-01	.1653E+00	.1851E+00	.3131E+01	.1345E+01
.8007E+01	.2320E-01	.2590E-01	.1821E+00	.2032E+00	.3658E+01	.1565E+01
.8996E+01	.2425E-01	.2682E-01	.1903E+00	.2104E+00	.4182E+01	.1651E+01
.1001E+02	.2474E-01	.2719E-01	.1943E+00	.2135E+00	.4605E+01	.1751E+01
.1100E+02	.2478E-01	.2713E-01	.1946E+00	.2130E+00	.4933E+01	.1851E+01
.1201E+02	.2594E-01	.2817E-01	.2038E+00	.2213E+00	.5532E+01	.1921E+01
.1300E+02	.2730E-01	.2944E-01	.2144E+00	.2312E+00	.6164E+01	.2010E+01
.1402E+02	.2650E-01	.2851E-01	.2082E+00	.2240E+00	.6401E+01	.2038E+01

B IS (PM-PO)(Q)
C IS (PM)(Q)

STEEL CYLINDERS (NO POLYMER - NO CAPS)   D/D=0.624

L/D	L(CM)	W(GMF)	PM(CM HG)	PO(CM.HG)	Q(CC/SEC)	M(G4)	VOL(CC)
.1975E+01	.6210E+01	.3285E+03	.2074E+01	.5530E+00	.3120E+04	.3767E+03	.4824E+02
.2973E+01	.9350E+01	.4945E+03	.3064E+01	.8720E+00	.4020E+04	.5671E+03	.7263E+02
.3993E+01	.1253E+02	.6591E+03	.3941E+01	.1085E+01	.4720E+04	.7564E+03	.9730E+02
.4975E+01	.1565E+02	.8321E+03	.5388E+01	.1215E+01	.5220E+04	.9576E+03	.1215E+03
.5999E+01	.1884E+02	.9929E+03	.5700E+01	.1234E+01	.5650E+04	.1139E+04	.1463E+03
.6991E+01	.2196E+02	.1166E+04	.6858E+01	.1258E+01	.6170E+04	.1336E+04	.1706E+03
.8000E+01	.2516E+02	.1325E+04	.7500E+01	.1236E+01	.6220E+04	.1521E+04	.1955E+03
.8992E+01	.2828E+02	.1498E+04	.8370E+01	.1346E+01	.6620E+04	.1718E+04	.2197E+03
.1000E+02	.3148E+02	.1659E+04	.8856E+01	.1401E+01	.6840E+04	.1903E+04	.2445E+03
.1100E+02	.3460E+02	.1832E+04	.1002E+02	.1466E+01	.7060E+04	.2100E+04	.2687E+03
.1201E+02	.3778E+02	.1991E+04	.1113E+02	.1524E+01	.7340E+04	.2284E+04	.2935E+03
.1300E+02	.4099E+02	.2164E+04	.1196E+02	.1586E+01	.7560E+04	.2482E+04	.3184E+03
.1398E+02	.4398E+02	.2323E+04	.1248E+02	.1600E+01	.7680E+04	.2665E+04	.3416E+03

STEEL CYLINDERS (NO POLYMER - NO CAPS)

D/D=0.624

L/D	CD/(L/D)	(PM-PO) (CM HG)	(PM-PO)(Q) (WATTS)	(PM)(Q) (WATTS)	UO (CM/SEC)	(UO)(UO) (CM2/SEC2)	(UU)(W) (WATTS)
.1975E+01	.1833E+01	.1521E+01	.6327E+01	.8627E+01	.1514E+03	.2293E+05	.4878E+01
.2973E+01	.1104E+01	.2192E+01	.1175E+02	.1642E+02	.1951E+03	.3806E+05	.9461E+01
.3993E+01	.7967E+00	.2856E+01	.1797E+02	.2480E+02	.2291E+03	.5247E+05	.1481E+02
.4975E+01	.6583E+00	.4173E+01	.2904E+02	.3750E+02	.2533E+03	.6417E+05	.2067E+02
.5999E+01	.5570E+00	.4466E+01	.3364E+02	.4294E+02	.2742E+03	.7518E+05	.2670E+02
.6991E+01	.4705E+00	.5600E+01	.4607E+02	.5641E+02	.2994E+03	.8966E+05	.3423E+02
.8000E+01	.4592E+00	.6264E+01	.5195E+02	.6219E+02	.3019E+03	.9112E+05	.3923E+02
.8992E+01	.4077E+00	.7024E+01	.6199E+02	.7387E+02	.3213E+03	.1032E+06	.4720E+02
.1000E+02	.3799E+00	.7455E+01	.6798E+02	.8076E+02	.3319E+03	.1102E+06	.5339E+02
.1100E+02	.3583E+00	.8549E+01	.8047E+02	.9427E+02	.3426E+03	.1174E+06	.6154E+02
.1201E+02	.3299E+00	.9606E+01	.9400E+02	.1089E+03	.3562E+03	.1269E+06	.6953E+02
.1300E+02	.3115E+00	.1037E+02	.1045E+03	.1205E+03	.3669E+03	.1346E+06	.7784E+02
.1398E+02	.3021E+00	.1088E+02	.1114E+03	.1278E+03	.3727E+03	.1389E+06	.8491E+02

140

STEEL CYLINDERS (NO POLYMER - NO CAPS)   D/D=0.674

L/D	B/M(WATTS/GM)	C/M(WATTS/GM)	B/V (WATTS/VOL)	C/V(WATTS/VOL)	PRESS COEF	VEL COEF
.1975E+01	.1679E-01	.2290E-01	.1311E+00	.1788E+00	.5929E+00	.6702E+00
.2973E+01	.2071E-01	.2896E-01	.1617E+00	.2261E+00	.8546E+00	.1113E+01
.3993E+01	.2376E-01	.3279E-01	.1847E+00	.2549E+00	.1119E+01	.1542E+01
.4975E+01	.3046E-01	.3932E-01	.2390E+00	.3085E+00	.1618E+01	.1866E+01
.5999E+01	.2953E-01	.3769E-01	.2299E+00	.2934E+00	.1747E+01	.2206E+01
.6991E+01	.3447E-01	.4221E-01	.2701E+00	.3308E+00	.2174E+01	.2611E+01
.8000E+01	.3416E-01	.4090E-01	.2658E+00	.3182E+00	.2452E+01	.2675E+01
.8992E+01	.3609E-01	.4300E-01	.2822E+00	.3363E+00	.2734E+01	.3013E+01
.1000E+02	.3572E-01	.4243E-01	.2780E+00	.3303E+00	.2917E+01	.3234E+01
.1100E+02	.3831E-01	.4488E-01	.2994E+00	.3508E+00	.3329E+01	.3429E+01
.1201E+02	.4116E-01	.4769E-01	.3203E+00	.3712E+00	.3759E+01	.3724E+01
.1300E+02	.4211E-01	.4855E-01	.3283E+00	.3785E+00	.4050E+01	.3943E+01
.1398E+02	.4180E-01	.4794E-01	.3260E+00	.3740E+00	.4245E+01	.4067E+01

B IS(PM-PO)(Q)
C_IS_(PM)(Q)

STEEL CYLINDERS (NO POLYMER - NO CAPS)

D/D=0.434

L/D	L(CM)	W(GMF)	PM(CM HG)	PO(CM HG)	Q(CC/SEC)	M(GM)	VOL(CC)
.1946E+01	.4330E+01	.1140E+03	.7210E+00	.3640E+00	.2800E+04	.1308E+03	.1684E+02
.2924E+01	.6505E+01	.1695E+03	.1483E+01	.9070E+00	.4100E+04	.1948E+03	.2529E+02
.3926E+01	.8735E+01	.2283E+03	.2102E+01	.1200E+01	.5000E+04	.2622E+03	.3396E+02
.4903E+01	.1091E+02	.2838E+03	.2456E+01	.1230E+01	.5670E+04	.3262E+03	.4242E+02
.5917E+01	.1317E+02	.3401E+03	.3067E+01	.1236E+01	.6160E+04	.3912E+03	.5119E+02
.6894E+01	.1534E+02	.3956E+03	.3506E+01	.1380E+01	.6620E+04	.4552E+03	.5965E+02
.7912E+01	.1761E+02	.4548E+03	.4091E+01	.1476E+01	.7140E+04	.5232E+03	.6845E+02
.8890E+01	.1978E+02	.5103E+03	.4516E+01	.1589E+01	.7480E+04	.5872E+03	.7691E+02
.9901E+01	.2203E+02	.5645E+03	.4717E+01	.1610E+01	.7720E+04	.6501E+03	.8566E+02
.1088E+02	.2421E+02	.6200E+03	.5142E+01	.1644E+01	.7920E+04	.7141E+03	.9411E+02
.1190E+02	.2647E+02	.6780E+03	.5664E+01	.1675E+01	.8120E+04	.7809E+03	.1029E+03

STEEL CYLINDERS (NO POLYMER - NO CAPS)

D/D=0.434

L/D	CD/(L/D)	(PM-PO) (CM HG)	(PM-PO)(Q) (WATTS)	(PM)(Q) (WATTS)	UO (CM/SEC)	(UO)(UO) (CM2/SEC2)	(UO)(W) (WATTS)
.1946E+01	.1601E+01	.3570E+00	.1333E+01	.2692E+01	.1359E+03	.1846E+05	.1519E+01
.2924E+01	.7390E+00	.5760E+00	.3149E+01	.8106E+01	.1990E+03	.3959E+05	.3307E+01
.3926E+01	.4983E+00	.9020E+00	.6013E+01	.1401E+02	.2426E+03	.5888E+05	.5431E+01
.4903E+01	.3857E+00	.1226E+01	.9268E+01	.1857E+02	.2752E+03	.7571E+05	.7657E+01
.5917E+01	.3245E+00	.1831E+01	.1504E+02	.2519E+02	.2989E+03	.8937E+05	.9969E+01
.6894E+01	.2805E+00	.2126E+01	.1876E+02	.3094E+02	.3213E+03	.1032E+06	.1246E+02
.7912E+01	.2416E+00	.2615E+01	.2489E+02	.3894E+02	.3465E+03	.1201E+06	.1545E+02
.8890E+01	.2198E+00	.2927E+01	.2919E+02	.4504E+02	.3630E+03	.1318E+06	.1816E+02
.9901E+01	.2050E+00	.3107E+01	.3198E+02	.4855E+02	.3746E+03	.1404E+06	.2074E+02
.1088E+02	.1947E+00	.3498E+01	.3694E+02	.5429E+02	.3844E+03	.1477E+06	.2337E+02
.1190E+02	.1852E+00	.3989E+01	.4318E+02	.6132E+02	.3941E+03	.1553E+06	.2620E+02

STEEL CYLINDERS (NO POLYMER - NO CAPS)

D/D=0.434

L/D	B/M(WATTS/GM)	C/M(WATTS/GM)	B/V (WATTS/VOL)	C/V(WATTS/VOL)	PRESS COEF	VEL COEF
.1946E+01	.1019E-01	.2057E-01	.7916E-01	.1599E+00	.1399E+00	.5429E+00
.2924E+01	.1616E-01	.4162E-01	.1245E+00	.3205E+00	.2281E+00	.1176E+01
.3926E+01	.2293E-01	.5344E-01	.1770E+00	.4126E+00	.3562E+00	.1744E+01
.4903E+01	.2841E-01	.5692E-01	.2185E+00	.4377E+00	.4865E+00	.2253E+01
.5917E+01	.3844E-01	.6438E-01	.2938E+00	.4921E+00	.7316E+00	.2678E+01
.6894E+01	.4122E-01	.6798E-01	.3146E+00	.5188E+00	.8509E+00	.3098E+01
.7912E+01	.4758E-01	.7443E-01	.3637E+00	.5689E+00	.1045E+01	.3598E+01
.8890E+01	.4971E-01	.7670E-01	.3795E+00	.5856E+00	.1171E+01	.3954E+01
.9901E+01	.4919E-01	.7468E-01	.3733E+00	.5668E+00	.1251E+01	.4240E+01
.1088E+02	.5173E-01	.7604E-01	.3925E+00	.5769E+00	.1409E+01	.4465E+01
.1190E+02	.5530E-01	.7852E-01	.4196E+00	.5958E+00	.1607E+01	.4693E+01

B IS (PM-PO)(Q)
C IS (PM)(Q)

STEEL CYLINDERS (NO POLYMER - WITH BOTH CAPS)

L/D	L(CM)	W(GMF)	PM(CM HG)	PO(CM HG)	Q(CC/SEC)	M(G4)	VOL(CC)
D/D=0.864							
.2667E+01	.1180E+02	.1204E+04	.5033E+01	.2500E+00	.1800E+04	.1385E+04	.1815E+03
.5667E+01	.2508E+02	.2585E+04	.1169E+02	.3820E+00	.2470E+04	.2971E+04	.3856E+03
.8667E+01	.3835E+02	.3971E+04	.1588E+02	.4330E+00	.2640E+04	.4561E+04	.5898E+03
.1167E+02	.5163E+02	.5341E+04	.2252E+02	.4870E+00	.2840E+04	.6134E+04	.7939E+03
D/D=0.731							
.2667E+01	.9988E+01	.7496E+03	.2974E+01	.6180E+00	.3120E+04	.8596E+03	.1100E+03
.5667E+01	.2122E+02	.1595E+04	.7118E+01	.1119E+01	.4840E+04	.1829E+04	.2338E+03
.8667E+01	.3246E+02	.2453E+04	.1110E+02	.1256E+01	.5500E+04	.2810E+04	.3575E+03
.1167E+02	.4369E+02	.3300E+04	.1390E+02	.1390E+01	.6350E+04	.3782E+04	.4813E+03
D/D=0.624							
.2667E+01	.8388E+01	.4380E+03	.2904E+01	.8925E+00	.3700E+04	.5032E+03	.6516E+02
.5667E+01	.1782E+02	.9316E+03	.5571E+01	.1407E+01	.5860E+04	.1070E+04	.1385E+03
.8667E+01	.2726E+02	.1435E+04	.8636E+01	.1627E+01	.7800E+04	.1647E+04	.2118E+03

STEEL CYLINDERS (NO POLYMER - WITH BOTH CAPS)

L/D	CD/(L/D)	(PM-PO) (CM.HG)	(PM-PO)(Q) (WATTS)	(PM)(Q) (WATTS)	UO (CM/SEC)	(UO)(UO) (CM2/SEC2)	(UO)(W) (WATTS)
D/D=0.864							
.2667E+01	.7546E+01	.4783E+01	.1148E+02	.1208E+02	.8735E+02	.7631E+04	.1031E+02
.5667E+01	.4050E+01	.1130E+02	.3722E+02	.3848E+02	.1199E+03	.1437E+05	.3039E+02
.8667E+01	.3561E+01	.1545E+02	.5437E+02	.5589E+02	.1281E+03	.1641E+05	.4989E+02
.1167E+02	.3074E+01	.2203E+02	.8343E+02	.8527E+02	.1378E+03	.1900E+05	.7218E+02
D/D=0.731							
.2667E+01	.2184E+01	.2356E+01	.9800E+01	.1237E+02	.1514E+03	.2293E+05	.1113E+02
.5667E+01	-.9089E+00	.5999E+01	.3871E+02	.4593E+02	.2349E+03	.5517E+05	.3675E+02
.8667E+01	.7075E+00	.9845E+01	.7219E+02	.8140E+02	.2669E+03	.7124E+05	.6420E+02
.1167E+02	.5306E+00	.1251E+02	.1059E+03	.1177E+03	.3082E+03	.9496E+05	.9974E+02
D/D=0.624							
.2667E+01	.1286E+01	.2012E+01	.9923E+01	.1433E+02	.1795E+03	.3224E+05	.7713E+01
.5667E+01	.5134E+00	.4164E+01	.3253E+02	.4352E+02	.2844E+03	.8087E+05	.2598E+02
.8667E+01	.2918E+00	.7009E+01	.7789E+02	.8981E+02	.3785E+03	.1433E+06	.5326E+02

STEEL CYLINDERS (NO POLYMER - WITH BOTH CAPS)

L/D	B/M(WATTS/GM)	C/M(WATTS/GM)	B/V (WATTS/VOL)	C/V(WATTS/VOL)	PRESS COEF	VEL COEF
D/D=0.864						
.2667E+01	.8288E-02	.8721E-02	.6325E-01	.6656E-01	.1914E+01	.2291E+00
.5667E+01	.1253E-01	.1295E-01	.9653E-01	.9979E-01	.4476E+01	.4267E+00
.8667E+01	.1192E-01	.1225E-01	.9218E-01	.9476E-01	.6089E+01	.4853E+00
.1167E+02	.1360E-01	.1390E-01	.1051E+00	.1074E+00	.8694E+01	.5622E+00
D/D=0.731						
.2667E+01	.1140E-01	.1439E-01	.8908E-01	.1124E+00	.9178E+00	.6699E+00
.5667E+01	.2116E-01	.2511E-01	.1656E+00	.1965E+00	.2333E+01	.1609E+01
.8667E+01	.2569E-01	.2897E-01	.2019E+00	.2277E+00	.3809E+01	.2067E+01
.1167E+02	.2801E-01	.3112E-01	.2201E+00	.2445E+00	.4842E+01	.2757E+01
D/D=0.624						
.2667E+01	.1972E-01	.2847E-01	.1523E+00	.2198E+00	.7943E+00	.9549E+00
.5667E+01	.3040E-01	.4068E-01	.2350E+00	.3144E+00	.1643E+01	.2393E+01
.8667E+01	.4427E-01	.5454E-01	.3442E+00	.4241E+00	.2745E+01	.4210E+01

B IS(PM-PO)(Q)
C IS (PM)(Q)

STEEL CYLINDERS (NO POLYMER - WITH TRAILING GAP)

L/D	L(CM)	W(GMF)	PM(CM HG)	PO(CM HG)	Q(CC/SEC)	M(GM)	VOL(CC)
D/D=0.864							
.3333E+01	.1473E+02	.1531E+04	.5938E+01	.2200E+00	.1830E+04	.1758E+04	.2265E+03
.6333E+01	.2801E+02	.2920E+04	.1223E+02	.3430E+00	.2340E+04	.3351E+04	.4308E+03
.9333E+01	.4127E+02	.4299E+04	.1851E+02	.3980E+00	.2520E+04	.4933E+04	.6346E+03
.1233E+02	.5448E+02	.5672E+04	.2379E+02	.4530E+00	.2700E+04	.6510E+04	.8377E+03
D/D=0.731							
.3333E+01	.1239E+02	.9221E+03	.4177E+01	.5840E+00	.3100E+04	.1059E+04	.1365E+03
.6333E+01	.2368E+02	.1777E+04	.8521E+01	.1020E+01	.4460E+04	.2038E+04	.2609E+03
.9333E+01	.3491E+02	.2623E+04	.1231E+02	.1170E+01	.5600E+04	.3008E+04	.3846E+03
.1233E+02	.4622E+02	.3481E+04	.1751E+02	.1330E+01	.6800E+04	.3990E+04	.5091E+03
D/D=0.624							
.3333E+01	.1042E+02	.5421E+03	.3230E+01	.9840E+00	.3940E+04	.6230E+03	.8098E+02
.6333E+01	.1992E+02	.1042E+04	.5631E+01	.1090E+01	.5750E+04	.1197E+04	.1548E+03
.9333E+01	.2938E+02	.1549E+04	.8550E+01	.1370E+01	.6900E+04	.1777E+04	.2282E+03
.1233E+02	.3885E+02	.2042E+04	.1143E+02	.1540E+01	.7510E+04	.2344E+04	.7918E+03

STEEL CYLINDERS (NO POLYMER - WITH TRAILING GAP)

L/D	CD/(L/D)	(PM-PO) (CM HG)	(PM-PO)(Q) (WATTS)	(PM)(Q) (WATTS)	UO (CM/SEC)	(UO)(UO) (CM2/SEC2)	(UO)(W) (WATTS)
D/D=0.864							
.3333E+01	.7442E+01	.5718E+01	.1395E+02	.1449E+02	.8881E+02	.7887E+04	.1334E+02
.6333E+01	.4564E+01	.1189E+02	.3709E+02	.3816E+02	.1136E+03	.1290E+05	.3252E+02
.9333E+01	.3932E+01	.1811E+02	.6083E+02	.6217E+02	.1223E+03	.1496E+05	.5155E+02
.1233E+02	.3424E+01	.2334E+02	.8400E+02	.8563E+02	.1310E+03	.1717E+05	.7288E+02
D/D=0.731							
.3333E+01	.2194E+01	.3593E+01	.1485E+02	.1726E+02	.1504E+03	.2263E+05	.1360E+02
.6333E+01	.1069E+01	.7501E+01	.4460E+02	.5067E+02	.2164E+03	.4685E+05	.3772E+02
.9333E+01	.6786E+00	.1114E+02	.8320E+02	.9194E+02	.2718E+03	.7386E+05	.6991E+02
.1233E+02	.4614E+00	.1618E+02	.1467E+03	.1588E+03	.3300E+03	.1089E+06	.1127E+03
D/D=0.624							
.3333E+01	.1130E+01	.2246E+01	.1180E+02	.1697E+02	.1912E+03	.3656E+05	.1016E+02
.6333E+01	.5336E+00	.4541E+01	.3481E+02	.4317E+02	.2790E+03	.7787E+05	.2852E+02
.9333E+01	.3734E+00	.7180E+01	.6605E+02	.7865E+02	.3349E+03	.1121E+06	.5085E+02
.1233E+02	.3143E+00	.9890E+01	.9902E+02	.1144E+03	.3645E+03	.1328E+06	.7298E+02

STEEL CYLINDERS (NO POLYMER - WITH TRAILING CAP)

L/D	B/M(WATTS/GM)	C/M(WATTS/GM)	B/V (WATTS/VOL)	C/V(WATTS/VOL)	PRESS COEF	VEL C
D/D=0.864						
.3333E+01	.7936E-02	.8241E-02	.6159E-01	.6395E-01	.2245E+01	.2323E+00
.6333E+01	.1107E-01	.1139E-01	.8611E-01	.8860E-01	.4656E+01	.3787E+00
.9333E+01	.1233E-01	.1260E-01	.9586E-01	.9797E-01	.7095E+01	.4395E+00
.1233E+02	.1290E-01	.1315E-01	.1003E+00	.1022E+00	.9148E+01	.5048E+00
D/D=0.731						
.3333E+01	.1403E-01	.1631E-01	.1088E+00	.1265E+00	.1411E+01	.6669E+00
.6333E+01	.2188E-01	.2486E-01	.1710E+00	.1942E+00	.2922E+01	.1369E+01
.9333E+01	.2766E-01	.3057E-01	.2163E+00	.2391E+00	.4336E+01	.2156E+01
.1233E+02	.3677E-01	.3979E-01	.2882E+00	.3119E+00	.6282E+01	.3171E+01
D/D=0.624						
.3333E+01	.1894E-01	.2723E-01	.1457E+00	.2095E+00	.8906E+00	.1087E+01
.6333E+01	.2909E-01	.3607E-01	.2249E+00	.2789E+00	.1790E+01	.2302E+01
.9333E+01	.3718E-01	.4427E-01	.2894E+00	.3446E+00	.2809E+01	.3290E+01
.1233E+02	.4225E-01	.4883E-01	.3281E+00	.3792E+00	.3880E+01	.3909E+01

B IS(PM-PO)(Q)
C IS (Q)(PM)(Q)

STEEL CYLINDERS   (NO POLYMER, WITH LEADING CAP)

L/D	L(CM)	W(GMF)	PM(CM HG)	PO(CM HG)	Q(CC/SEC)	M(GM)	VOL(CC)
D/D=0.864							
.3333E+01	.1473E+02	.1510E+04	.6719E+01	.2820E+00	.2100E+04	.1737E+04	.2265E+03
.6333E+01	.2801E+02	.2899E+04	.1211E+02	.3780E+00	.2460E+04	.3329E+04	.4308E+03
.9333E+01	.4127E+02	.4277E+04	.1880E+02	.4600E+00	.2740E+04	.4912E+04	.6346E+03
.1233E+02	.5448E+02	.5650E+04	.2418E+02	.4950E+00	.2840E+04	.6488E+04	.8377E+03
D/D=0.731							
.3333E+01	.1239E+02	.9426E+03	.4711E+01	.8860E+00	.4080E+04	.1133E+04	.1905E+03
.6333E+01	.2368E+02	.1798E+04	.8486E+01	.8930E+00	.5120E+04	.2162E+04	.3642E+03
.9333E+01	.3491E+02	.2644E+04	.1293E+02	.1140E+01	.6090E+04	.3181E+04	.5369E+03
.1233E+02	.4622E+02	.3502E+04	.1733E+02	.1240E+01	.6310E+04	.4212E+04	.7108E+03
D/D=0.624							
.3333E+01	.1042E+02	.5555E+03	.3706E+01	.1090E+01	.5430E+04	.7158E+03	.1603E+03
.6333E+01	.1992E+02	.1056E+04	.6464E+01	.1370E+01	.6880E+04	.1362E+04	.3964E+03
.9333E+01	.2940E+02	.1562E+04	.9792E+01	.1600E+01	.7780E+04	.2014E+04	.4521E+03

157

STEEL CYLINDERS (NON-POLYMER - WITH LEADING CAP)

L/D	CD/(L/D)	(PM-PO) (CM HG)	(PM-PO)(Q) (WATTS)	(PM)(Q) (WATTS)	UO (CM/SEC)	(UO)(UO) (CM2/SEC2)	(UO)(W) (WATTS)
D/D=0.864							
.3333E+01	.5572E+01	.6437E+01	.1802E+02	.1881E+02	.1019E+03	.1039E+05	.1509E+02
.6333E+01	.4099E+01	.1174E+02	.3849E+02	.3973E+02	.1194E+03	.1425E+05	.3393E+02
.9333E+01	.3310E+01	.1834E+02	.6698E+02	.6866E+02	.1330E+03	.1768E+05	.5578E+02
.1233E+02	.3083E+01	.2368E+02	.8967E+02	.9155E+02	.1378E+03	.1900E+05	.7637E+02
D/D=0.731							
.3333E+01	.1096E+01	.3825E+01	.2081E+02	.2563E+02	.1980E+03	.3920E+05	.1930E+02
.6333E+01	.6941E+00	.7593E+01	.5183E+02	.5793E+02	.2485E+03	.6174E+05	.4391E+02
.9333E+01	.4894E+00	.1179E+02	.9573E+02	.1050E+03	.2955E+03	.8735E+05	.7663E+02
.1233E+02	.4561E+00	.1609E+02	.1354E+03	.1458E+03	.3062E+03	.9377E+05	.1052E+03
D/D=0.624							
.3333E+01	.4332E+00	.2616E+01	.1894E+02	.2683E+02	.2635E+03	.6944E+05	.1435E+02
.6333E+01	.2683E+00	.5094E+01	.4672E+02	.5929E+02	.3339E+03	.1115E+06	.3456E+02
.9333E+01	.2104E+00	.8192E+01	.8497E+02	.1016E+03	.3775E+03	.1426E+06	.5783E+02

STEEL CYLINDERS (NO POLYMER - WITH LEADING CAP)

L/D B/M(WATTS/GM)	C/M(WATTS/GM)	B/V (WATTS/VOL)	C/V(WATTS/VOL)	PRESS COEF	VEL COEF

D/D=0.864

L/D	B/M(WATTS/GM)	C/M(WATTS/GM)	B/V (WATTS/VOL)	C/V(WATTS/VOL)	PRESS COEF	VEL COEF
.3333E+01	.1038E-01	.1083E-01	.7956E-01	.8304E-01	.2563E+01	.3102E+00
.6333E+01	.1156E-01	.1193E-01	.8935E-01	.9223E-01	.4629E+01	.4217E+00
.9333E+01	.1364E-01	.1398E-01	.1055E+00	.1082E+00	.7220E+01	.5222E+00
.1233E+02	.1382E-01	.1411E-01	.1070E+00	.1093E+00	.9320E+01	.5607E+00

D/D=0.731

L/D	B/M(WATTS/GM)	C/M(WATTS/GM)	B/V (WATTS/VOL)	C/V(WATTS/VOL)	PRESS COEF	VEL COEF
.3333E+01	.1836E-01	.2262E-01	.1092E+00	.1345E+00	.2052E+01	.1578E+01
.6333E+01	.2397E-01	.2679E-01	.1423E+00	.1590E+00	.4083E+01	.2490E+01
.9333E+01	.3010E-01	.3301E-01	.1783E+00	.1955E+00	.6355E+01	.3532E+01
.1233E+02	.3213E-01	.3461E-01	.1904E+00	.2051E+00	.8668E+01	.3789E+01

D/D=0.624

L/D	B/M(WATTS/GM)	C/M(WATTS/GM)	B/V (WATTS/VOL)	C/V(WATTS/VOL)	PRESS COEF	VEL COEF
.3333E+01	.2646E-01	.3748E-01	.1181E+00	.1674E+00	.2004E+01	.3990E+01
.6333E+01	.3431E-01	.4354E-01	.1525E+00	.1935E+00	.3925E+01	.6442E+01
.9333E+01	.4219E-01	.5043E-01	.1880E+00	.2247E+00	.6293E+01	.8214E+01

B IS (PM-PO)(Q)
C IS (PM)(Q)

ALUMINUM CYLINDERS (NO POLYMER - NO CAPS)

L/D	L(CM)	W(GMF)	PM(CM HG)	PO(CM HG)	Q(CC/SEC)	M(GM)	VOL(CC)
D/D=0.864							
.2993E+01	.1323E+02	.3449E+03	.1404E+01	.4400E-01	.8200E+03	.5479E+03	.2030E+03
.5963E+01	.2636E+02	.6862E+03	.2895E+01	.8200E-01	.1080E+04	.1091E+04	.4044E+03
.8958E+01	.3960E+02	.1032E+04	.4345E+01	.1100E+00	.1240E+04	.1639E+04	.6075E+03
.1195E+02	.5282E+02	.1381E+04	.6018E+01	.1240E+00	.1320E+04	.2191E+04	.8105E+03
D/D=0.731							
.2922E+01	.1147E+02	.2162E+03	.1014E+01	.1620E+00	.1560E+04	.3504E+03	.1342E+03
.5933E+01	.2290E+02	.4275E+03	.2070E+01	.2640E+00	.2040E+04	.6955E+03	.2687E+03
.8916E+01	.3442E+02	.6412E+03	.3157E+01	.3430E+00	.2340E+04	.1044E+04	.4027E+03
.1183E+02	.4565E+02	.8516E+03	.4071E+01	.3980E+00	.2530E+04	.1386E+04	.5342E+03
D/D=0.624							
.2983E+01	.9425E+01	.1246E+03	.7040E+00	.2640E+00	.2040E+04	.1985E+03	.7392E+02
.5949E+01	.1880E+02	.2486E+03	.1395E+01	.4680E+00	.2760E+04	.3960E+03	.1474E+03
.8922E+01	.2820E+02	.3723E+03	.2138E+01	.6320E+00	.3260E+04	.5934E+03	.2211E+03
.1189E+02	.3758E+02	.4954E+03	.2696E+01	.7410E+00	.3600E+04	.7901E+03	.2947E+03

ALUMINUM CYLINDERS (NO POLYMER - NO CAPS)

L/D	CD/(L/D)	(PM-PO) (CM HG)	(PM-PO)(Q) (WATTS)	(PM)(Q) (WATTS)	UO (CM/SEC)	(UO)(UO) (CM2/SEC2)	(UO)(W) (WATTS)
D/D=0.864							
.2993E+01	.9304E+01	.1360E+01	.1487E+01	.1535E+01	.3979E+02	.1584E+04	.1346E+01
.5963E+01	.5357E+01	.2813E+01	.4050E+01	.4168E+01	.5241E+02	.2747E+04	.3527E+01
.8958E+01	.4066E+01	.4235E+01	.7001E+01	.7183E+01	.6018E+02	.3621E+04	.6085E+01
.1195E+02	.3601E+01	.5894E+01	.1037E+02	.1059E+02	.6406E+02	.4104E+04	.8675E+01
D/D=0.731							
.2922E+01	.2128E+01	.8520E+00	.1772E+01	.2109E+01	.7571E+02	.5731E+04	.1605E+01
.5933E+01	.1233E+01	.1806E+01	.4912E+01	.5630E+01	.9900E+02	.9801E+04	.4150E+01
.8916E+01	.9350E+00	.2814E+01	.8779E+01	.9849E+01	.1136E+03	.1290E+05	.7141E+01
.1183E+02	.8009E+00	.3673E+01	.1239E+02	.1373E+02	.1228E+03	.1507E+05	.1025E+02
D/D=0.624							
.2983E+01	.1066E+01	.4400E+00	.1197E+01	.1915E+01	.9900E+02	.9801E+04	.1209E+01
.5949E+01	.5826E+00	.9270E+00	.3411E+01	.5133E+01	.1339E+03	.1794E+05	.3265E+01
.8922E+01	.4171E+00	.1506E+01	.6546E+01	.9292E+01	.1582E+03	.2503E+05	.5776E+01
.1189E+02	.3415E+00	.1955E+01	.9383E+01	.1294E+02	.1747E+03	.3052E+05	.8488E+01

161

ALUMINIUM CYLINDERS (NO POLYMER - NO CAPS)

L/D	B/M(WATTS/GM)	C/M(WATTS/GM)	B/V (WATTS/VOL)	C/V(WATTS/VOL)	PRESS COEF	VEL COE
D/D=0.864						
.2993E+01	.2714E-02	.2801E-02	.7324E-02	.7561E-02	.2125E+01	.1856E+00
.5963E+01	.3714E-02	.3822E-02	.1002E-01	.1031E-01	.4400E+01	.3223E+00
.8958E+01	.4271E-02	.4382E-02	.1152E-01	.1182E-01	.6620E+01	.4246E+00
.1195E+02	.4733E-02	.4833E-02	.1280E-01	.1307E-01	.9181E+01	.4794E+00
D/D=0.731						
.2922E+01	.5057E-02	.6019E-02	.1320E-01	.1571E-01	.1404E+01	.7085E+00
.5933E+01	.7063E-02	.8095E-02	.1833E-01	.2101E-01	.3005E+01	.1223E+01
.8916E+01	.8410E-02	.9435E-02	.2180E-01	.2446E-01	.4691E+01	.1612E+01
.1183E+02	.8940E-02	.9909E-02	.2319E-01	.2571E-01	.6115E+01	.1883E+01
D/D=0.624						
.2983E+01	.6030E-02	.9648E-02	.1619E-01	.2590E-01	.6931E+00	.1158E+01
.5949E+01	.8614E-02	.1296E-01	.2313E-01	.3481E-01	.1460E+01	.2119E+01
.8922E+01	.1103E-01	.1566E-01	.2960E-01	.4202E-01	.2374E+01	.2959E+01
.1189E+02	.1188E-01	.1638E-01	.3184E-01	.4391E-01	.3087E+01	.3615E+01

B IS(PM-PO)(Q)
C IS (PM)(Q)

STEEL CYLINDERS (WITH POLYMER - NO CAPS)

D/D=0.864

POLYMER CONCENTRATION 100 WPPM

L/D	L(CM)	W(GMF)	PM(CM HG)	PO(CM HG)	Q(CC/SEC)	M(GM)	VOL(CC)
.2000E+01	.8850E+01	.9257E+03	.3722E+01	.1040E+00	.1495E+03	.1062E+04	.1361E+03
.2998E+01	.1327E+02	.1383E+04	.5550E+01	.1510E+00	.1859E+04	.1587E+04	.2040E+03
.3998E+01	.1769E+02	.1848E+04	.7603E+01	.1810E+00	.2081E+04	.2120E+04	.2720E+03
.4995E+01	.2211E+02	.2305E+04	.9179E+01	.2230E+00	.2364E+04	.2644E+04	.3399E+03
.5998E+01	.2654E+02	.2772E+04	.1158E+02	.2470E+00	.2505E+04	.3190E+04	.4081E+03
.6995E+01	.3096E+02	.3229E+04	.1258E+02	.2710E+00	.2667E+04	.3705E+04	.4760E+03
.7998E+01	.3539E+02	.3693E+04	.1461E+02	.2910E+00	.2798E+04	.4237E+04	.5442E+03
.8995E+01	.3981E+02	.4150E+04	.1690E+02	.3120E+00	.2929E+04	.4762E+04	.6121E+03
.9990E+01	.4421E+02	.4606E+04	.1899E+02	.3340E+00	.3040E+04	.5286E+04	.6798E+03
.1099E+02	.4862E+02	.5063E+04	.2033E+02	.3540E+00	.3172E+04	.5810E+04	.7477E+03
.1199E+02	.5305E+02	.5524E+04	.2310E+02	.3670E+00	.3232E+04	.6340E+04	.8158E+03
.1299E+02	.5746E+02	.5981E+04	.2567E+02	.3780E+00	.3303E+04	.6865E+04	.8837E+03
.1398E+02	.6186E+02	.6442E+04	.2674E+02	.4010E+00	.3434E+04	.7393E+04	.9512E+03

STEEL CYLINDERS (WITH POLYMER - NO CAPS) POLYMER CONCENTRATION 100 WPPM

163

D/D=0.864

L/D	CO/(L/D)	(PM-PO) (CM HG)	(PM-PO)(Q) (WATTS)	(PM)(Q) (WATTS)	UO (CM/SEC)	(UO)(UO) (CM2/SEC2)	(UO)(W) (WATTS)
.2000E+01	.1122E+04	.3618E+01	.7211E+00	.7418E+00	.7255E+01	.5263E+02	.6586E+00
.2998E+01	.7233E+01	.5399E+01	.1338E+02	.1375E+02	.9020E+02	.8135E+04	.1223E+02
.3998E+01	.5782E+01	.7422E+01	.2059E+02	.2109E+02	.1010E+03	.1020E+05	.1830E+02
.4995E+01	.4472E+01	.8956E+01	.2823E+02	.2893E+02	.1147E+03	.1316E+05	.2593E+02
.5998E+01	.3990E+01	.1133E+02	.3784E+02	.3867E+02	.1216E+03	.1478E+05	.3305E+02
.6995E+01	.3516E+01	.1231E+02	.4377E+02	.4473E+02	.1294E+03	.1675E+05	.4098E+02
.7998E+01	.3195E+01	.1432E+02	.5342E+02	.5451E+02	.1358E+03	.1844E+05	.4918E+02
.8995E+01	.2913E+01	.1659E+02	.6477E+02	.6599E+02	.1422E+03	.2021E+05	.5795E+02
.9990E+01	.2702E+01	.1866E+02	.7563E+02	.7698E+02	.1475E+03	.2177E+05	.6664E+02
.1099E+02	.2481E+01	.1997E+02	.8445E+02	.8595E+02	.1539E+03	.2369E+05	.7642E+02
.1199E+02	.2389E+01	.2273E+02	.9796E+02	.9954E+02	.1569E+03	.2461E+05	.8499E+02
.1299E+02	.2287E+01	.2529E+02	.1114E+03	.1130E+03	.1603E+03	.2569E+05	.9402E+02
.1398E+02	.2117E+01	.2634E+02	.1206E+03	.1224E+03	.1667E+03	.2778E+05	.1053E+03

STEEL CYLINDERS (WITH POLYMER - NO CAPS)

POLYMER CONCENTRATION 100 WPPM

L/D	B/M(WATTS/GM)	C/M(WATTS/GM)	B/V (WATTS/VOL)	C/V(WATTS/VOL)	PRESS COEF	VEL COEF
.2000E+01	.6791E-03	.6986E-03	.5298E-02	.5450E-02	.1412E+01	.1540E-02
.2998E+01	.8432E-02	.8667E-02	.6558E-01	.6742E-01	.2114E+01	.2389E+00
.3998E+01	.9714E-02	.9951E-02	.7568E-01	.7753E-01	.2901E+01	.2989E+00
.4995E+01	.1067E-01	.109?E-01	.8303E-01	.8510E-01	.3506E+01	.3865E+00
.5998E+01	.1190E-01	.1216E-01	.9272E-01	.9474E-01	.4428E+01	.4332E+00
.6995E+01	.1181E-01	.1207E-01	.9194E-01	.9397E-01	.4817E+01	.4915E+00
.7998E+01	.1261E-01	.1286E-01	.9816E-01	.1002E+00	.5602E+01	.5409E+00
.8995E+01	.1360E-01	.1386E-01	.1058E+00	.1078E+00	.6493E+01	.5934E+00
.9990E+01	.1431E-01	.1456E-01	.1112E+00	.1132E+00	.7309E+01	.6397E+00
.1099E+02	.1453E-01	.1479E-01	.1129E+00	.1150E+00	.7829E+01	.6966E+00
.1199E+02	.1545E-01	.1570E-01	.1201E+00	.1220E+00	.8909E+01	.7233E+00
.1299E+02	.1622E-01	.1647E-01	.1260E+00	.1279E+00	.9917E+01	.7557E+00
.1398E+02	.1631E-01	.1656E-01	.1268E+00	.1287E+00	.1032E+02	.8166E+00

D/D=0.864

B IS (PM-PO)(Q)
C IS (PM)(Q)

164

STEEL CYLINDERS (WITH POLYMER - NO CAPS)   POLYMER CONCENTRATION   50 WPPM

D/D=0.864

L/D	L(CM)	W(GMF)	PM(CM HG)	PO(CM HG)	Q(CC/SEC)	M(GM)	VOL(CC)
.2000E+01	.8850E+01	.9257E+03	.3640E+01	.9300E-01	.1456E+04	.1062E+04	.1361E+03
.2998E+01	.1327E+02	.1383E+04	.5560E+01	.1360E+00	.1887E+04	.1587E+04	.2040E+03
.3998E+01	.1769E+02	.1848E+04	.7430E+01	.1660E+00	.2144E+04	.2120E+04	.2720E+03
.4995E+01	.2211E+02	.2305E+04	.9086E+01	.1830E+00	.2297E+04	.2644E+04	.3399E+03
.5998E+01	.2654E+02	.2772E+04	.1096E+02	.2030E+00	.2472E+04	.3180E+04	.4081E+03
.6995E+01	.3096E+02	.3229E+04	.1283E+02	.2200E+00	.2615E+04	.3705E+04	.4760E+03
.7998E+01	.3539E+02	.3693E+04	.1475E+02	.2450E+00	.2810E+04	.4237E+04	.5442E+03
.8995E+01	.3981E+02	.4150E+04	.1686E+02	.2550E+00	.2903E+04	.4762E+04	.6121E+03
.9990E+01	.4421E+02	.4606E+04	.1866E+02	.2720E+00	.3026E+04	.5286E+04	.6798E+03
.1099E+02	.4862E+02	.5063E+04	.1992E+02	.2930E+00	.3180E+04	.5810E+04	.7477E+03
.1199E+02	.5305E+02	.5524E+04	.2224E+02	.3070E+00	.3280E+04	.6340E+04	.8158E+03
.1299E+02	.5746E+02	.5981E+04	.2433E+02	.3150E+00	.3360E+04	.6865E+04	.8837E+03
.1398E+02	.6186E+02	.6442E+04	.2725E+02	.3330E+00	.3490E+04	.7393E+04	.9512E+03

STEEL CYLINDERS (WITH POLYMER - NO CAPS)   POLYMER CONCENTRATION   50 WPPM

D/D=0.864

L/D	CD/(L/D)	(PM-PO) (CM HG)	(PM-PO)(Q) (WATTS)	(PM)(Q) (WATTS)	UO (CM/SEC)	(UO)(UO) (CM2/SEC2)	(UO)(W) (WATTS)
.2000E+01	.1182E+02	.3547E+01	.6887E+01	.7068E+01	.7068E+02	.4995E+04	.6416E+01
.2998E+01	.7016E+01	.5424E+01	.1365E+02	.1399E+02	.9158E+02	.8388E+04	.1242E+02
.3998E+01	.5448E+01	.7264E+01	.2076E+02	.2123E+02	.1040E+03	.1082E+05	.1385E+02
.4995E+01	.4735E+01	.8903E+01	.2727E+02	.2783E+02	.1115E+03	.1243E+05	.2520E+02
.5998E+01	.4098E+01	.1076E+02	.3546E+02	.3613E+02	.1200E+03	.1439E+05	.3261E+02
.6995E+01	.3656E+01	.1261E+02	.4396E+02	.4473E+02	.1269E+03	.1611E+05	.4019E+02
.7998E+01	.3167E+01	.1451E+02	.5435E+02	.5527E+02	.1364E+03	.1860E+05	.4939E+02
.8995E+01	.2966E+01	.1660E+02	.6425E+02	.6524E+02	.1409E+03	.1944E+05	.5733E+02
.9990E+01	.2728E+01	.1839E+02	.7417E+02	.7527E+02	.1468E+03	.2156E+05	.6632E+02
.1099E+02	.2468E+01	.1962E+02	.8319E+02	.8444E+02	.1543E+03	.2382E+05	.7662E+02
.1199E+02	.2320E+01	.2194E+02	.9592E+02	.9726E+02	.1592E+03	.2534E+05	.8623E+02
.1299E+02	.2210E+01	.2402E+02	.1076E+03	.1090E+03	.1631E+03	.2659E+05	.9564E+02
.1398E+02	.2050E+01	.2692E+02	.1253E+03	.1268E+03	.1694E+03	.2869E+05	.1070E+03

STEEL CYLINDERS (WITH POLYMER - NO CAPS.) POLYMER CONCENTRATION 50 WPPM

D/D=0.864

L/D	B/M(WATTS/GM)	C/M(WATTS/GM)	B/V (WATTS/VOL)	C/V(WATTS/VOL)	PRESS COEF	VEL COEF
.2000E+01	.6486E-02	.6656E-02	.5060E-01	.5193E-01	.1384E+01	.1462E+00
.2998E+01	.8601E-02	.8817E-02	.6690E-01	.6858E-01	.2124E+01	.2464E+00
.3998E+01	.9794E-02	.1002E-01	.7631E-01	.7805E-01	.2839E+01	.3172E+00
.4995E+01	.1031E-01	.1052E-01	.8022E-01	.8187E-01	.3486E+01	.3650E+00
.5998E+01	.1115E-01	.1136E-01	.8689E-01	.8853E-01	.4205E+01	.4218E+00
.6995E+01	.1186E-01	.1207E-01	.9234E-01	.9395E-01	.4933E+01	.4728E+00
.7998E+01	.1283E-01	.1304E-01	.9986E-01	.1015E+00	.5674E+01	.5457E+00
.8995E+01	.1349E-01	.1370E-01	.1050E+00	.1066E+00	.6501E+01	.5827E+00
.9990E+01	.1403E-01	.1424E-01	.1091E+00	.1107E+00	.7204E+01	.6335E+00
.1099E+02	.1432E-01	.1453E-01	.1113E+00	.1129E+00	.7692E+01	.7002E+00
.1199E+02	.1513E-01	.1534E-01	.1176E+00	.1192E+00	.8597E+01	.7449E+00
.1299E+02	.1567E-01	.1588E-01	.1217E+00	.1233E+00	.9417E+01	.7820E+00
.1398E+02	.1694E-01	.1715E-01	.1317E+00	.1333E+00	.1055E+02	.8433E+00

B IS (PM-PO)(Q)
C IS (PM)(Q)

STEEL CYLINDERS (WITH POLYMER - 10 CASES)   POLYMER CONCENTRATION   20 WPPM

D/D=0.864

L/D	L(CM)	H(GMF)	PM(CM HG)	PO(CM HG)	Q(CC/SEC)	M(GM)	VOL(CC)
.2000E+01	.8850E+01	.9257E+03	.3622E+01	.8700E-01	.1498E+04	.1062E+04	.1361E+03
.2998E+01	.1327E+02	.1383E+04	.5556E+01	.1200E+00	.1858E+04	.1587E+04	.2040E+03
.3998E+01	.1769E+02	.1848E+04	.7240E+01	.1400E+00	.2053E+04	.2120E+04	.2720E+03
.4995E+01	.2211E+02	.2305E+04	.9084E+01	.1650E+00	.2295E+04	.2644E+04	.3399E+03
.5998E+01	.2654E+02	.2772E+04	.1125E+02	.1790E+00	.2463E+04	.3190E+04	.4081E+03
.6995E+01	.3096E+02	.3229E+04	.1259E+02	.1920E+00	.2590E+04	.3705E+04	.4760E+03
.7998E+01	.3539E+02	.3693E+04	.1478E+02	.2090E+00	.2779E+04	.4237E+04	.5442E+03
.8995E+01	.3981E+02	.4150E+04	.1683E+02	.2280E+00	.2979E+04	.4762E+04	.6121E+03
.9990E+01	.4421E+02	.4606E+04	.1865E+02	.2310E+00	.3042E+04	.5286E+04	.6798E+03
.1099E+02	.4862E+02	.5063E+04	.2007E+02	.2440E+00	.3080E+04	.5810E+04	.7477E+03
.1199E+02	.5305E+02	.5524E+04	.2164E+02	.2500E+00	.3160E+04	.6340E+04	.8158E+03
.1299E+02	.5746E+02	.5981E+04	.2384E+02	.2600E+00	.3260E+04	.6865E+04	.8837E+03
.1398E+02	.6186E+02	.6442E+04	.2608E+02	.2610E+00	.3325E+02	.7393E+04	.9512E+03

STEEL CYLINDERS (WITH POLYMER - NO CAPS)   POLYMER CONCENTRATION   20 WPPM

D/D=0.864

L/D	CD/(L/D)	(PM-PO) (CM HG)	(PM-PO)(Q) (WATTS)	(PM)(Q) (WATTS)	UO (CM/SFC)	(UO)(UO) (CM2/SECZ)	(UO)(W) (WATTS)
.2000E+01	.1118E+02	.3535E+01	.7059E+01	.7232E+01	.7268E+02	.5283E+04	.6598E+01
.2998E+01	.7239E+01	.5436E+01	.1346E+02	.1376E+02	.9016E+02	.8179E+04	.1223E+02
.3998E+01	.5942E+01	.7100E+01	.1943E+02	.1981E+02	.9961E+02	.9922E+04	.1805E+02
.4995E+01	.4746E+01	.8919E+01	.2729E+02	.2779E+02	.1114E+03	.1240E+05	.2517E+02
.5998E+01	.4127E+01	.1107E+02	.3636E+02	.3694E+02	.1195E+03	.1429E+05	.3250E+02
.6995E+01	.3729E+01	.1240E+02	.4282E+02	.4348E+02	.1257E+03	.1579E+05	.3979E+02
.7998E+01	.3239E+01	.1457E+02	.5399E+02	.5476E+02	.1349E+03	.1819E+05	.4884E+02
.8995E+01	.2816E+01	.1660E+02	.6592E+02	.6683E+02	.1446E+03	.2090E+05	.5883E+02
.9990E+01	.2699E+01	.1842E+02	.7470E+02	.7564E+02	.1476E+03	.2180E+05	.6668E+02
.1099E+02	.2631E+01	.1983E+02	.8142E+02	.8242E+02	.1495E+03	.2234E+05	.7-21E+02
.1199E+02	.2500E+01	.2139E+02	.9013E+02	.9119E+02	.1534E+03	.2352E+05	.8308E+02
.1299E+02	.2348E+01	.2358E+02	.1025E+03	.1036E+03	.1582E+03	.2503E+05	.9280E+02
.1398E+02	.2258E+05	.2581E+02	.1144E+01	.1156E+01	.1614E+01	.2604E+01	.1019E+01

L/D	B/M(WATTS/GM)	C/M(WATTS/GM)	B/V (WATTS/VOL)	C/V(WATTS/VOL)	PRESS COEF	VEL COEF
.2000E+01	.6648E-02	.6811E-02	.5186E-01	.5314E-01	.1379E+01	.1546E+00
.2998E+01	.8486E-02	.8673E-02	.6601E-01	.6746E-01	.2129E+01	.2388E+00
.3998E+01	.9167E-02	.9348E-02	.7142E-01	.7283E-01	.2775E+01	.2909E+00
.4995E+01	.1032E-01	.1051E-01	.8027E-01	.8175E-01	.3492E+01	.3642E+00
.5998E+01	.1143E-01	.1162E-01	.8908E-01	.9052E-01	.4327E+01	.4189E+00
.6995E+01	.1156E-01	.1174E-01	.8994E-01	.9133E-01	.4853E+01	.4635E+00
.7998E+01	.1274E-01	.1292E-01	.9920E-01	.1006E+00	.5700E+01	.5336E+00
.8995E+01	.1384E-01	.1403E-01	.1077E+00	.1092E+00	.6499E+01	.6137E+00
.9990E+01	.1413E-01	.1431E-01	.1099E+00	.1113E+00	.7216E+01	.6404E+00
.1099E+02	.1401E-01	.1419E-01	.1089E+00	.1102E+00	.7772E+01	.6569E+00
.1199E+02	.1422E-01	.1438E-01	.1105E+00	.1118E+00	.8385E+01	.6913E+00
.1299E+02	.1493E-01	.1509E-01	.1160E+00	.1172E+00	.9245E+01	.7361E+00

D/D=0.864

B IS (PM-PO)(Q)
C IS (PM)(Q)

STEEL CYLINDERS (WITH POLYMER - NO CAPS) D/D=0.731

L/D	L(CM)	W(GMF)	-PM(CM HG)	PO(CM HG)	Q(CC/SEC)	M(GM)	VOL(CC)
POLYMER CONCENTRATION · 20 WPPM							
.2981E+01	.1117E+02	.8380E+03	.3581E+01	.3600E+00	.3185E+09	.9610E+03	.1230E+03
.5997E+01	.2246E+02	.1693E+04	.7339E+01	.5660E+00	.4540E+04	.1941E+04	.2474E+03
.8996E+01	.3369E+02	.2539E+04	.1044E+02	.6400E+00	.5430E+04	.2910E+04	.3711E+03
.201E+02	.4499E+02	.3398E+04	.1415E+02	.6730E+00	.5630E+04	.3894E+04	.4956E+03
POLYMER CONCENTRATION 50 WPPM							
.2981E+01	.1117E+02	.8380E+03	.3504E+01	.2940E+00	.3180E+04	.9610E+03	.1230E+03
.5997E+01	.2246E+02	.1693E+04	.7238E+01	.4590E+00	.4530E+04	.1941E+04	.2474E+03
.8996E+01	.3369E+02	.2539E+04	.1039E+02	.5330E+00	.5500E+04	.2910E+04	.3711E+03
.201E+02	.4499E+02	.3398E+04	.1471E+02	.5520E+00	.5950E+04	.3894E+04	.4956E+03
POLYMER CONCENTRATION 100 WPPM							
.2981E+01	.1117E+02	.8380E+03	.3378E+01	.2440E+00	.3160E+04	.9610E+03	.1230E+03

STEEL CYLINDERS (WITH POLYMER - NO CAPS)

D/D=0.731

L/D	CD/(L/D)	(PM-PO) (CM HG)	(PM-PO)(Q) (WATTS)	(PM)(Q) (WATTS)	UO (CM/SEC)	(UO)(UO) (CM2/SEC2)	(UO)(W) (WATTS)
POLYMER CONCENTRATION 20 WPPM							
997E+01	.1036E+01	.6773E+01	.4100E+02	.4442E+02	.2203E+03	.4854E+05	.3658E+02
996E+01	.7240E+00	.9796E+01	.7092E+02	.7555E+02	.2635E+03	.6944E+05	.6562E+02
.1201E+02	.6750E+00	.1347E+02	.1011E+03	.1062E+03	.2732E+03	.7465E+05	.9106E+02
POLYMER CONCENTRATION 50 WPPM							
981E+01	.2102E+01	.3210E+01	.1361E+02	.1486E+02	.1543E+03	.2392E+05	.1268E+02
997E+01	.1041E+01	.6779E+01	.4094E+02	.4371E+02	.2198E+03	.4833E+05	.3650E+02
996E+01	.7057E+00	.9854E+01	.7226E+02	.7616E+02	.2669E+03	.7124E+05	.6646E+02
201E+02	.6043E+00	.1416E+02	.1123E+03	.1167E+03	.2888E+03	.8338E+05	.9623E+02
POLYMER CONCENTRATION 100 WPPM							
981E+01	.2129E+01	.3134E+01	.1320E+02	.1423E+02	.1534E+03	.2352E+05	.1260E+02

STEEL CYLINDERS (WITH POLYMER - NO CAPS)

D/D=0.731

L/D	B/M(WATTS/GM)	C/M(WATTS/GM)	B/V (WATTS/VOL)	C/V(WATTS/VOL)	PRESS COEF	VEL COEF
POLYMER CONCENTRATION 20 WPPM						
.5997E+01	.2113E-01	.2289E-01	.1657E+00	.1796E+00	.2627E+01	.1412E+01
.8996E+01	.2437E-01	.2596E-01	.1911E+00	.2036E+00	.3800E+01	.2020E+01
.1201E+02	.2597E-01	.2727E-01	.2041E+00	.2143E+00	.5215E+01	.2167E+01
POLYMER CONCENTRATION 50 WPPM						
.2981E+01	.1416E-01	.1546E-01	.1107E+00	.1208E+00	.1250E+01	.6958E+00
.5997E+01	.2110E-01	.2253E-01	.1655E+00	.1767E+00	.2629E+01	.1406E+01
.8996E+01	.2483E-01	.2617E-01	.1947E+00	.2052E+00	.3822E+01	.2073E+01
.1201E+02	.2884E-01	.2996E-01	.2266E+00	.2354E+00	.5479E+01	.2421E+01
POLYMER CONCENTRATION 100 WPPM						
.2981E+01	.1374E-01	.1481E-01	.1074E+00	.1157E+00	.1221E+01	.6871E+00

B IS(PM-PO)(Q)
C IS (PM2)(Q)

STEEL CYLINDERS (WITH POLYMER - NO CAPS)

D/D=0.624

L/D	L(CM)	W(GMF)	PM(CM HG)	PO(CM HG)	Q(CC/SEC)	M(GM)	VOL(CC)
POLYMER CONCENTRATION 20 WPPM							
.2973E+01	.9350E+01	.4915E+03	.2992E+01	.4840E+00	.4040E+04	.5641E+03	.7263E+02
.5999E+01	.1884E+02	.9929E+03	.4533E+01	.6590E+00	.5600E+04	.1139E+04	.1463E+03
.8992E+01	.2828E+02	.1498E+04	.6955E+01	.8350E+00	.7130E+04	.1718E+04	.2197E+03
.1201E+02	.3778E+02	.1991E+04	.9219E+01	.8890E+00	.7975E+04	.2284E+04	.2935E+03
POLYMER CONCENTRATION 50 WPPM							
.2973E+01	.9350E+01	.4915E+03	.2082E+01	.4130E+00	.4120E+04	.5641E+03	.7263E+02
.5999E+01	.1884E+02	.9929E+03	.4249E+01	.5470E+00	.5750E+04	.1139E+04	.1463E+03
.8992E+01	.2828E+02	.1498E+04	.6772E+01	.5780E+00	.7300E+04	.1718E+04	.2197E+03

STEEL CYLINDERS (WITH POLYMER - NO CAPS)

D/D=0.624

L/D	CD/(L/D)	(PM-PO) (CM.HG)	(PM-PO)(G) (WATTS)	(PM)(Q) (WATTS)	UO (CM/SEC)	(UO)(UO) (CM2/SEC2)	(UO)(W) (WATTS)
POLYMER CONCENTRATION 20 WPPM							
.2973E+01	.1086E+01	.2508E+01	.1351E+02	.1612E+02	.1961E+03	.3844E+05	.9449E+01
.5999E+01	.5670E+00	.3874E+01	.2892E+02	.3384E+02	.2718E+03	.7386E+05	.2646E+02
.8992E+01	.3515E+00	.6120E+01	.5818E+02	.6611E+02	.3460E+03	.1197E+06	.5084E+02
.1201E+02	.2794E+00	.8330E+01	.8857E+02	.9802E+02	.3870E+03	.1498E+06	.7555E+02
POLYMER CONCENTRATION 50 WPPM							
.2973E+01	.1044E+01	.1669E+01	.9168E+01	.1144E+02	.1999E+03	.3998E+05	.9636E+01
.5999E+01	.5378E+00	.3702E+01	.2838E+02	.3257E+02	.2790E+03	.7787E+05	.2717E+02
.8992E+01	.3353E+00	.6194E+01	.6028E+02	.6591E+02	.3543E+03	.1255E+06	.5205E+02

STEEL CYLINDERS (WITH POLYMER - NO C/PS)

D/D=0.624

L/D	B/M(WATTS/GM)	C/M(WATTS/GM)	B/V (WATTS/VOL)	C/V(WATTS/VOL)	PRESS COEF	VEL COEF
POLYMER CONCENTRATION 20 WPPM						
.2973E+01	.2395E-01	.2857E-01	.1860E+00	.2219E+00	.9838E+00	.1131E+01
.5999E+01	.2539E-01	.2971E-01	.1977E+00	.2313E+00	.1515E+01	.2167E+01
.8992E+01	.3386E-01	.3848E-01	.2648E+00	.3009E+00	.2382E+01	.3495E+01
.1201E+02	.3878E-01	.4292E-01	.3018E+00	.3340E+00	.3259E+01	.4396E+01
POLYMER CONCENTRATION 50 WPPM						
.2973E+01	.1625E-01	.2027E-01	.1262E+00	.1574E+00	.6547E+00	.1176E+01
.5999E+01	.2491E-01	.2859E-01	.1940E+00	.2226E+00	.1448E+01	.2284E+01
.8992E+01	.3509E-01	.3836E-01	.2744E+00	.3000E+00	.2411E+01	.3664E+01

B IS (PM-PO)(Q)
C IS (PM)(Q)

STEEL CYLINDERS (WITH POLYMER - NO CAPS)

D/D=0.434

* L/D	L(CM)	M(GMF)	PM(CM HG)	PO(CM HG)	Q(CC/SEC)	M(GM)	VOL(CC)
			POLYMER CONCENTRATION 20 WPPM				
.2924E+01	.6505E+01	.1695E+03	.1100E+01	.5130E+00	.4140E+04	.1948E+03	.2529E+02
.5917E+01	.1317E+02	.3401E+03	.2121E+01	.7080E+00	.6550E+04	.3912E+03	.5119E+02
.8890E+01	.1978E+02	.5103E+03	.3162E+01	.9140E+00	.8070E+04	.5872E+03	.7691E+02
			POLYMER CONCENTRATION 50 WPPM				
.2924E+01	.6505E+01	.1695E+03	.1019E+01	.4260E+00	.4230E+04	.1948E+03	.2529E+02
.5917E+01	.1317E+02	.3401E+03	.1923E+01	.5960E+00	.6560E+04	.3912E+03	.5119E+02

STEEL CYLINDERS (WITH POLYMER - NO CAPS)

D/D=0.434

L/D	CD/(L/D)	(PM-PO) (CM HG)	(PM-PO)(Q) (WATTS)	(PM)(Q) (WATTS)	UO (CM/SEC)	(UO)(UO) (CM2/SEC2)	(UO)(W) (WATTS)
POLYMER CONCENTRATION 20 WPPM							
924E+01	.7248E+00	.5870E+00	.3240E+01	.6071E+01	.2009E+03	.4037E+05	.3340E+01
517E+01	.2870E+00	.1413E+01	.1234E+02	.1852E+02	.3179E+03	.1010E+06	.1060E+02
890E+01	.1888E+00	.2248E+00	.2419E+02	.3402E+02	.3916E+03	.1534E+06	.1960E+02
POLYMER CONCENTRATION 50 WPPM							
.2924E+01	.6943E+00	.5930E+00	.3344E+01	.5747E+01	.2053E+03	.4214E+05	.3412E+01
.5917E+01	.2861E+00	.1327E+01	.1161E+02	.1682E+02	.3184E+03	.1013E+06	.1062E+02

STEEL CYLINDERS (WITH POLYMER - NO CAPS)

D/D=0.434

L/D	B/M(WATTS/GM)	C/M(WATTS/GM)	B/V (WATTS/VOL)	C/V(WATTS/VOL)	PRESS COEF	VEL COEF
POLYMER CONCENTRATION	20 WPPM					
.2924E+01	.1663E-01	.3117E-01	.1281E+00	.2400E+00	.2325E+00	.1199E+01
.5917E+01	.3154E-01	.4734E-01	.2411E+00	.3618E+00	.5645E+00	.3028E+01
.8890E+01	.4119E-01	.5794E-01	.3145E+00	.4423E+00	.8993E+00	.4602E+01
POLYMER CONCENTRATION	50 WPPM					
.2924E+01	.1717E-01	.2950E-01	.1322E+00	.2272E+00	.2349E+00	.1252E+01
.5917E+01	.2966E-01	.4299E-01	.2267E+00	.3286E+00	.5302E+00	.3037E+01

B IS (PM-PO)(Q)
C IS (PM)(Q)